

The development of new dual-target antibiotics: Synthesis of Mur ligase inhibitors

Open Source Antibiotics

THESIS

submitted by

Kato LEONARD

Matthew Todd Research Group, University College London

Academic promotor: Prof. Dr. Matthew Todd

Co-promotor: Prof. Dr. Arthur Van Aerschot

Supervisors: Dr. Dana Klug and Dr. Edwin Tse

LEUVEN

Academic year 2021-2022

© Copyright by KU Leuven

Without written permission of the promotor and the authors it is forbidden to reproduce or adapt in any form or by any means any part of this publication.

A written permission of the promotor is also required to use the methods, products, schematics and programs described in this work for industrial or commercial use, and for submitting this publication in scientific context.

Acknowledgements

Looking back on these past months, I am beyond grateful for the people who supported me both in my professional and personal life and who made my Erasmus adventure in London a success.

*First of all, I would like to express my gratitude to my supervisor **Prof. Dr. Matthew Todd**, in whose lab I was given the chance to do research. It was incredibly inspiring to learn about Open Source Science first-hand from one of the pioneers. I cannot express in words how thankful I am for the confidence you had in my abilities and for all the opportunities you gave me to engage in various experiences, which undoubtedly helped shape the scientist I am today.*

*In addition, a big thank you goes to my mentors, who supported me in the lab daily. **Dr. Edwin Tse and Dr. Dana Klug** at UCL, I have deeply appreciated your immense patience and exceptional ability to train a chemistry newbie. Without you, I would never have been able to successfully complete this project. I wish you both all the best with your further, and presumably very impressive, careers. **Dr. Lizbe Koekemoer** at the University of Oxford, thank you so much for welcoming me to your lab for a month and introducing me to high-throughput bio-crystallography. This triggered my interest in structural biology and played a major role in my decision to start the postgraduate master's in plant biotechnology next academic year. No less importantly, I would like to thank my family friend **Dr. Gerardine Quaghebeur**, for being so hospitable to accommodate me in their home during my research period in Oxford.*

*Furthermore, also the remote assistance from my university in Belgium, KU Leuven, was tremendously appreciated. **Prof. Dr. Arthur Van Aerschot**, it was an honour to be a student in your organic chemistry classes at the beginning of my academic journey and to have you as my co-supervisor for my master's thesis five years later. I hope you have enjoyed this last year of your academic career to the fullest and wish you a wonderful retirement.*

*Not to be forgotten are **all the members of the G25 lab**. Thank you for making me feel welcome from the first second I entered the lab. Of course, I would like to give extra credit to **all the members of the Todd group**. Tom, Yuhang, Dmitrij, and Daniel, every day has been a pleasure to work with you. Time and time again, I have been impressed by your knowledge, helpfulness, and resilience. I most certainly look up to you.*

*Finally, I would like to thank my **family and friends**, who believed in me even at times when I did not, for their unconditional support. Thank you for the numerous phone and video calls and the unforgettable visits to make me forget the physical distance that was between us for nine months. **Mom, Dad**, I will be forever grateful to you for making this international experience possible.*

TABLE OF CONTENTS

LIST OF ABBREVIATIONS.....	ii
SUMMARY.....	iv
SAMENVATTING.....	v
1 INTRODUCTION.....	1
1.1 ANTIBIOTIC RESISTANCE AND ECONOMICAL CHALLENGES	1
1.2 OPEN SOURCE DRUG DISCOVERY OF ANTIBIOTICS	2
1.3 MULTITARGET INHIBITORS FOR MUR LIGASES	3
1.4 KNOWN INHIBITORS OF THE MUR LIGASES	6
1.5 FRAGMENT-BASED DRUG DISCOVERY OF MUR LIGASE INHIBITORS	8
2 OBJECTIVE.....	11
3 MATERIALS AND METHODS	12
3.1 GENERAL EXPERIMENTAL DETAILS	12
3.2 GENERAL SPECTROSCOPIC ANALYSIS	12
3.3 GENERAL EXPERIMENTAL PROCEDURES.....	13
4 RESULTS.....	23
4.1 SYNTHESIS OF BROMO SUBSTITUTED CORE (COMPOUND 3A AND 3B)	23
4.2 SYNTHESIS OF THE BORONIC ESTER SUBSTITUTED CORE (COMPOUND 5)	24
4.3 SYNTHESIS OF OSA_1054 – 1061 (ROUND 2) AND OSA_1062 – 1070 (ROUND 3)	24
4.4 X-RAY CRYSTALLOGRAPHY OF OSA_1054 – 1061	25
5 DISCUSSION.....	26
5.1 ELABORATION ROUND 1.....	26
5.1.1 SAR analysis	26
5.1.2 Analysis of the binding pocket.....	28
5.2 ELABORATION ROUND 2.....	29
5.3 ELABORATION ROUND 3.....	34
5.4 FUTURE PERSPECTIVES.....	38
5.5 RETROSPECTION ON OPEN SCIENCE.....	38
6 REFERENCES.....	40
ADDENDA.....	I
ADDENDUM 1 - NMR: SYNTHESIS OF BROMO SUBSTITUTED CORE (COMPOUND 3A AND 3B)	I
ADDENDUM 2 - NMR: SYNTHESIS OF THE BORONIC ESTER SUBSTITUTED CORE (COMPOUND 5)	III
ADDENDUM 3 - NMR: SYNTHESIS OF OSA_1054 – 1068.....	IV
ADDENDUM 4 - HRMS: SYNTHESIS OF OSA_1054 – 1065	XVIII

LIST OF ABBREVIATIONS

AMR: antimicrobial resistance

CC-BY: Creative Commons Attribution license

CLogP: partition coefficient

DCM: dichloromethane

DMSO: dimethyl sulfoxide

DMSO- d_6 : hexadeuterodimethyl sulfoxide

equiv.: equivalent

FBDD: fragment-based drug discovery

HTS: high-throughput screening

Hz: Hertz

IC₅₀: half maximal inhibitory concentration

K_d: dissociation rate constant

LCMS: liquid chromatography mass spectrometry

LRMS: low resolution mass spectrometry

mA2pm: *meso*-diaminopimelate

MeOD₄: tetradeuteromethanol

m.p.: melting point

MurC: UDP-*N*-acetylmuramate: L-Ala ligase

MurD: UDP-*N*-acetylmuramoyl-L-Ala: D-Glu ligase

MurE: UDP-*N*-acetylmuramoyl-L-Ala-D-Glu: *meso*-diaminopimelate (or L-Lys) ligase

MurF: UDP-*N*-acetylmuramoyl-L-Ala-D-Glu-meso-diaminopimelate (or L-Lys): D-Ala-D-Ala ligase

MW: molecular weight

NMR: nuclear magnetic resonance

OSA: Open Source Antibiotics

PG: peptidoglycan

ppm: parts per million

R&D: research and development

Ro3: Rule of Three

Ro5: Rule of Five

rt: room temperature

SAR: structure activity relationship

S_NAc: nucleophilic acyl substitution

SPR: surface plasmon resonance

TEA: triethylamine

TLC: thin layer chromatography

UDP-GlcNAc: uridine diphosphate *N*-acetylglucosamine

UDP-MurNAc: uridine diphosphate *N*-acetylmuramic acid

UMA: UDP-*N*-acetylmuramoyl-L-Ala

UMAG: UDP-*N*-acetylmuramoyl-L-Ala-D-Glu

UMPP: UDP-*N*-acetylmuramoyl pentapeptide

UMT: UDP-*N*-acetylmuramoyl: tripeptide

UNAM: UDP-*N*-acetylmuramoyl

SUMMARY

According to the World Health Organisation, antibiotic resistance is one of the biggest threats to global health. Action is required not only in terms of antibiotic stewardship but also in terms of the discovery and development of new antibiotics. Although there is a high need for new antibiotics, few pharmaceutical companies are investing in such research out of fear of not gaining profit. This has raised the question of whether an alternative model should be developed to incentivise antimicrobial research. One possible alternative is Open Source Drug Discovery, where all data and ideas are freely shared. This allows scientists of different expertise to cooperate without fear of breaching confidentiality, thereby accelerating the drug discovery process.

The Open Source Antibiotics consortium was founded based on these pillars. One of the two major projects that are part of this consortium is the Mur ligase project. The four Mur ligases (MurC, MurD, MurE and MurF) play an important role in the construction of the bacterial cell wall and this makes them essential for bacterial survival. In addition, the Mur ligases are highly conserved in various bacteria and absent in eukaryotes, making them an excellent target for drug discovery projects. The goal of the Open Source Antibiotics: Mur ligase project is to develop a small-molecule inhibitor of two or more Mur ligases whereby several complementary approaches are applied. These include attempts to improve existing inhibitors, develop *de novo* compounds, and fragment-based drug discovery approaches, usually supported by computational chemistry.

The specific aim of this thesis project was to develop fragment-based drug candidates targeting MurD, with the potential of dual inhibition against MurE. A commercially available fragment library was screened against MurD ligase which resulted in four fragment hits. The fragments made weak interactions with a potential allosteric pocket and needed to be optimised into lead compounds by fragment growing. Based on structural information obtained by X-ray crystallography and on the results of enzymatic inhibition assays from the first Elaboration Round, 22 new compounds were designed, synthesised, and characterised. Interestingly, six of the compounds from the first Elaboration Round appeared to inhibit both MurD and MurE, which was a promising starting point for the development of new antibiotics with dual-target activity.

SAMENVATTING

Volgens de Wereldgezondheidsorganisatie is antibioticaresistentie een van de grootste bedreigingen voor de wereldgezondheid. Er moet niet alleen actie worden ondernomen op het gebied van antibiotica-stewardship, maar ook op het gebied van de ontdekking en ontwikkeling van nieuwe antibiotica. Hoewel er een grote behoefte aan nieuwe antibiotica bestaat, investeren maar weinig farmaceutische bedrijven in dergelijk onderzoek uit vrees geen winst te maken. Dit heeft de vraag doen rijzen of er een alternatief model moet worden ontwikkeld om het antimicrobiële onderzoek te stimuleren. Eén mogelijk alternatief is Open Source ontdekking van geneesmiddelen, waarbij alle data en ideeën vrij worden gedeeld. Hierdoor kunnen wetenschappers met verschillende expertise samenwerken zonder te moeten vrezen voor schending van vertrouwelijkheid, waardoor het proces van geneesmiddelenontdekking wordt versneld.

Het Open Source Antibiotica consortium is opgericht op basis van deze pijlers. Eén van de twee grote projecten die deel uitmaken van dit consortium is het Mur ligase project. De vier Mur ligasen (MurC, MurD, MurE en MurF) spelen een belangrijke rol bij de opbouw van de bacteriële celwand en zijn daardoor essentieel voor het overleven van bacteriën. Bovendien zijn de Mur ligasen zeer geconserveerd in verschillende bacteriën en afwezig in eukaryoten, waardoor ze een uitstekend target vormen voor geneesmiddelen ontdekkingsprojecten. Het doel van het Open Source Antibiotica: Mur ligase project is het ontwikkelen van een small-molecule inhibitor van twee of meer Mur ligasen waarbij verschillende complementaire benaderingen worden toegepast. Deze omvatten pogingen om bestaande inhibitors te verbeteren, *de novo* verbindingen te ontwikkelen, en fragment-gebaseerde geneesmiddelen ontdekkingsstrategieën, meestal ondersteund door computationele chemie.

Het specifieke doel van dit thesisproject was het ontwikkelen van fragment-gebaseerde kandidaat-geneesmiddelen gericht tegen MurD, met de mogelijkheid tot duale inhibitie van MurE. Een commercieel verkrijgbare fragmentenbibliotheek werd gescreend tegen MurD ligase wat resulteerde in vier fragmenten hits. De fragmenten vertoonden zwakke interacties met een potentiële allosterische pocket en moesten worden geoptimaliseerd tot lead-verbindingen door middel van fragmentgroei. Gebaseerd op structurele informatie verkregen door X-ray kristallografie en op de resultaten van enzymatische inhibitie testen uit de eerste Elaboratieronde, werden 22 nieuwe verbindingen ontworpen, gesynthetiseerd en gekarakteriseerd. Interessant was dat zes van de verbindingen uit de eerste Elaboratieronde zowel MurD als MurE bleken te inhiberen, wat een veelbelovend vertrekpunt was voor de ontwikkeling van antibiotica met een duale target activiteit.

1 INTRODUCTION

1.1 ANTIBIOTIC RESISTANCE AND ECONOMICAL CHALLENGES

For several years, antimicrobial resistance (AMR) has been classified by the World Health Organisation as one of the top ten threats to human health.^(1,2) Antimicrobial drug-resistant diseases affect 700.000 lives globally each year, but this could rise to a horrendous ten million if no action is taken.⁽³⁾ In addition to effects on morbidity and mortality, AMR also causes increased financial stress on healthcare systems.⁽⁴⁾ More specifically, the annual economic cost in the USA associated with bacterial resistance is estimated at \$55 billion.⁽⁵⁾

Worldwide, there is significant dependence on antibiotics to meet our medical needs, however this is contrasted as their effectiveness continues to decline due to their misuse and overuse.⁽⁶⁾ The current situation, in which Covid-19 is still apparent, emphasises the need for effective antibiotics as patients with this viral infection are often prone to develop a secondary bacterial infection.⁽⁷⁾ To combat antibiotic resistance, the implementation of antibiotic stewardship and the development of new antibiotics are crucial to our efforts. However, it has been proven difficult to make these two strategies go hand in hand. Even more, the efforts to limit AMR counteract the development and marketing of new antibiotics by creating significant economical burdens.⁽⁴⁾ This is referred to as the antibiotic paradox, which implies that pharmaceutical companies cannot afford to create life-saving drugs.⁽⁷⁾

The period when the discovery and development of new antibiotics reached its peak is referred to as the golden era of antibiotics. However, this golden era has come to an end and has shifted into a post-antibiotic era. Despite the urgent need for new antibiotics, the post-antibiotic era is characterised by a drug discovery pipeline depleted of new antibacterial agents, especially those targeting multi-drug resistant Gram-negative strains.^(5,8) This is the result of an economical failure of the market for antibiotics rather than scientific failure. The antibiotic market is broken because it is not compatible with the traditional business model, in which drug revenue is linked to sales volume and price.⁽⁹⁾ Because of AMR, sales volume is limited through antibiotic stewardship and low, yet unsustainable, prices are imposed by governmental agencies with reference to cost-effectiveness.⁽¹⁰⁾ The effectiveness of antibiotics is at risk once they are on the market and extensively used, as antibiotic resistance then has the potential to develop and spread among the population worldwide. Thus, the limitations on sales volume and price drive pharmaceutical firms into overmarketing and overconsumption of antibiotics, which, in turn, facilitates and reinforces the spread of AMR.⁽⁵⁾

Both the limitations in marketability and the risk of reduced effectiveness of new antibiotics cause the antibiotics market to be financially unattractive. Thus, the unprofitability of antibiotics made the pharmaceutical industry averse to investing in new antibacterial classes.⁽⁵⁾ Consequently, private efforts in research and development (R&D) have shifted focus towards areas of medicine that are more profitable, such as oncology.⁽¹¹⁾

There is therefore an urgent need to revise the business model and investigate other ways of bringing antibiotics to the market in order to make their R&D financially attractive again without compromising the public health objective of responsible use.⁽⁹⁾

The most widespread response to the antibiotics market failure was an attempt to fix it by providing new incentives. ‘Push’ incentives, usually financed by public funding, have been adopted to a considerable extent to reduce the early-stage developmental costs. Complementary to push funding, there also is a need for appropriate financial rewarding after market approval of the new antibiotic. Such “pull” incentives, aimed at delinking profits from sales volume and price, have not yet been introduced globally because they are often considered too costly or politically unfeasible. As a harmonised, holistic approach with both push and pull mechanisms is required to fix the broken market for antibiotics, its implementation has proven problematic.⁽⁹⁾

1.2 OPEN SOURCE DRUG DISCOVERY OF ANTIBIOTICS

Another, though more radical approach to stimulate the development and commercialisation of antibiotics, is to abandon the traditional profit-driven market model. This opens the possibility to recognise antibiotics as a global public good which do not require an economical return.⁽¹¹⁾

Several initiatives have shown that antibiotic R&D would greatly benefit from a multi-sectorial collaboration which allows the risk to be distributed by the private and public partners while encouraging open sharing of information and resources. However, this framework was received reluctantly as it would still require public funding and delinked market forces.⁽¹¹⁾ Additionally, it forces the private sector to distance itself from the traditional patent-based business model where secrecy is vital to obtain market exclusivity and thus financial rewards.⁽⁵⁾

As there is no functioning market for antibiotics, this permits to exit the notion of secrecy and intellectual property protection and to adopt an open approach for antibiotic R&D. In this ‘Open Source’ approach, all data and ideas are shared openly, anyone at any level can participate, and no patents are applied for. Instead, ownership of chemical structures, the data associated and the website content in general can be

ensured with appropriate licensing. The most straightforward type of licence is the Creative Commons Attribution License (CC-BY), which is also used by Wikipedia, however, adjusted to the requirements of pharmaceutical products. The licence enables the distribution, modification and utilisation of data on the condition that adequate credit is given to its originator.⁽¹²⁾

In comparison with the traditional business model, there are several advantages to 'Open Source' drug discovery: 1) pre-clinical R&D becomes more efficient as cooperation between highly qualified people is stimulated. 2) the risk of unnecessary duplication is greatly reduced. 3) antibiotic R&D is considered a shared responsibility between the private and public sectors, while antibiotics are considered a public good.⁽¹¹⁾ With this in mind, the Open Source Antibiotics (OSA) consortium, within which the research for this thesis was conducted, was founded to enable and support the discovery and development of novel, low-cost medicines against bacterial infections.⁽¹³⁾

1.3 MULTITARGET INHIBITORS FOR MUR LIGASES

To date, the bacterial cell wall has proven to be a valuable source of antibacterial targets, with many successful antibiotics interfering with its structure. The crucial component of the bacterial cell wall in both Gram-positive and -negative bacteria is peptidoglycan (PG). PG is a glycopeptide polymer which consists of a chain of alternating UDP-*N*-acetylglucosamine (UDP-GlcNAc) and UDP-*N*-acetylmuramic acid (UDP-MurNAc) units, the latter being linked to a chain of five peptides, also known as the pentapeptide (Figure 1.1). Although having a similar composition, Gram-positive bacteria show a PG layer that is more voluminous and contains more cross-linking of pentapeptides.⁽¹⁴⁾

PG is essential in maintaining cell flexibility and integrity, allowing the bacterial cell to grow and divide whilst withstanding turgor. Thus, interference with PG biosynthesis is a highly effective anti-bacterial mechanism exploited by many clinically relevant antibiotics such as beta-lactams, glycopeptides, fosfomycin and cycloserine. They target various steps of the biosynthetic pathway, however, none of them interrupt the growth of the pentapeptide chain, which is realised by ligation of the individual peptides to the UDP-GlcNAc PG precursor. This series of peptide bond formations is catalysed by the amide ligases MurC, D, E and F (Figure 1.1).⁽¹⁴⁾

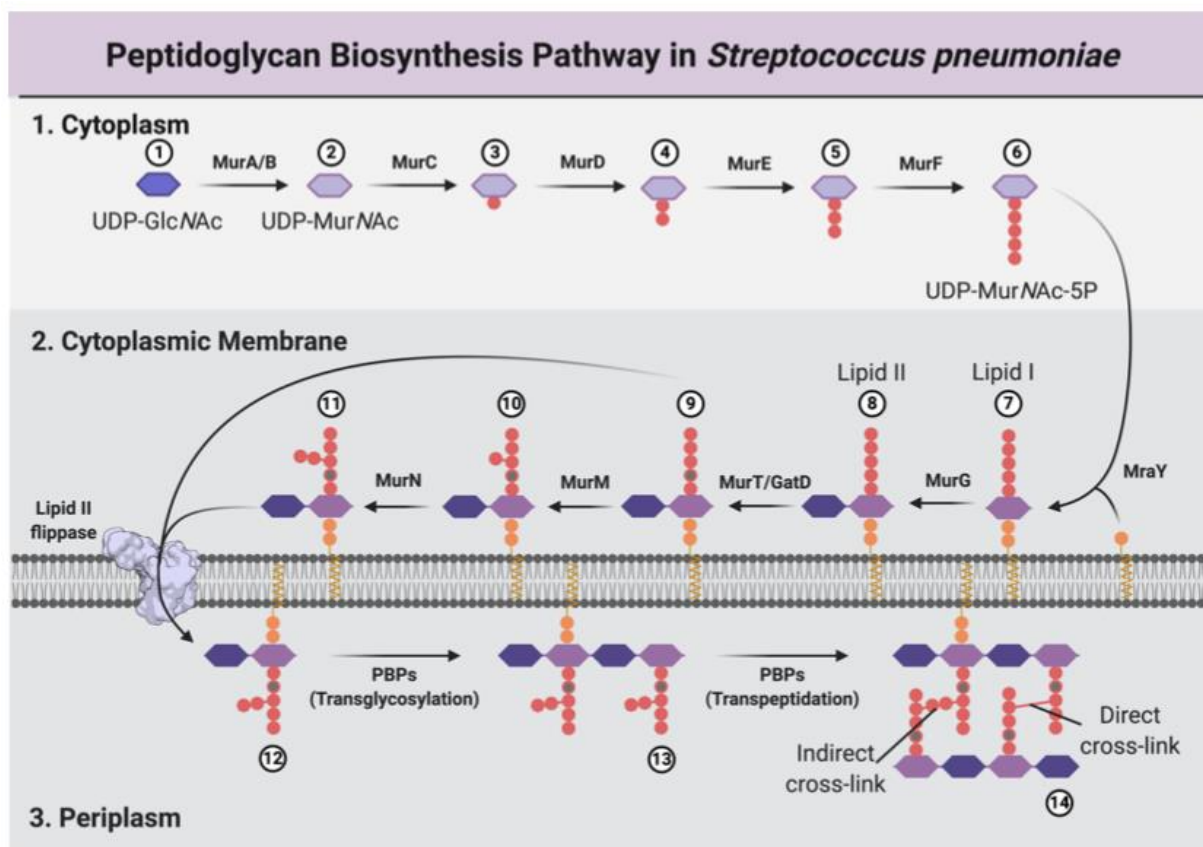


Figure 1.1: "Diagram illustrating stages of the PG biosynthesis pathway". (Figure copied from York A, et al. is licensed under [CC-BY-NC-ND 4.0](#).⁽¹⁵⁾)

The four Mur ligases essential for bacterial survival are conserved amongst the most important bacteria, and are absent in eukaryotic cells, making them an excellent antibacterial target. Moreover, they share a common catalytic mechanism, have well-preserved regions of amino acid sequences, and are structurally similar. This can be exploited to design antibacterial agents targeting multiple enzymes at once. For antibiotics, this is particularly beneficial since the multi-target approach reduces the chances of resistance development as resistance inducing mutations would need to be present in multiple target genes during the same generation.⁽¹⁴⁾

Following a common catalytic mechanism, the ATP-dependent Mur ligases sequentially add L-Ala (MurC), D-Glu (MurD), L-Lys or *meso*-diaminopimelate (mA2pm) (MurE, in Gram-positive and Gram-negative bacteria respectively), and dipeptide D-Ala-D-Ala (MurF) to the UDP-*N*-acetylmuramoyl (UNAM) precursor, yielding the UDP-*N*-acetylmuramoyl pentapeptide (UMPP) in Figure 1.2.⁽¹⁶⁾

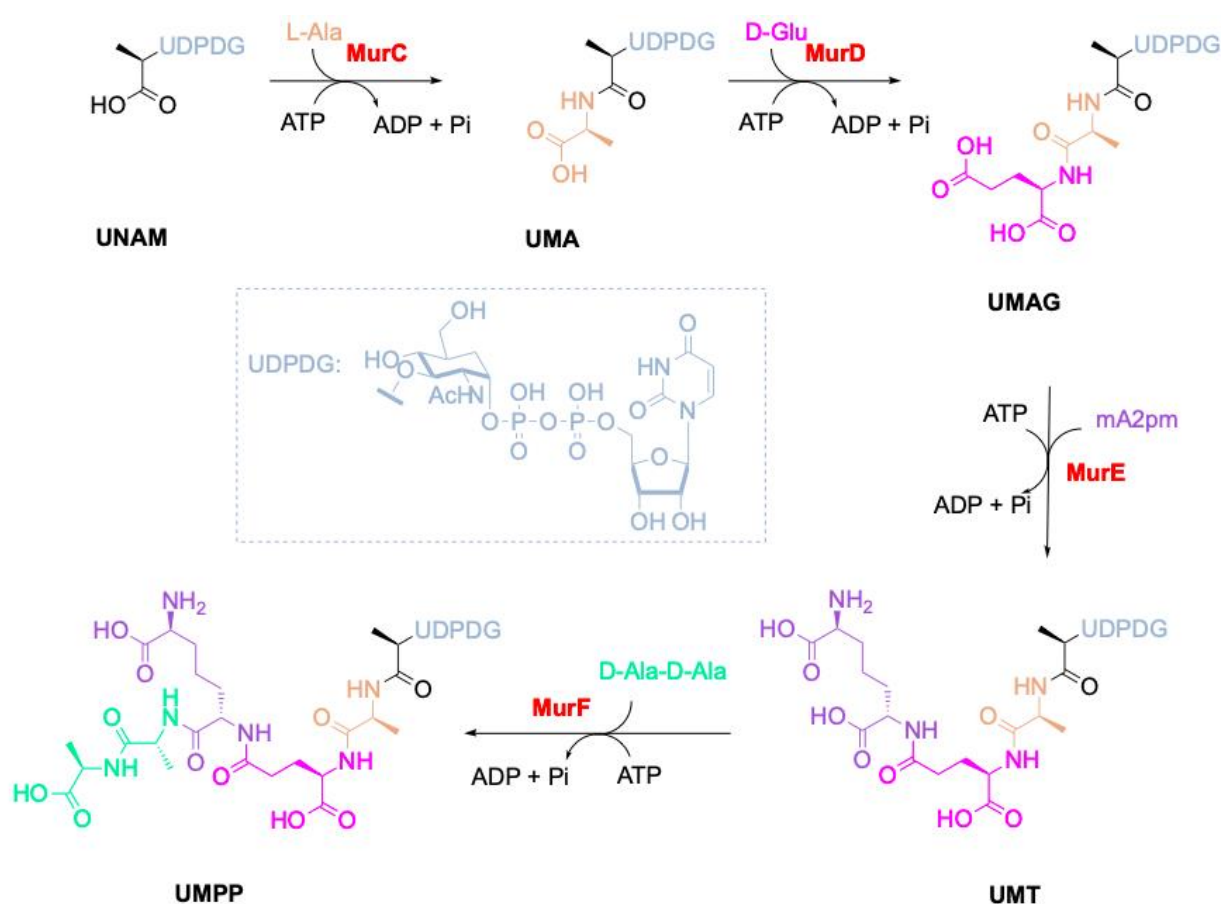


Figure 1.2: MurC – F cascade. Step 1: MurC or UDP-N-acetylmuramoyl: L-Ala ligase adds L-Ala to UDP-N-acetylmuramoyl (**UNAM**) and generates UDP-N-acetylmuramoyl-L-Ala (**UMA**). Step 2: MurD or UDP-N-acetylmuramoyl-L-Ala: D-Glu ligase adds D-Glu to **UMA** and generates UDP-N-acetylmuramoyl-L-Ala-D-Glu (**UMAG**). Step 3: MurE or UDP-N-acetylmuramoyl-L-Ala-D-Glu: meso-diaminopimelate (or L-Lys) ligase adds meso-diaminopimelate (mA2pm) (or L-Lys) to **UMAG** and forms UDP-N-acetylmuramoyl-L-Ala-D-Glu-mA2pm (or L-Lys), also known as UDP-N-acetylmuramoyl: tripeptide (**UMT**). Step 4: MurF or UDP-N-acetylmuramoyl-L-Ala-D-Glu-meso-diaminopimelate(or L-Lys): D-Ala-D-Ala ligase adds the dipeptide D-Ala-D-Ala to **UMT** and ultimately generates UDP-N-acetylmuramoyl-L-Ala-D-Glu-mA2pm/L-Lys-D-Ala-D-Ala, also known as UDP-N-acetylmuramoyl: pentapeptide (**UMPP**).⁽¹⁴⁾

In each reaction, the incorporation of the amino acid into the UDP precursor occurs according to a stepwise mechanism based on the topology and dynamics of the three domains common to all Mur ligases (Figure 1.3). First, ATP is bound to the central domain of the Mur enzyme in its free state. Then, the UDP precursor binds to the N-terminal domain and is phosphorylated by ATP, resulting in an acyl phosphate intermediate along with ADP. Next, the C-terminal domain binds the condensing amino acid that attacks the acyl phosphate intermediate, creating a tetrahedral intermediate. The high-energy intermediate dissociates, which involves the release of inorganic phosphate and simultaneous generation of the resulting peptide bond (Figure 1.4).⁽¹⁶⁾ Important to note is that the Mur enzymes are subject to significant conformational changes while they give rise to a potent active site. Upon binding of the ATP substrate, the C-terminal domain moves to form a closed conformation which accommodates binding of the two other substrates.⁽¹⁴⁾

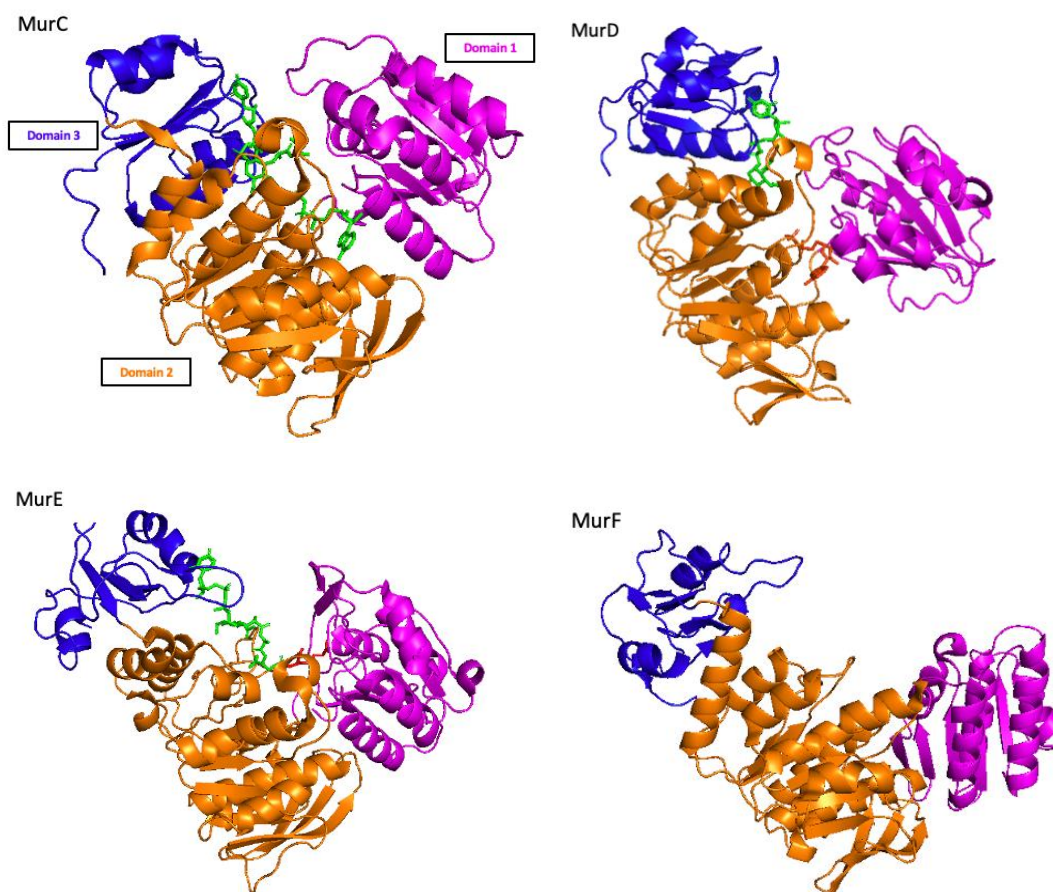


Figure 1.3: Tri-dimensional representation of the four Mur ligases: MurC (PDB: 1P3D), MurD (PDB: 2UAG), MurE (PDB: 1E8C), and MurF (PDB: 1GG4). The C-terminal domain is shown in magenta (domain 1), the central domain in orange (domain 2), and the N-terminal domain in blue (domain 3). The image was generated with PyMOL, Schrödinger, Version 4.2.4.

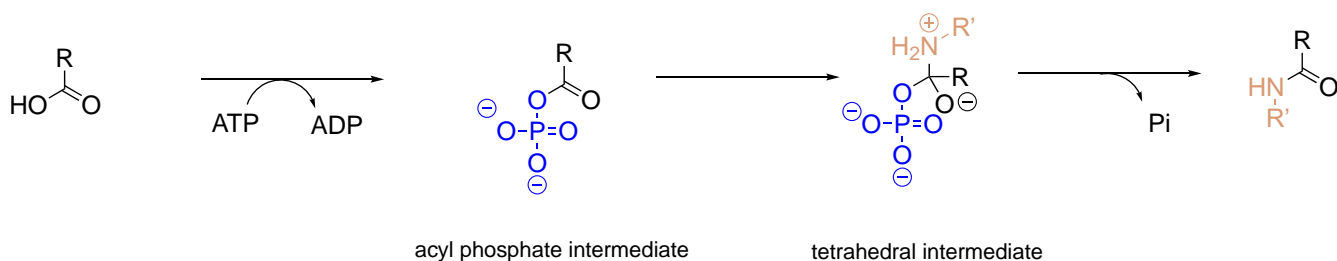


Figure 1.4: Catalytic mechanism of the ATP-dependent Mur ligases.

1.4 KNOWN INHIBITORS OF THE MUR LIGASES

A frequently used method for the development of antibiotics against newly identified bacterial targets relies exclusively on libraries of synthetic compounds.⁽¹⁷⁾ In this regard, several high-throughput screenings (HTS) have been carried out by, for example, GlaxoSmithKline (GSK) and AstraZeneca, but without any success. AstraZeneca's 65 HTS programmes produced some leads, but none succeeded in killing multi-drug resistant Gram-negative bacteria.⁽⁸⁾ This was not due to insufficient hit or lead identification, but rather due to the challenging process of extending the activity against the isolated target to general antibacterial activity.⁽¹⁸⁾

Lack of activity against wild-type bacteria indeed occurred in a pyrazolopyrimidine (Figure 1.5 – a) hit series derived from an AstraZeneca HTS targeting *Escherichia coli* and *Pseudomonas aeruginosa* MurC. However, the elaborated lead series showed promising antibacterial potency against efflux-deficient strains. This suggests that an efflux problem is at the root of the poor performance in wild-type cells, possibly in combination with poor permeability often seen in Gram-negative bacteria. Multidrug efflux pumps indeed appear to be a key mechanism in antibacterial resistance, leading to suboptimal intracellular compound concentrations.^(19,20)

A more rational drug design of inhibitors of the Mur ligases involved attempts to mimic substrates, products, and tetrahedral intermediates.⁽¹⁶⁾ Since the tetrahedral structures have both product-like features for one Mur ligase and substrate-like features for the subsequent Mur ligase, this is promising for the development of dual-target inhibitors. Various phosphinate and *N*-sulfonyl derivatives (Figure 1.5 – b) based on the tetrahedral intermediate of MurD, which contains a glutamic acid group, have been reported as inhibitors.⁽²¹⁾

A successful attempt at the initial development of multitarget antibacterial agents, based on the tetrahedral intermediate of MurD, involved a series of hydroxy-substituted 5-benzylethazolidine-4-ones (Figure 1.5 – c). The most potent inhibitor had IC₅₀ values for MurD-F in the micromolar range, which makes it a promising lead compound for further investigation of multitarget inhibitory properties.⁽¹⁶⁾

Another structure-based drug design approach using the MurD tetrahedral intermediate as a starting point combined molecular docking calculations and 3D structure-based pharmacophores. The hit compounds that emerged from the virtual screening were assayed against MurD and MurE. This led to the discovery of benzene 1,3-dicarboxylic acid derivatives (Figure 1.5 – d and e) as a novel class of inhibitors of both Mur ligases.⁽²¹⁾ To extend the activity of these novel inhibitors to all four Mur ligases, further optimisation was carried out. In turn, this led to the discovery of two classes of compound: benzene 1,3-dicarboxylic acid 2,5-dimethylpyrrole derivatives (Figure 1.5 – f) and furan-based benzene mono- and dicarboxylic acid derivatives (Figure 1.5 – g). These compounds act in a competitive way towards the ATP and D-Glu substrate of MurD respectively and both inhibit the whole MurC-F cascade in the micromolar range. As in the case of HTS, further studies are needed to optimise the physical-chemical properties to achieve efficient bacterial cell penetration.^(22,23)

The active site of MurD enzymes is largely (but not entirely) conserved amongst different important bacterial pathogens. Some examples of virulent bacteria, some of which are multi-drug resistant, include *Escherichia coli*, *Mycobacterium tuberculosis*, *Staphylococcus aureus*, *Borrelia burgdorferi* and *Streptococcus pneumoniae*. Most glutamic acid-based inhibitors that were developed to target MurD of

Escherichia coli specifically inhibit this orthologue, while having weaker activity against MurD orthologues of the other mentioned bacteria. Most likely, this is caused by differences in topologies as well as amino acid sequences between the MurD active site of the different bacterial pathogens. Consequently, some MurD inhibitors are incapable of generating a broad-spectrum effect. However, this does not imply that conversion of inhibitors based on one particular orthologue into broad-spectrum antibiotics is not possible. Only, to achieve this the structural properties of other MurD orthologues must also be taken into account.⁽²⁴⁾

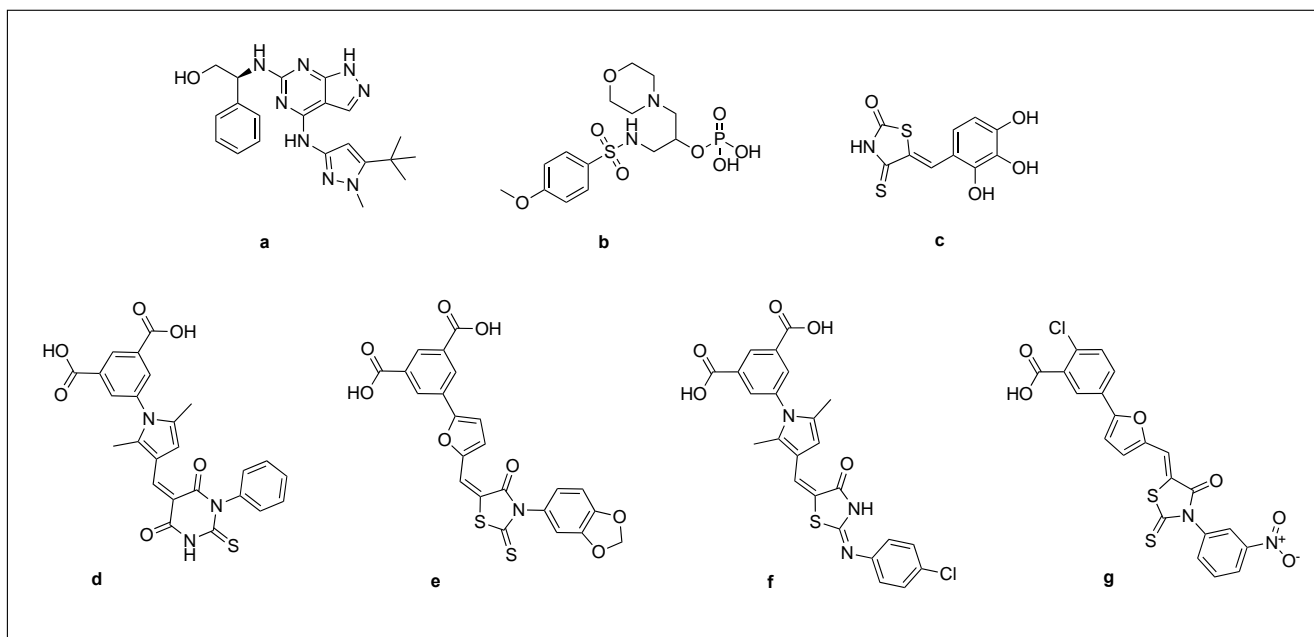


Figure 1.5: Overview of known inhibitors of the Mur ligases. (a) pyrazolopyrimidine derivative, (b) phosphinate and N-sulfonyl derivative of the tetrahedral intermediate, (c) hydroxy-substituted 5-benzylethazolidine-4-one, (d) and (e) benzene 1,3-dicarboxylic acid derivatives, (f) 1,3-dicarboxylic acid 2,5-dimethylpyrrole derivative, and (g) furan-based benzene mono- and dicarboxylic acid derivative.

1.5 FRAGMENT-BASED DRUG DISCOVERY OF MUR LIGASE INHIBITORS

The Mur ligases, which are promising targets for antibacterial drug design, function as the foundation of the Open Source Antibiotics: Mur ligase project. The project aims to develop small molecules that inhibit at least two of the Mur ligases at the same time. To achieve this, several complementary approaches are applied and are usually supported by computational chemistry. These include attempts to improve existing inhibitors so that they meet the criteria of Gram-negative cell penetration and accumulation, to develop *de novo* compounds, and fragment-based drug discovery (FBDD) approaches, which is the objective of this thesis.

To date, FBDD is receiving increasing interest, particularly from academia. Fragments are very small molecules of low molecular weight that are intended to bind a pre-specified target. The binding of the fragments occurs through weak interactions (μM – mM range) with so-called ‘sweet spots’ in the target protein and can be

detected through biophysical or biochemical methods. These "sweet spots" may be areas that can only be accessed using fragments given their small size, which would otherwise be difficult to target, such as allosteric pockets. In addition, because of their low degree of complexity, fragment hits are considered an ideal starting point for Hit-to-Lead optimisation campaigns.⁽²⁵⁾

The purpose of FBDD is to identify weakly binding fragments and grow them into drug-sized inhibitors.⁽²⁶⁾ It involves two key steps, fragment screening and fragment optimisation.⁽²⁷⁾ In the screening step, a commercially available library of 860 fragments was screened against apo MurD from *Streptococcus agalactiae* using X-ray crystallography, optimised for the detection of weak affinities.^(28,29) This resulted in four fragment hits, shown in Figure 1.6.⁽³⁰⁾ Subsequently, these hits were evaluated for their biological activity against purified MurD at a concentration of 1mM to investigate the functional significance of the binding.

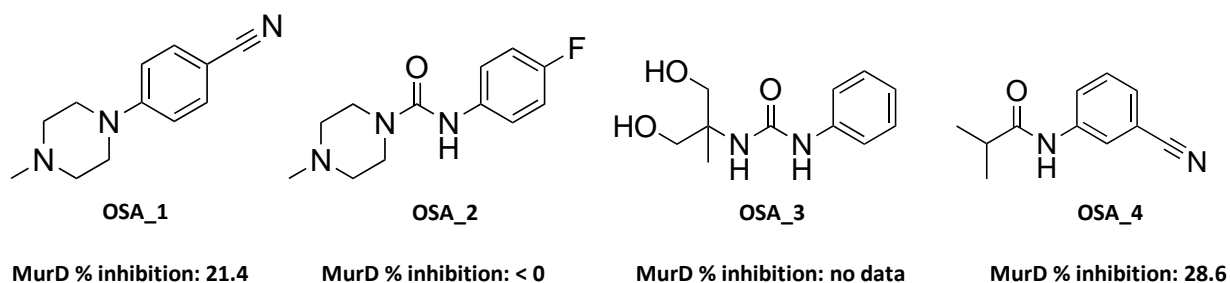


Figure 1.6: Four fragment hits identified from the screening of commercially available fragment library.

Important to note is that, in contrast to known inhibitors, these fragment hits occupy a potential allosteric pocket that is remote from the precursor binding site, and adjacent to the ADP binding site.⁽³⁰⁾

After fragment screening and hit identification, the fragments needed to be optimised by carrying out various rounds of elaboration. The initially screened fragment library was specifically designed to easily allow for follow-up synthesis of various analogues.^(28,29) In the first Elaboration Round, specific small changes were introduced for each of the fragment hits, after which they were tested against MurD. This provided data for the structure-activity relationship (SAR) analysis. In Figure 1.7, the MurD % inhibition of the 73 compounds after fragment elaboration is represented in a histogram with the most active fragments located above the red cut-off line.⁽³¹⁾

There were 11 structures out of the total of 73 compounds from Elaboration Round 1 with inhibitory activity greater than 80%. From these 11 compounds, the ones that also passed the assay interference checks were evaluated against MurE as a further exploration of potential dual-target capability. Encouragingly, as can be seen in Figure 1.8, most compounds that had good activity against MurD had good

activity against MurE as well. Therefore, they will be referred to as dual inhibitors throughout this thesis. However, it must be borne in mind that the inhibition assays were carried out at a high concentration (1 mM) so it is necessary to perform and investigate dose-response curves in the future.⁽³¹⁾

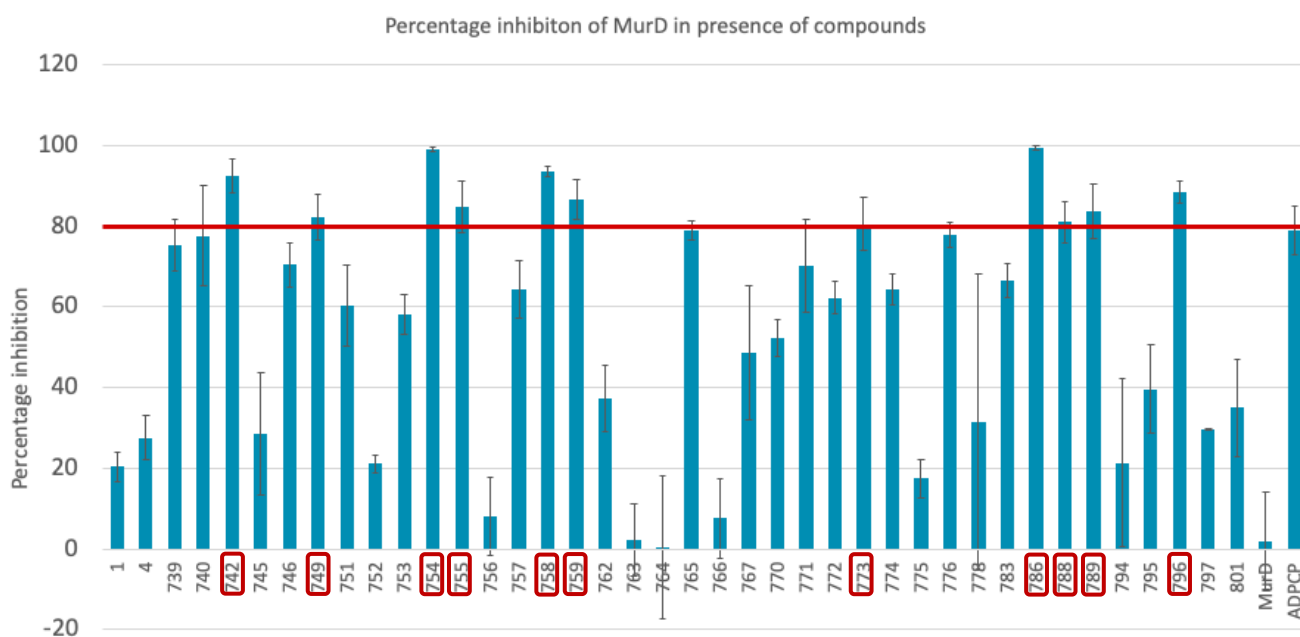


Figure 1.7: Diagram representing the MurD % inhibition of the elaborated compounds from Elaboration Round 1. 38 compounds are not included as their MurD % inhibition fell outside the range of the graph either due to precipitation or assay interference. (Figure adapted from <https://github.com/opensourceantibiotics/murliqase/wiki/MurD-Round-1>.⁽³¹⁾)

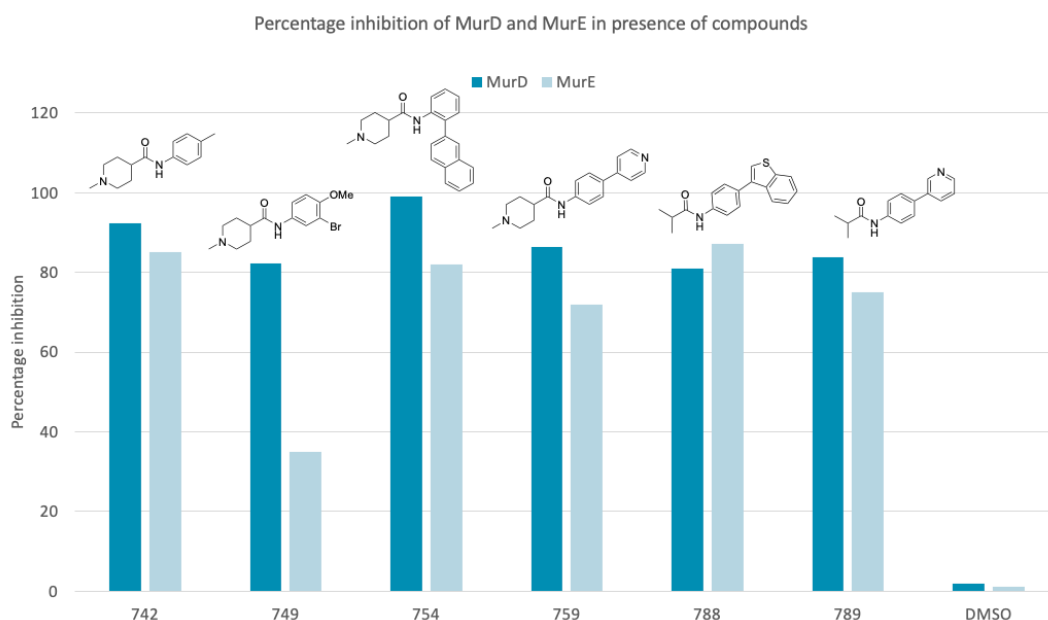


Figure 1.8: **The Dual Inhibitors.** Diagram representing the MurD and MurE % inhibition of the 6 compounds with the best initial MurD inhibition activity. (Figure adapted from <https://github.com/opensourceantibiotics/murliqase/wiki/Dual-Inhibitors>.⁽³²⁾)

Based on the previously obtained data within our research group, further rounds of elaboration can be carried out to further explore the properties of the allosteric pocket, so that the affinity of the initially weakly binding fragment hits can be increased.

2 OBJECTIVE

AMR is on the rise, and it is expected that this trend will continue if no action is taken. The need for the development of new antibiotics has never been more urgent. Various approaches are being investigated, including the inhibition of Mur ligases, which was discussed in detail in the previous chapter.

The scope of this 'Mur ligase: Fragment Hit-to-Lead' project is to carry out further elaboration of compounds which were identified as dual inhibitors of MurD and MurE in a semi-rational way. The foundation of the project is provided by previous FBDD research performed by Dr. Dana Klug, Dr. Fahima Idiris, and other collaborators of the OSA Mur ligase project. Ultimately, the original fragment hits are intended to be transformed into lead compounds with greater affinity and potency for the target.

Further exploration of the potential allosteric binding pocket is essential in this next stage. This can be achieved by creating analogues of the previously identified dual inhibitors.

With regards to the chemistry, I will design, synthesise, and characterise analogues at the UCL – School of Pharmacy based on existing data in the project. Semi-rational design concerns analysing target % inhibition data of previously synthesised compounds and assessing the features of the allosteric pocket where the original fragment hits bind. Synthesis of the analogues is expected to be straightforward as the SAR to be investigated requires reactions that are frequently used by Dr. Klug, for instance amide coupling, reductive amination, Suzuki-Miyaura coupling, and aromatic nucleophilic substitution.⁽²⁸⁾ For characterisation of the synthesised analogues, I will prepare and analyse samples using melting point determination, LCMS, and proton and carbon NMR. Characterisation with HRMS will be carried out by Mr. Emmanuel Samuel.

As for biology, I will attempt to elucidate the structure of the compounds bound to MurD and MurE at the University of Oxford. This biophysical assay, also referred to as X-ray crystallography, will be carried out remotely at the Diamond Light Source facility. Preparation of the crystals for screening will be my responsibility, while data interpretation will be performed by our collaborators there.

Figure 2.1 shows an overview of the course of the FBDD Hit-to-Lead approach for the OSA Mur ligase project to date in blue, and the goal of this thesis project in grey.

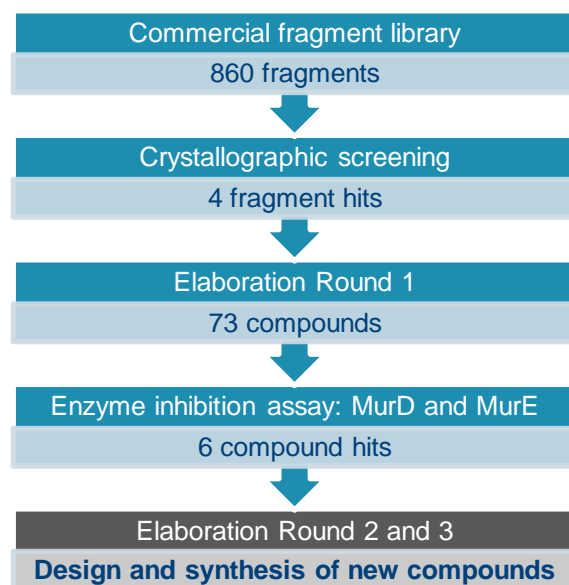


Figure 2.1: Overview of fragment Hit-to-Lead approach of the OSA Mur ligase project.

3 MATERIALS AND METHODS

3.1 GENERAL EXPERIMENTAL DETAILS

Reagents and solvents were purchased from commercial suppliers Sigma Aldrich, Fisher Scientific, Merck and Fluorochem. Unless specified in experimental protocols, reagents were analytical grade and used as provided without further purification. Anhydrous dioxane was stored over 4 Å molecular sieves. Analytical thin layer chromatography (TLC) was performed on precoated TLC Silica gel 60 F254, 20 × 20 cm aluminium sheets (Merck) and visualisation was done under UV light (254 nm). Compound purification was performed on Biotage Selekt flash chromatography system. Normal phase purification was performed on Biotage Sfär Silica 60 µm 5 g/10 g/25 g/50 g columns. Reactions were carried out in oven-dried (40 °C) glassware with stirring at room temperature (rt), unless indicated otherwise. Reactions with air sensitive reagents were conducted under argon atmosphere. All reported yields refer to chromatographically and spectroscopically pure products, unless indicated otherwise.

3.2 GENERAL SPECTROSCOPIC ANALYSIS

Structural product characterisation was performed on the following analytical instrumentation:

¹H and ¹³C Nuclear Magnetic Resonance (NMR) spectra were taken on Bruker UltraShield Avance 400/500 instruments at 400, 500 MHz (¹H) and 126 MHz (¹³C). Chemical shifts were measured in parts per million (ppm) and expressed as δ values. Tetradeuteromethanol (MeOD₄) and hexadeuterodimethyl sulfoxide (DMSO-d₆) were used as sample solvents and the residual solvent peaks (MeOD₄ ¹H, δ = 3.31 ppm and ¹³C, δ = 49.00 ppm; DMSO-d₆ ¹H, δ = 2.50 ppm and ¹³C, δ = 39.52 ppm) served as a reference. ¹H peak splitting patterns have the following assigned definitions: s (singlet), d (doublet), t (triplet), q (quartet), m (multiplet), ds (doublet of singlets), dd (doublet of doublets) and dt (doublet of triplets). Coupling constants are reported in Hertz (Hz).

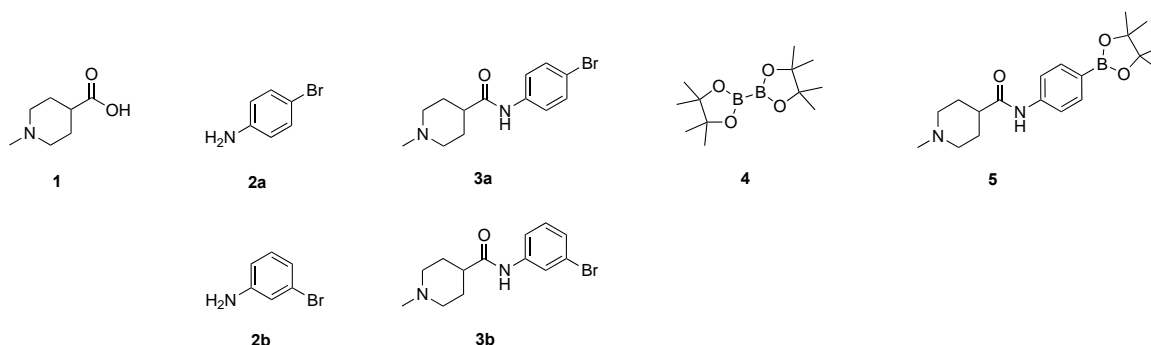
Liquid Chromatography Mass Spectrometry (LCMS) data were acquired on Agilent 1260 Infinity II system and were used for Low Resolution Mass Spectrometry (LRMS) analysis.

High Resolution Mass Spectrometry (HRMS) analysis was performed on Waters Q-ToF Premier Tandem Mass Spectrometer with papaverine [M+H]⁺ = 340.1549 or reserpine [M+H]⁺ = 609.2812 alkaloid used as an internal standard.

Melting points (m.p.) were obtained on Stuart SMP10 Melting Point Apparatus using glass capillary tubes (ø = 1.8-1.9 mm, 100 mm).

The NMR spectra of all synthesised compounds and the mass spectra (high resolution) of the final **OSA** compounds can be found in the addenda.

3.3 GENERAL EXPERIMENTAL PROCEDURES



Synthetic Procedure A: Amide coupling

In a 100 mL round-bottom flask, 1-methylpiperidine-4-carboxylic acid (**1**) (1.0 equiv.) was dissolved in thionyl chloride (15.0 equiv.) and the reaction was heated at reflux at 75 °C for 4 h. The reaction mixture was concentrated by removing solvents under reduced pressure and the resulting white solid was azeotroped with toluene. In a separate flask, compound **2** (1.0 equiv.) was dissolved in DCM (0.21 M, 1.0 equiv.). TEA (2.1 equiv.) was added, and the reaction mixture was cooled to 0 °C. The acid chloride was added to the reaction mixture portionwise, and the reaction was stirred overnight and allowed to warm to room temperature. Reaction completion was monitored by LCMS. The slightly cloudy reaction mixture was filtered into a round-bottom flask and concentrated under reduced pressure to remove excess TEA. The crude material was purified by flash chromatography (DCM: 5% NH₄OH in MeOH 98:2 → 80:20, step gradient).

Synthetic Procedure B: Suzuki reaction

In a 20 mL reaction vial, compound **3** (1.0 equiv.), the boronic acid or boronic acid pinacol ester (1.2 equiv.), K₂CO₃ (3.0 equiv.), and PdCl₂(dppf)·CH₂Cl₂ (0.1 equiv.) were combined and closed off with a septum cap. The vial was filled with argon and put under vacuum, and this was repeated three times. An amount of 3:1 dioxane:water (to obtain 0.10 M per 1.0 equiv.) was added and argon was bubbled through the reaction mixture to degas. The reaction was heated at 100 °C and stirred overnight. Reaction completion was monitored by LCMS. The reaction mixture was diluted with ethyl acetate and filtered through celite. The solvents were removed under reduced pressure and the crude was purified by flash chromatography (DCM: 5% NH₄OH in MeOH 95:5 → 80:20, step gradient).

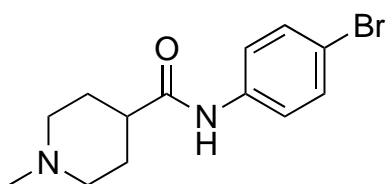
Synthetic Procedure C: Miyaura borylation - microwave

In a 20 mL microwave vial, compound **3** (1.0 equiv.), bis(pinacolato)diboron (**4**) (1.49 equiv.), KOAc (3.0 equiv.) and PdCl₂(dppf)·CH₂Cl₂ (0.05 equiv.) were combined and closed off with a septum cap. The vial was filled with argon and put under vacuum, and this was repeated three times. Dry, degassed dioxane (0.15 M, 1.0 equiv.) was added and the reaction was run in the microwave at 145 °C for 1 h. Reaction completion was monitored by LCMS. The reaction mixture was cooled to room temperature, diluted with ethyl acetate and filtered through celite. The solvents were removed under reduced pressure and the crude was purified by flash chromatography (DCM: MeOH 98:2 → 75:25, step gradient).

Synthetic procedure D: Suzuki reaction – microwave

In a 10 mL microwave vial, compound **5** (1.2 equiv.), aryl bromide (1.0 equiv.) K_2CO_3 (3.0 equiv.), and $PdCl_2(dppf) \cdot CH_2Cl_2$ (0.1 equiv.) were combined and closed off with a septum cap. The vial was filled with argon and put under vacuum, and this was repeated three times. An amount of 3:1 dioxane:water (to obtain 0.05 M per 1.0 equiv.) was added and argon was bubbled through the reaction mixture to degas. The reaction was run in the microwave at 120 °C for 30 min. Reaction completion was monitored by LCMS. The reaction mixture was cooled to room temperature, diluted with ethyl acetate and filtered through celite. The solvents were removed under reduced pressure and the crude was purified by flash chromatography (DCM: 5% NH_4OH in MeOH 95:5 → 80:20, step gradient).

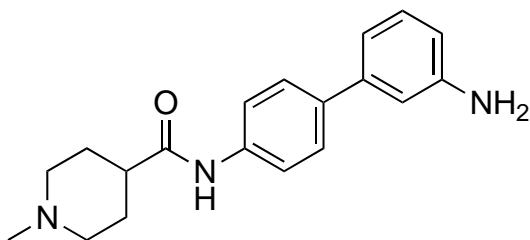
N-(4-Bromophenyl)-1-methylpiperidine-4-carboxamide (**3a**)



Compound **3a** was synthesised following synthetic procedure A, using 1-methylpiperidine-4-carboxylic acid (**1**) (500 mg, 3.49 mmol), thionyl chloride (3.80 mL, 52.4 mmol), 4-bromoaniline (**2a**) (601 mg, 3.49 mmol), DCM (16.60 mL, 3.49 mmol) and TEA (1.00 mL, 7.16 mmol) to give the crude

product which was purified by flash silica gel chromatography. The reaction was carried out twice on a 500 mg scale and once on a 1000 mg scale, affording respectively 700 mg, 561 mg and 1089 mg of compound **3a**. The title compound was obtained as a white solid with TEA impurities and was used in subsequent reactions that follow synthetic procedure B. 1H NMR (500 MHz, $MeOD_4$) δ ppm 7.55 – 7.48 (m, 2H), 7.48 – 7.41 (m, 2H), 3.14 – 3.09 (m, 2H), 2.52 – 2.31 (m, 6H), 1.99 – 1.83 (m, 4H) (*addendum 1* – Figure 1). ^{13}C NMR (126 MHz, $MeOD_4$) δ ppm 175.5, 139.3, 132.8, 122.8, 117.4, 55.5, 47.8, 43.2, 28.9 (*addendum 1* – Figure 2). LRMS m/z (ESI+) 296.8 ($[M+H]^+$, ^{79}Br) 298.8 ($[M+H]^+$, ^{81}Br). The data obtained corresponded to those from previous experimental work by Dr. Klug (Dana Klug, unpublished work, 2021).

N-(3'-Amino-[1,1'-biphenyl]-4-yl)-1-methylpiperidine-4-carboxamide (**OSA_1054**)

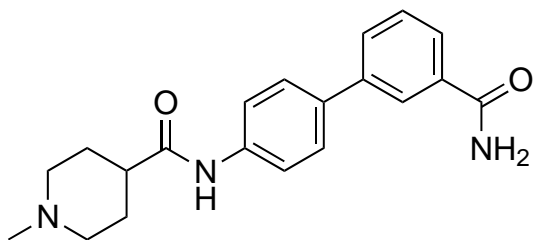


Compound **OSA_1054** was synthesised following synthetic procedure B, using compound **3a** (150 mg, 0.50 mmol), (3-aminophenyl)boronic acid (83 mg, 0.61 mmol), K_2CO_3 (209 mg, 1.51 mmol), $PdCl_2(dppf) \cdot CH_2Cl_2$ (41 mg, 0.05 mmol) and dioxane:water (5.05 mL, 0.50 mmol) to give the crude product

which was purified by flash silica gel chromatography. The purified product was vacuum filtered with hexane to remove grease. The title compound was obtained as a brown solid (46 mg, 29% yield). **m.p.** 175 – 177 °C (no lit m.p.). 1H NMR (400 MHz, $MeOD_4$) δ ppm 7.59 (d, J = 8.5 Hz, 2H), 7.52 (d, J = 8.0 Hz, 2H), 7.14 (t, J = 7.9 Hz, 1H), 6.96 (d, J = 2.2 Hz, 1H), 6.91 (d, J = 7.7 Hz, 1H), 6.68 (d, J = 7.9 Hz, 1H), 2.97 (d, J = 11.5 Hz, 2H), 2.38 (q, J = 7.6 Hz, 1H), 2.30 (s, 3H), 2.12 (t, J = 13.3 Hz, 2H), 1.90 (dd, J = 8.0, 3.3 Hz, 4H) (*addendum 3* – Figure 6). ^{13}C NMR (126 MHz, $DMSO-d_6$) δ ppm 173.8, 149.3, 140.6, 138.7, 135.8, 129.5, 126.8, 119.5, 114.1, 112.9, 111.9, 54.9, 46.3,

42.5, 28.6 (*addendum 3* – Figure 7). **LRMS** m/z (ESI+) 309.9 ([M+H]⁺) 155.5 (M+2H)²⁺. **HRMS** (ESI+): calcd. for C₁₉H₂₄N₃O [M+H]⁺: 310.1919; found: 310.1928 (*addendum 4* – figure 33).

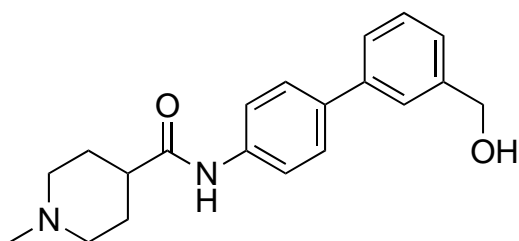
***N*-(3'-Carbamoyl-[1,1'-biphenyl]-4-yl)-1-methylpiperidine-4-carboxamide (OSA 1055)**



Compound **OSA_1055** was synthesised following synthetic procedure B, using compound **3a** (150 mg, 0.50 mmol), (3-carbamoylphenyl)boronic acid (100 mg, 0.61 mmol), K₂CO₃ (209 mg, 1.51 mmol), PdCl₂(dppf)·CH₂Cl₂ (41 mg, 0.05 mmol) and dioxane:water (5.05 mL, 0.50 mmol) to give the crude

product which was purified by flash silica gel chromatography. The title compound was obtained as a brown solid (43 mg, 26% yield). **m.p.** 222 – 225 °C (no lit m.p.). **¹H NMR** (400 MHz, MeOD₄) δ ppm 8.13 (d, J = 1.9 Hz, 1H), 7.87 – 7.77 (m, 2H), 7.70 (d, J = 8.7 Hz, 2H), 7.66 (d, J = 8.8 Hz, 2H), 7.53 (t, J = 7.8 Hz, 1H), 3.57 (d, J = 12.3 Hz, 2H), 3.12 (s, 2H), 2.89 (s, 3H), 2.74 (d, J = 11.1 Hz, 1H), 2.22 – 1.99 (m, 4H) (*addendum 3* – Figure 8). **¹³C NMR** (126 MHz, DMSO-*d*₆) δ ppm 172.1, 167.8, 139.6, 139.0, 134.9, 134.2, 128.9, 128.7, 127.1, 126.2, 125.2, 119.6, 52.4, 42.6, 29.1, 25.8 (*addendum 3* – Figure 9). **LRMS** m/z (ESI+) 337.8 ([M+H]⁺). **HRMS** (ESI+): calcd. for C₂₀H₂₄N₃O₂ [M+H]⁺: 338.1869; found: 338.1868 (*addendum 4* – figure 34).

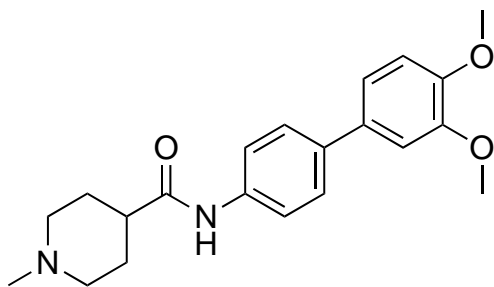
***N*-(3'-(Hydroxymethyl)-[1,1'-biphenyl]-4-yl)-1-methylpiperidine-4-carboxamide (OSA 1056)**



Compound **OSA_1056** was synthesised following synthetic procedure B, using compound **3a** (150 mg, 0.50 mmol), (3-(hydroxymethyl)phenyl)boronic acid (92 mg, 0.61 mmol), K₂CO₃ (209 mg, 1.51 mmol), PdCl₂(dppf)·CH₂Cl₂ (41 mg, 0.05 mmol) and dioxane:water (5.05 mL, 0.50 mmol) to give the crude product

which was purified by flash silica gel chromatography. The title compound was obtained as a brown solid (85 mg) with impurities. Further purification is necessary. **¹H NMR** (500 MHz, MeOD₄) δ ppm 7.65 (d, J = 8.5 Hz, 2H), 7.59 (d, J = 8.4 Hz, 3H), 7.50 (d, J = 7.8 Hz, 1H), 7.42 – 7.37 (m, 1H), 7.32 (t, J = 8.7 Hz, 1H), 3.35 (dt, J = 12.9, 3.7 Hz, 2H), 2.80 – 2.70 (m, 2H), 2.67 (s, 3H), 2.61 (tt, J = 10.9, 4.2 Hz, 1H), 2.09 – 1.94 (m, 4H) (*addendum 3* – Figure 10). **¹³C NMR** (126 MHz, MeOD₄) δ ppm 174.7, 143.3, 141.9, 139.2, 138.3, 129.9, 128.3, 126.8, 126.6, 126.3, 121.5, 65.4, 65.2, 55.0, 44.8, 28.2 (*addendum 4* – Figure 11). **LRMS** m/z (ESI+) 325.8 ([M+H]⁺). **HRMS** (ESI+): calcd. for C₂₀H₂₅N₂O₂ [M+H]⁺: 325.1916; found: 325.1909 (*addendum 4* – figure 35).

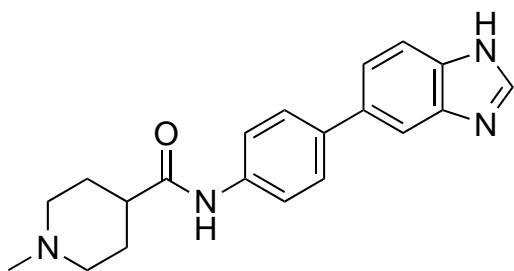
N-(3',4'-Dimethoxy-[1,1'-biphenyl]-4-yl)-1-methylpiperidine-4-carboxamide (**OSA 1057**)



Compound **OSA_1057** was synthesised following synthetic procedure B, using compound **3a** (150 mg, 0.50 mmol), (3,4-dimethoxyphenyl)boronic acid (110 mg, 0.61 mmol), K₂CO₃ (209 mg, 1.51 mmol), PdCl₂(dppf)·CH₂Cl₂ (41 mg, 0.05 mmol) and dioxane:water (5.05 mL, 0.50 mmol) to give the crude product which was purified by flash silica gel chromatography. The title

compound was obtained as a brown solid (49 mg, 27% yield). **m.p.** 221 – 224 °C (no lit m.p.). **¹H NMR** (400 MHz, MeOD₄) δ ppm 7.61 (d, *J* = 8.3 Hz, 2H), 7.54 (d, *J* = 8.4 Hz, 2H), 7.16 (d, *J* = 10.0 Hz, 2H), 7.01 (d, *J* = 8.2 Hz, 1H), 3.90 (s, 3H), 3.86 (s, 3H), 3.23 (d, *J* = 12.1 Hz, 2H), 2.55 (s, 6H), 1.97 (d, *J* = 21.6 Hz, 4H) (*addendum 3* – Figure 12). **¹³C NMR** (126 MHz, MeOD₄) δ ppm 175.1, 150.7, 150.0, 138.7, 138.1, 135.0, 127.9, 121.5, 120.3, 113.3, 111.6, 56.5, 56.5, 55.4, 45.3, 42.7, 28.7 (*addendum 3* – Figure 13). **LRMS** *m/z* (ESI⁺) 355.2 ([M+H]⁺). **HRMS** (ESI⁺): calcd. for C₂₁H₂₇N₂O₃ [M+H]⁺: 355.2022; found: 355.2024 (*addendum 4* – figure 36).

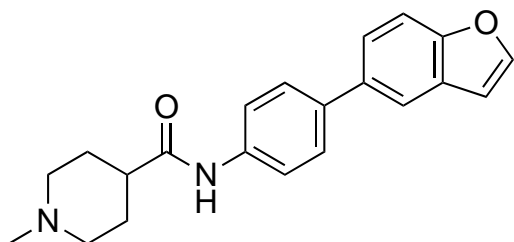
N-(4-(1H-Benzo[d]16midazole-5-yl)phenyl)-1-methylpiperidine-4-carboxamide (**OSA 1058**)



Compound **OSA_1058** was synthesised following synthetic procedure B, using compound **3a** (150 mg, 0.50 mmol), 1H-benzimidazole-5-boronic acid pinacol ester (148 mg, 0.61 mmol), K₂CO₃ (209 mg, 1.51 mmol), PdCl₂(dppf)·CH₂Cl₂ (41 mg, 0.05 mmol) and dioxane:water (5.05 mL, 0.50 mmol). The reaction was incomplete as not all starting material (**3a**) was

converted and another 0.5 equiv. PdCl₂(dppf)·CH₂Cl₂ (206 mg, 0.25 mmol) was added. As even prolonged reaction did not lead to completion, the reaction was halted after 36 h and the resulting crude product was purified by flash silica gel chromatography. The title compound was obtained as a brown solid (32.6 mg, 19% yield). **m.p.** 175 – 177 °C (no lit m.p.). **¹H NMR** (400 MHz, MeOD₄) δ ppm 7.80 (s, 1H), 7.75 – 7.46 (m, 7H), 3.35 (s, 2H), 2.64 (d, *J* = 13.4 Hz, 6H), 2.03 (d, *J* = 13.0 Hz, 4H) (*addendum 3* – Figure 14). **¹³C NMR** (101 MHz, MeOD₄) δ ppm 175.8, 159.7, 145.3, 138.7, 137.6, 135.0, 127.1, 126.8, 121.6, 110.2, 55.9, 46.3, 44.0, 29.6 (*addendum 3* – Figure 15). **LRMS** *m/z* (ESI⁺) 355.0 ([M+H]⁺) 168.0 ([M+2H]²⁺). **HRMS** (ESI⁺): calcd. for C₂₀H₂₃N₄O [M+H]⁺: 335.1872; found: 335.1866 (*addendum 4* – figure 37).

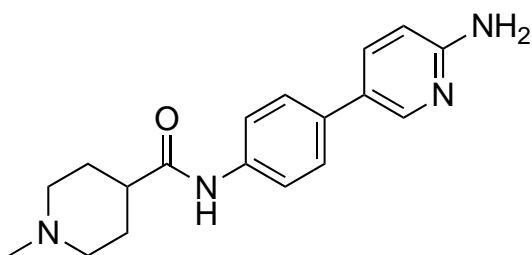
N-(4-(Benzofuran-5-yl)phenyl)-1-methylpiperidine-4-carboxamide (**OSA 1059**)



Compound **OSA_1059** was synthesised following synthetic procedure B, using compound **3a** (100 mg, 0.34 mmol), benzofuran-5-boronic acid pinacol ester (99 mg, 0.40 mmol), K₂CO₃ (140 mg, 1.01 mmol), PdCl₂(dppf)·CH₂Cl₂ (28 mg, 0.03 mmol) and dioxane:water (3.36 mL, 0.34 mmol) to give the crude

product which was purified by flash silica gel chromatography (DCM: 5% NH₄OH in MeOH 98:2 → 80:20, step gradient). The title compound was obtained as a brown solid (25 mg, 23% yield). **m.p.** 205 – 209 °C (no lit m.p.). **¹H NMR** (400 MHz, MeOD₄) δ ppm 7.81 (s, 1H), 7.76 (d, *J* = 2.3 Hz, 1H), 7.68 – 7.62 (m, 2H), 7.62 – 7.56 (m, 2H), 7.53 (s, 2H), 6.88 (s, 1H), 3.17 (d, *J* = 11.9 Hz, 2H), 2.47 (d, *J* = 20.8 Hz, 6H), 1.95 (d, *J* = 18.8 Hz, 4H) (*addendum 3* – Figure 16). **¹³C NMR** (126 MHz, MeOD₄) δ ppm 175.3, 155.9, 147.1, 138.8, 138.7, 137.1, 129.5, 128.6, 124.6, 121.6, 120.2, 112.3, 107.8, 55.5, 45.6, 43.1, 28.9 (*addendum 3* – Figure 17). **LRMS** *m/z* (ESI+) 355.0 ([M+H]⁺). **HRMS** (ESI+): calcd. for C₂₁H₂₃N₂O₂ [M+H]⁺: 335.1760; found: 335.1767 (*addendum 4* – figure 38).

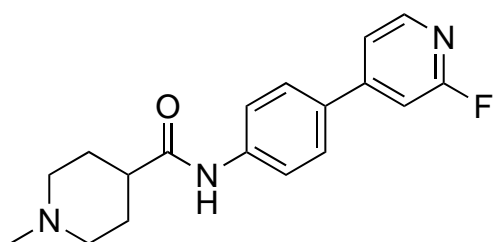
N-(4-(2-Aminopyridin-5-yl)phenyl)-1-methylpiperidine-4-carboxamide (OSA 1060)



Compound **OSA_1060** was synthesised following synthetic procedure B, using compound **3a** (100 mg, 0.34 mmol), 2-aminopyridine-5-boronic acid pinacol ester (89 mg, 0.40 mmol), K₂CO₃ (140 mg, 1.01 mmol), PdCl₂(dppf)·CH₂Cl₂ (28 mg, 0.03 mmol) and dioxane:water (3.36 mL, 0.34 mmol) to give the crude product which was purified by flash silica gel

chromatography. The title compound was obtained as a beige solid (41 mg, 39% yield). **m.p.** 249 – 251 °C (no lit m.p.). **¹H NMR** (500 MHz, MeOD₄) δ ppm 8.13 (d, *J* = 2.5 Hz, 1H), 7.73 (dd, *J* = 8.7, 2.5 Hz, 1H), 7.65 – 7.57 (m, 2H), 7.51 – 7.44 (m, 2H), 6.65 (d, *J* = 8.6 Hz, 1H), 2.97 (dt, *J* = 12.0, 3.5 Hz, 2H), 2.38 (td, *J* = 9.9, 5.4 Hz, 1H), 2.30 (s, 3H), 2.16 – 2.05 (m, 2H), 1.88 (td, *J* = 9.2, 3.9 Hz, 4H) (*addendum 3* – Figure 18). **¹³C NMR** (126 MHz, MeOD₄) δ ppm 176.0, 159.9, 145.5, 138.9, 137.8, 135.2, 127.2, 127.0, 121.7, 110.3, 55.9, 46.3, 44.0, 29.5 (*addendum 3* – Figure 19). **LRMS** *m/z* (ESI+) 310.9 ([M+H]⁺) 156.1 ([M+2H]²⁺). **HRMS** (ESI+): calcd. for C₁₈H₂₃N₄O [M+H]⁺: 311.1872; found: 311.1872 (*addendum 4* – figure 39).

N-(4-(2-Fluoropyridin-4-yl)phenyl)-1-methylpiperidine-4-carboxamide (OSA 1061)

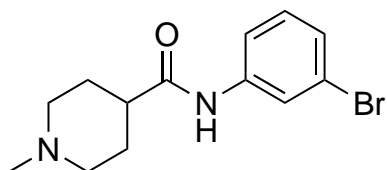


Compound **OSA_1061** was synthesised following synthetic procedure B, using compound **3a** (100 mg, 0.34 mmol), (2-fluoropyridin-4-yl)boronic acid (57 mg, 0.40 mmol), K₂CO₃ (140 mg, 1.01 mmol), PdCl₂(dppf)·CH₂Cl₂ (28 mg, 0.03 mmol) and dioxane:water (3.36 mL, 0.34 mmol) to give the crude product

which was purified by flash silica gel chromatography. The title compound was obtained as a beige solid (50 mg, 47% yield). **m.p.** 193 – 195 °C (no lit m.p.). **¹H NMR** (400 MHz, MeOD₄) δ ppm 8.20 (d, *J* = 5.4 Hz, 1H), 7.74 (d, *J* = 1.8 Hz, 4H), 7.61 – 7.55 (m, 1H), 7.34 (s, 1H), 2.97 (d, *J* = 11.3 Hz, 2H), 2.46 – 2.36 (m, 1H), 2.30 (s, 3H), 2.17 – 2.06 (m, 2H), 1.93 – 1.81 (m, 4H) (*addendum 3* – Figure 20). **¹³C NMR** (126 MHz, MeOD₄) δ ppm 176.2, 166.0 (d, ¹*J*_{CF} = 237.5 Hz, 2-C_{pyridinyl}), 155.4 (d, ⁴*J*_{CCCF} = 8.3 Hz, 4-C_{pyridinyl}), 148.7 (d, ³*J*_{CNCF} = 14.7 Hz, 6-C_{pyridinyl}), 142.0, 133.0 (d, ⁶*J*_{CCCCF} = 3.1 Hz, 4-C_{phenyl}), 128.7, 121.4, 120.3 (d, ⁵*J*_{CCNCF} = 3.1 Hz, 5-C_{pyridinyl}), 107.3 (d, ²*J*_{CCF} = 37.6 Hz, 3-C_{pyridinyl}), 55.9, 46.3, 44.1, 29.5 (*addendum 3* – Figure 21). **LRMS** *m/z* (ESI+) 313.8 ([M+H]⁺). **HRMS** (ESI+): calcd. for C₁₈H₂₁FN₃O [M+H]⁺:

314.1669; found: 314.1664 (*addendum 4* – figure 40). The values for the C-F coupling constants of the 2-fluoropyridine substituent matched those in the literature.⁽³³⁾

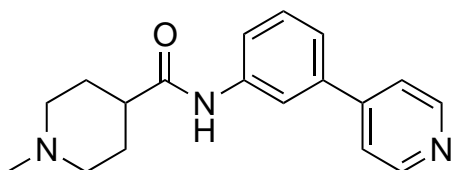
N-(3-Bromophenyl)-1-methylpiperidine-4-carboxamide (**3b**)



Compound **3b** was synthesised following synthetic procedure A, using 1-methylpiperidine-4-carboxylic acid (Scheme 4.1 - **1**) (500 mg, 3.49 mmol), thionyl chloride (3.80 mL, 52.4 mmol), 3-bromoaniline (Scheme 4.1- **2b**) (0.38 mL, 3.5 mmol), DCM (16.60 mL, 3.49 mmol) and TEA (1.00 mL, 7.16

mmol) to give the crude product which was purified by flash silica gel chromatography. The title compound **3b** was obtained as a white solid (422 mg) with TEA impurities and used in subsequent reactions that follow synthetic procedure C. ¹H NMR (400 MHz, MeOD₄) δ ppm 7.92 – 7.88 (m, 1H), 7.47 (dt, *J* = 6.9, 2.1 Hz, 1H), 7.26 – 7.17 (m, 2H), 3.38 – 3.32 (m, 2H), 2.80 – 2.55 (m, 6H), 2.09 – 1.90 (m, 4H) (*addendum 1* – Figure 3). LRMS *m/z* (ESI⁺) 296.8 ([M+H]⁺, ⁷⁹Br) 298.8 (M+H]⁺, ⁸¹Br). The data obtained corresponded to those from previous experimental work by Dr. Klug (Dana Klug, unpublished work, 2021).

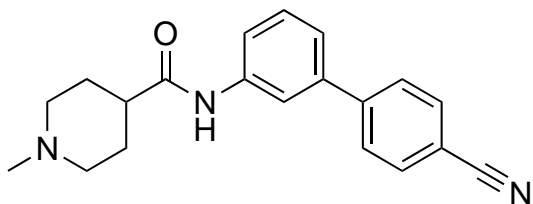
N-(3-(Pyridin-4-yl)phenyl)-1-methylpiperidine-4-carboxamide (**OSA 1062**)



Compound **OSA_1062** was synthesised following synthetic procedure B, using compound **3b** (150 mg, 0.50 mmol), pyridin-4-ylboronic acid (74 mg, 0.61 mmol), K₂CO₃ (209 mg, 1.51 mmol), PdCl₂(dppf)·CH₂Cl₂ (41 mg, 0.05 mmol) and dioxane:water (5.05 mL, 0.50 mmol) to give

the crude product which was purified by flash silica gel chromatography. The title compound was obtained as a brown solid (63 mg) with methanol impurities. Further purification is necessary. ¹H NMR (400 MHz, DMSO-*d*₆) δ ppm 10.04 (s, 1H), 8.64 (d, *J* = 5.0 Hz, 2H), 8.09 (d, *J* = 2.3 Hz, 1H), 7.70 – 7.56 (m, 3H), 7.45 (d, *J* = 4.7 Hz, 2H), 2.87 (d, *J* = 11.1 Hz, 2H), 2.32 (t, *J* = 11.7 Hz, 1H), 2.21 (d, *J* = 1.8 Hz, 3H), 1.96 (t, *J* = 11.6 Hz, 2H), 1.84 – 1.61 (m, 4H) (*addendum 3*- Figure 22). ¹³C NMR (101 MHz, MeOD₄) δ ppm 173.7, 150.3, 147.0, 140.2, 137.7, 129.6, 121.4, 121.2, 119.8, 117.3, 54.6, 45.9, 42.2, 28.2 (*addendum 3* – Figure 23). LRMS *m/z* (ESI⁺) 296.0 ([M+H]⁺). HRMS (ESI⁺): calcd. for C₁₈H₂₂N₃O [M+H]⁺: 296.1763; found: 296.1766 (*addendum 4* – figure 41).

N-(4'-Cyano-[1,1'-biphenyl]-3-yl)-1-methylpiperidine-4-carboxamide (**OSA 1063**)

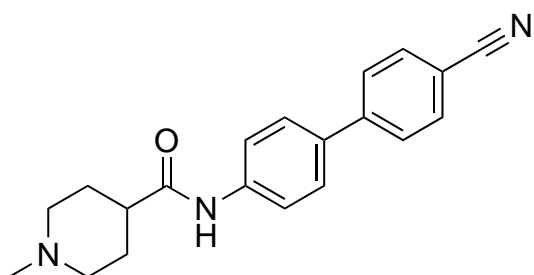


Compound **OSA_1063** was synthesised following synthetic procedure B, using compound **3b** (150 mg, 0.50 mmol), (4-cyanophenyl)boronic acid (89 mg, 0.61 mmol), K₂CO₃ (209 mg, 1.51 mmol), PdCl₂(dppf)·CH₂Cl₂ (41 mg, 0.05 mmol) and dioxane:water (5.05 mL, 0.50 mmol) to give the crude product

which was purified by flash silica gel chromatography. The title compound was obtained as a brown solid (113.1 mg, 70% yield). *m.p.* 174 – 178 °C (no lit *m.p.*). ¹H NMR (500 MHz, MeOD₄) δ ppm 7.96 (t, *J* = 1.8 Hz, 1H), 7.80 (s,

4H), 7.57 (dt, $J = 7.6, 1.9$ Hz, 1H), 7.46 – 7.38 (m, 2H), 2.97 (dt, $J = 12.1, 3.5$ Hz, 2H), 2.40 (tt, $J = 10.4, 5.9$ Hz, 1H), 2.30 (s, 3H), 2.10 (dt, $J = 11.4, 5.6$ Hz, 2H), 1.90 (qd, $J = 11.3, 4.3$ Hz, 4H) (*addendum 3* – Figure 24). $^{13}\text{C NMR}$ (126 MHz, MeOD₄) δ ppm 176.3, 146.8, 141.1, 140.8, 133.8, 130.7, 128.9, 123.8, 121.3, 119.8, 119.7, 112.1, 55.94, 46.4, 44.1, 29.6 (*addendum 3* – Figure 25). **LRMS** m/z (ESI+) 320.0 ([M+H]⁺). **HRMS** (ESI+): calcd. for C₂₀H₂₂N₃O [M+H]⁺: 320.1763; found: 320.1755 (*addendum 4* – figure 42).

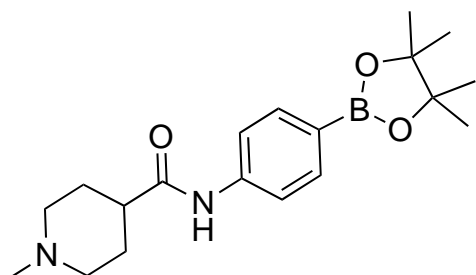
***N*-(4'-Cyano-[1,1'-biphenyl]-4-yl)-1-methylpiperidine-4-carboxamide (OSA_1064)**



Compound **OSA_1064** was synthesised following synthetic procedure B, using compound **3a** (100 mg, 0.34 mmol), (4-cyanophenyl)boronic acid (59 mg, 0.40 mmol), K₂CO₃ (140 mg, 1.01 mmol), PdCl₂(dppf)·CH₂Cl₂ (28 mg, 0.03 mmol) and dioxane:water (3.36 mL, 0.34 mmol) to give the crude product which was purified by flash silica gel chromatography. The title

compound was obtained as a brown solid (24.7 mg, 23% yield). **m.p.** 209 – 211 °C (no lit m.p.). $^1\text{H NMR}$ (500 MHz, MeOD₄) δ ppm 7.80 (d, $J = 8.6$ Hz, 2H), 7.77 (d, $J = 8.4$ Hz, 2H), 7.73 – 7.67 (m, 2H), 7.67 – 7.62 (m, 2H), 2.98 (dt, $J = 12.1, 3.5$ Hz, 2H), 2.40 (tt, $J = 10.2, 6.0$ Hz, 1H), 2.30 (s, 3H), 2.12 (td, $J = 11.1, 4.8$ Hz, 2H), 1.95 – 1.82 (m, 4H) (*addendum 3* – Figure 26). $^{13}\text{C NMR}$ (126 MHz, MeOD₄) δ ppm 176.2, 146.4, 140.8, 135.7, 133.8, 128.6, 128.4, 121.5, 119.9, 111.5, 55.9, 46.3, 44.1, 29.5 (*addendum 3* – Figure 27). **LRMS** m/z (ESI+) 320.0 ([M+H]⁺). **HRMS** (ESI+): calcd. for C₂₀H₂₂N₃O [M+H]⁺: 320.1763; found: 320.1766 (*addendum 4* – figure 43).

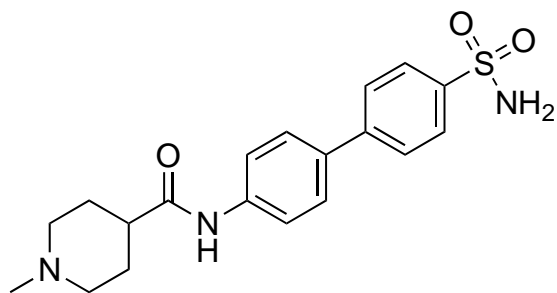
***N*-(4-(4,4,5,5-Tetramethyl-1,3,2-dioxaborolan-2-yl)phenyl)-1-methylpiperidine-4-carboxamide (5)**



Compound **5** was synthesised following synthetic procedure C, using compound **3a** (500 mg, 1.68 mmol), bis(pinacolato)diboron (**4**) (637 mg, 2.51 mmol), KOAc (495 mg, 5.05 mmol), PdCl₂(dppf)·CH₂Cl₂ (69 mg, 0.08 mmol) and dioxane (11.22 mL, 1.68 mmol) to give the crude product which was purified by flash silica gel chromatography. The title compound was obtained as a beige

solid (338 mg) with bis(pinacolato)diboron (**4**) impurities and used as such in subsequent reactions that follow synthetic procedure D. $^1\text{H NMR}$ (500 MHz, MeOD₄) δ ppm 7.69 – 7.66 (m, 2H), 7.58 – 7.55 (m, 2H), 3.14 (dt, $J = 11.8, 3.6$ Hz, 2H), 2.49 – 2.38 (m, 6H), 1.95 – 1.91 (m, 4H), 1.33 (s, 12H) (*addendum 2* – Figure 4). $^{13}\text{C NMR}$ (126 MHz, MeOD₄) δ ppm 175.5, 142.8, 136.5, 120.0, 112.0, 85.0, 55.5, 45.6, 43.1, 28.9, 25.2 (*addendum 2* – Figure 5). **LRMS** m/z (ESI+) 345.0 ([M+H]⁺).

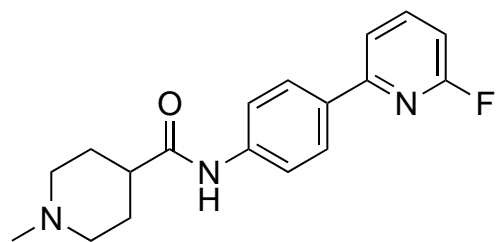
N-(4'-Sulfamoyl-[1,1'-biphenyl]-4-yl)-1-methylpiperidine-4-carboxamide (**OSA 1065**)



Compound **OSA_1065** was synthesised following synthetic procedure B, using compound **3a** (75 mg, 0.25 mmol), (4-sulfamoylphenyl)boronic acid (61 mg, 0.30 mmol), K₂CO₃ (105 mg, 0.76 mmol), PdCl₂(dppf)·CH₂Cl₂ (21 mg, 0.03 mmol) and dioxane:water (2.52 mL, 0.25 mmol) to give the crude product which was purified by flash silica gel chromatography. The title compound was obtained as a

brown solid (15.3 mg, 16% yield). **m.p.** 265 – 270 °C (no lit m.p.). ¹H NMR (500 MHz, MeOD₄) δ ppm 7.97 – 7.93 (m, 2H), 7.79 (d, *J* = 8.4 Hz, 2H), 7.72 – 7.68 (m, 2H), 7.66 (d, *J* = 8.8 Hz, 2H), 3.16 (d, *J* = 11.9 Hz, 2H), 2.56 – 2.40 (m, 6H), 1.95 (d, *J* = 17.1 Hz, 4H) (*addendum 3* – Figure 28). ¹³C NMR (126 MHz, MeOD₄) δ ppm 175.7, 145.7, 143.6, 140.5, 136.4, 128.8, 128.2, 127.9, 121.7, 55.7, 45.8, 43.4, 29.1 (*addendum 3* – Figure 29). **LRMS** *m/z* (ESI+) 373.9 ([M+H]⁺). **HRMS** (ESI+): calcd. for C₁₉H₂₄N₃O₂S [M+H]⁺: 374.1538; found: 374.1541 (*addendum 4* – figure 44).

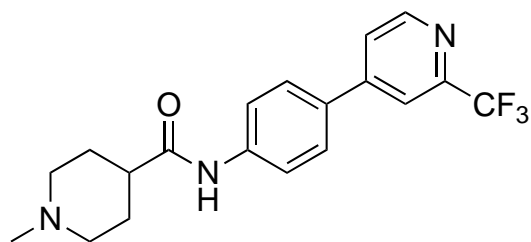
N-(4-(6-fluoropyridin-2-yl)phenyl)-1-methylpiperidine-4-carboxamide (**OSA 1066**)



Compound **OSA_1066** was synthesised following synthetic procedure D, using compound **5** (50 mg, 0.15 mmol), 2-bromo-6-fluoropyridine (21 mg, 0.12 mmol), K₂CO₃ (50 mg, 0.36 mmol), PdCl₂(dppf)·CH₂Cl₂ (10 mg, 0.01 mmol) and dioxane:water (1.68 mL, 0.12 mmol) to give the crude product which was purified by

flash silica gel chromatography. The title compound was obtained as a brown solid (31.8 mg) with impurities. Further purification by reversed-phase chromatography is necessary. ¹H NMR (500 MHz, MeOD₄) δ ppm 7.99 (dd, *J* = 9.3, 2.3 Hz, 2H), 7.97 – 7.91 (m, 1H), 7.75 (dd, *J* = 7.6, 2.5 Hz, 1H), 7.72 – 7.67 (m, 2H), 6.93 (dd, *J* = 8.0, 2.7 Hz, 1H), 2.98 (dt, *J* = 12.7, 3.4 Hz, 2H), 2.41 (tt, *J* = 10.6, 5.8 Hz, 1H), 2.31 (s, 3H), 2.13 (td, *J* = 11.3, 4.8 Hz, 2H), 1.92 – 1.83 (m, 4H) (*addendum 3* – Figure 30). **LRMS** *m/z* (ESI+) 313.9 ([M+H]⁺).

N-(4-(2-(Trifluoromethyl)pyridin-4-yl)phenyl)-1-methylpiperidine-4-carboxamide (**OSA 1067**)

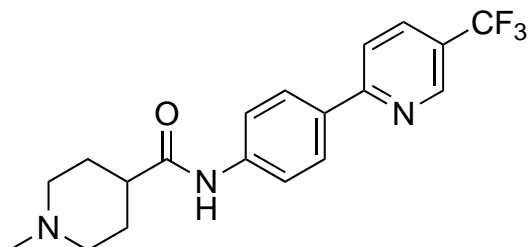


Compound **OSA_1067** was synthesised following synthetic procedure D, using compound **5** (50 mg, 0.15 mmol), 4-bromo-2-(trifluoromethyl)pyridine (16.0 μL, 0.12 mmol), K₂CO₃ (50 mg, 0.36 mmol), PdCl₂(dppf)·CH₂Cl₂ (10 mg, 0.01 mmol) and dioxane:water (1.68 mL, 0.12 mmol). The reaction was

considered incomplete and another 0.5 equiv. 4-bromo-2-(trifluoromethyl)pyridine (8.0 μL, 0.06 mmol) was added. After running the reaction in the microwave at 120 °C for another 10 min, the reaction was completed. The resulting crude product was purified by flash silica gel chromatography. The title compound was obtained as

a brown solid (37.8 mg) with impurities. Further purification by reverse-phase chromatography is necessary. ¹H NMR (500 MHz, MeOD₄) δ ppm 8.71 (d, *J* = 5.2 Hz, 1H), 8.07 (d, *J* = 1.8 Hz, 1H), 7.92 (dd, *J* = 5.2, 1.8 Hz, 1H), 7.81 (d, *J* = 8.9 Hz, 2H), 7.77 (d, *J* = 8.9 Hz, 2H), 3.01 (dt, *J* = 12.1, 3.5 Hz, 2H), 2.43 (tt, *J* = 10.4, 5.3 Hz, 1H), 2.33 (s, 3H), 2.17 (td, *J* = 11.6, 4.1 Hz, 2H), 1.94 – 1.84 (m, 4H) (addendum 3 – Figure 31). LRMS *m/z* (ESI+) 364.0 ([M+H]⁺).

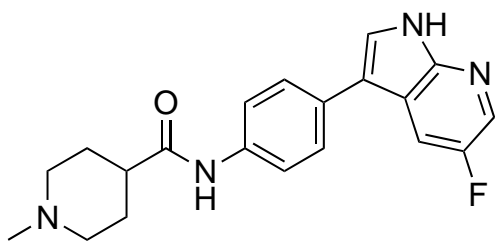
N-(4-(5-(Trifluoromethyl)pyridin-2-yl)phenyl)-1-methylpiperidine-4-carboxamide (OSA 1068)



Compound **OSA_1068** was synthesised following synthetic procedure D, using compound **5** (50 mg, 0.15 mmol), 2-bromo-5-(trifluoromethyl)pyridine (27 mg, 0.12 mmol), K₂CO₃ (50 mg, 0.36 mmol), PdCl₂(dppf)·CH₂Cl₂ (10 mg, 0.01 mmol) and dioxane:water (1.68 mL, 0.12 mmol) to give the crude product which was purified by flash silica gel chromatography. The title

compound was obtained as a brown solid (40.8 mg) with impurities. Further purification by reverse-phase chromatography is necessary. ¹H NMR (500 MHz, MeOD₄) δ ppm 8.90 – 8.87 (m, 1H), 8.15 – 8.02 (m, 4H), 7.77 – 7.72 (m, 2H), 2.98 (d, *J* = 11.9 Hz, 2H), 2.42 (tt, *J* = 10.1, 5.6 Hz, 1H), 2.31 (s, 3H), 2.12 (td, *J* = 11.2, 4.6 Hz, 2H), 1.89 (td, *J* = 9.9, 3.4 Hz, 4H) (addendum 3 – Figure 32). LRMS *m/z* (ESI+) 363.8 ([M+H]⁺).

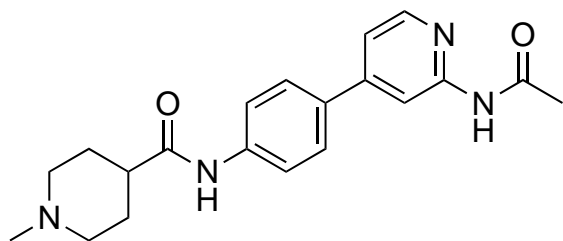
N-(4-(5-Fluoro-1H-pyrrolo[2,3-*b*]pyridin-3-yl)phenyl)-1-methylpiperidine-4-carboxamide (OSA 1069)



Compound **OSA_1069** was synthesised following synthetic procedure D, using compound **5** (50 mg, 0.15 mmol), 3-bromo-5-fluoro-1H-pyrrolo[2,3-*b*]pyridine (26 mg, 0.12 mmol), K₂CO₃ (50 mg, 0.36 mmol), PdCl₂(dppf)·CH₂Cl₂ (10 mg, 0.01 mmol) and dioxane: water (1.68 mL, 0.12 mmol). The reaction was considered

incomplete and another 0.5 equiv. 3-bromo-5-fluoro-1H-pyrrolo[2,3-*b*]pyridine (13 mg, 0.06 mmol) was added. The reaction was run in the microwave at 120 °C for another 10 min. As even prolonged reaction did not lead to completion, the reaction was halted. The reaction mixture was concentrated, and the resulting crude product will be purified by Dr. Edwin Tse. LRMS *m/z* (ESI+) 352.9 ([M+H]⁺) 177.0 ([M+2H]²⁺).

N-(4-(2-Acetamidopyridin-4-yl)phenyl)-1-methylpiperidine-4-carboxamide (OSA 1070)



Compound **OSA_1070** was synthesised following synthetic procedure D, using compound **5** (50 mg, 0.15 mmol), *N*-(4-bromopyridin-2-yl)acetamide (26 mg, 0.12 mmol), K₂CO₃ (50 mg, 0.36 mmol), PdCl₂(dppf)·CH₂Cl₂ (10 mg, 0.01 mmol) and dioxane:water (1.68 mL, 0.12 mmol) to give the crude

product which will be purified by Dr. Edwin Tse. LRMS *m/z* (ESI+) 352.9 ([M+H]⁺) 177.0 ([M+2H]²⁺).

The design of the following compounds: 1-methyl-N-(3-(4,4,5,5-tetramethyl-1,3,2-dioxaborolan-2-yl)phenyl)piperidine-4-carboxamide, 1-methyl-N-(3-(2-oxo-1,2-dihydroquinolin-6-yl)phenyl)piperidine-4-carboxamide (**OSA_1088**), N-(3-(1-(2-aminoethyl)-1H-pyrazol-4-yl)phenyl)-1-methylpiperidine-4-carboxamide (**OSA_1089**), 1-methyl-N-(3-(1-(2-(methylamino)-2-oxoethyl)-1H-pyrazol-4-yl)phenyl)piperidine-4-carboxamide (**OSA_1090**), N-(3-(5-carbamoylfuran-3-yl)phenyl)-1-methylpiperidine-4-carboxamide (**OSA_1091**), and 1-methyl-N-(3'-ureido-[1,1'-biphenyl]-3-yl)piperidine-4-carboxamide (**OSA_1092**) falls within the scope of this thesis project and will be described in the Discussion. However, the synthesis and characterisation will be performed by Dr. Edwin Tse and will therefore not be described here.

Biological procedure A: X-ray crystallography

After synthesis, purification, and characterisation of the compounds from Elaboration Round 2 (**OSA_1054 - 1061**), they were taken to the bio-crystallography lab of Prof. Dr. Frank Von Delft at the University of Oxford. After generating crystals of *Escherichia coli* apo MurD, using non-optimised conditions, and MurE, using optimised conditions, each compound was soaked in the drops of both protein crystals. The soaked crystals were harvested after 2.5 h and 12 h and sent to Diamond Light Source's synchrotron. Here, X-ray diffraction was used to determine the structure of the compounds in complex with the protein target.

Biological procedure B: Enzymatic inhibition assay

After synthesis, purification, and characterisation of the compounds from Elaboration Round 2 and 3 (**OSA_1054 - 1070**), they will be sent to the microbiology lab of Prof. Dr. Christopher Dowson at the University of Warwick. Here, PhD candidate Rebecca Steventon will carry out the enzymatic assay which is referred to as "stopped Pi release assay". The compounds will be incubated with the Mur ligase in the presence of assay components for 10 min at 37 °C. The inorganic phosphate released during the hydrolysis of ATP by the Mur ligase, which occurs during their catalytic reaction, will be measured and provides an indication for the residual Mur ligase activity. The % activity of the Mur ligase will be converted to % inhibition and then plotted. DMSO and ADPCP, a known inhibitor, will be used as control samples.⁽³¹⁾

It should be noted that this is the same assay used for the MurD % inhibition determination of the compounds from Elaboration Round 1, synthesised by Dr. Klug and Dr. Idiris and mentioned in the Introduction and Discussion (Figure 1.7 and Figure 5.1, respectively).

Biological procedure C: Surface plasmon resonance (SPR)

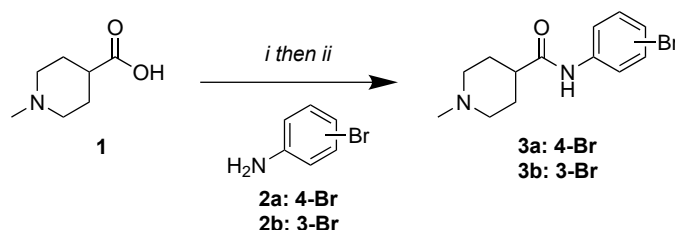
Dr. Laura Diaz Saez will carry out the SPR experiment for **OSA_1054 – 1070** at the University of Warwick. SPR is an optical technique used for the detection of molecular interactions between the compounds and the Mur ligases. Here, dose-response curves of the dissociation rate constant (K_d), which is a measure of binding affinity, will be generated.⁽³⁴⁾

4 RESULTS

The synthesis of the elaborated compounds from Elaboration Round 2 and 3 will be discussed in this chapter, while their design will be extensively described in the Discussion chapter.

4.1 SYNTHESIS OF BROMO SUBSTITUTED CORE (compound **3a** and **3b**)

The two bromo substituted cores have previously been synthesised by Dr. Klug in the context of Elaboration Round 1 (**OSA_752 and 751**). However, throughout this thesis they are referred to as compound **3a** and **3b** respectively, as they merely serve as intermediates for the synthesis of the elaborated compounds from Round 2 and 3.



*Scheme 4.1: Synthesis of the bromo substituted core (compound **3a** and **3b**). Reagents and conditions: (i) thionyl chloride, 75 °C, 4 h, reflux; (ii) 4-bromoaniline (**2a**) or 3-bromoaniline (**2b**), DCM, TEA, 0 °C to rt, overnight.*

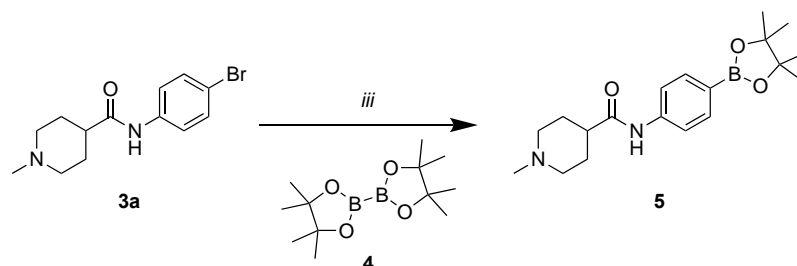
For the synthesis of all elaborated compounds, either a para- or meta-bromo substituted 1-methylpiperidine-4-(*N*-phenyl)carboxamide core (**3a** and **3b**) had to be constructed first. This was achieved by conversion of a carboxylic acid (**1**) into an acid chloride using thionyl chloride (step i) and subsequent coupling with a bromoaniline (**2a** and **2b**), thereby forming an amide bond (step ii) (Scheme 4.1). These reaction conditions were based on previous work by Dr. Klug *et al.*⁽³⁵⁾

In the first step, thionyl chloride undergoes nucleophilic addition of carboxylic acid, yielding a chlorosulfite intermediate. The chlorosulfite intermediate, which forms a better leaving group, undergoes nucleophilic attack by the displaced chloride anion on the carbonyl moiety, resulting in the removal of SO₂ and formation of the acid chloride (S_NAc). After the acid chloride was formed, excess thionyl chloride was removed under reduced pressure using toluene. Thionyl chloride and toluene form an azeotropic mixture, which has a lower boiling point than either of the two individual components.

Since SO₂ is a toxic gas formed in both the intended reaction and the exothermic reaction of thionyl chloride with moisture in the air, it was necessary to take appropriate precautions.

In the second step, which is referred to as a Schotten-Baumann reaction, the acyl chloride underwent a nucleophilic attack (likewise in an S_NAc reaction) by the primary amine of bromoaniline (**2a** and **2b**), obtaining the corresponding amide (**3a** and **3b**), and one equivalent of hydrogen chloride. The acid was neutralised with a base (TEA) to drive the reaction equilibrium towards the product. As not all starting material was converted to the desired amide product, purification was necessary before proceeding to the next reaction.

4.2 SYNTHESIS OF THE BORONIC ESTER SUBSTITUTED CORE (compound **5**)



Scheme 4.2: Synthesis of the boronic ester substituted core (compound **5**). Reagents and conditions: (iii) bis(pinacolato)diboron (**4**), $PdCl_2(dppf) \cdot CH_2Cl_2$, KOAc, dioxane, 145 °C, 1 h, microwave.

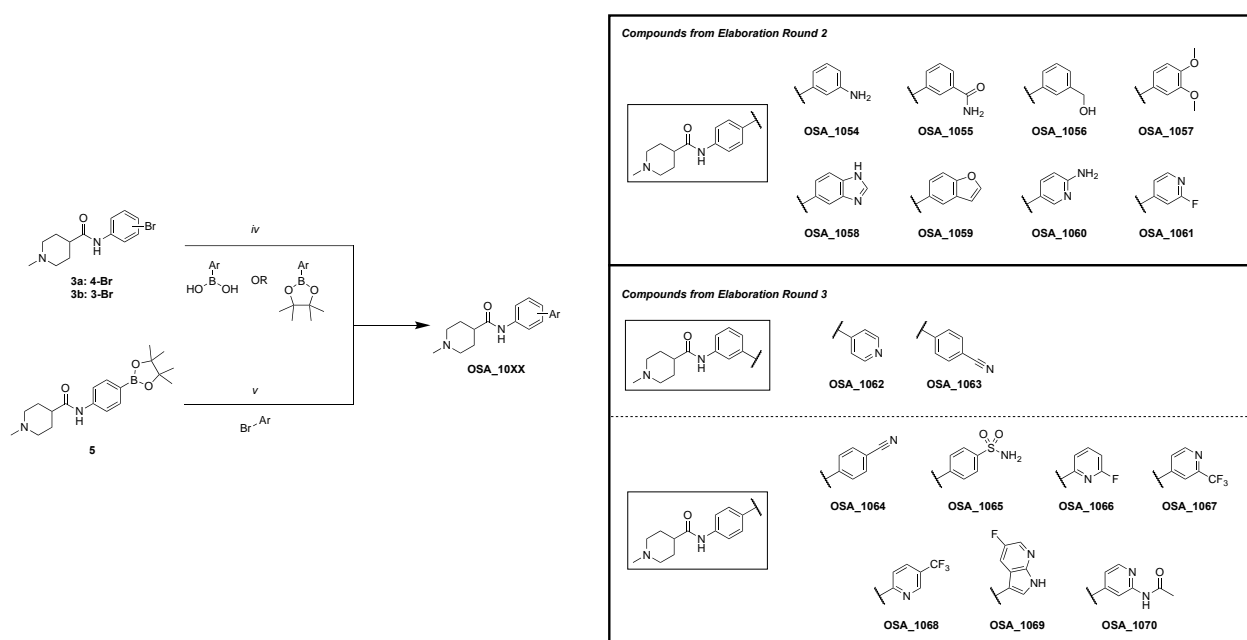
The bromo substituted 1-methylpiperidine-4-(N-phenyl)carboxamide core (**3a**) generated in the previous reaction, was converted to the corresponding boronic ester *via* a Miyaura borylation reaction (Scheme 4.2). In this process, the aryl bromide (**3a**) was reacted with bis(pinacolato)diboron (**4**) *via* a cross-coupling with a palladium catalyst to give the aryl boronic ester. These reaction conditions were based on previous work by Dr. Klug *et al.* ⁽³⁵⁾ In a study by Neeve E.C. *et al.*, it was found that careful selection of an appropriate base (KOAc) was necessary to obtain the desired aryl boronic ester product in high yields. The base is considered crucial for the activation of the transmetalation process in a way that formation of the homocoupling by-product is avoided. ⁽³⁶⁾ As not all the starting material was converted into the desired boronic ester product, purification was necessary before proceeding to the next reaction.

4.3 SYNTHESIS OF OSA_1054 – 1061 (Round 2) AND OSA_1062 – 1070 (Round 3)

After generating the desired bromo substituted core (**3a** and **3b**) and the boronic ester substituted core (**5**), various (hetero)aryl moieties were introduced either at the para- or meta- position of the phenyl ring *via* a Suzuki-Miyaura reaction (Scheme 4.3). The Suzuki-Miyaura reaction requires two coupling partners, an organohalide and a boronic acid or ester, which react *via* cross-coupling with a palladium catalyst, forming a carbon-carbon single bond between the coupling partners. As in the preceding reactions, these reaction conditions were also based on previous work by Dr. Klug *et al.* ⁽³⁵⁾

For compounds **OSA_1054 – 1065** from Elaboration Round 2 and 3, the bromo substituted core (**3a**) served as the organohalide, while the different (hetero)aryl substituents were used in the form of boronic acids or esters. All reactions were run at 100 °C overnight and the crude products were purified by flash chromatography.

For compounds **OSA_1066 – 1070** from Elaboration Round 3, this was the other way around. The (hetero)aryl moieties were used as bromides and thus acted as the organohalide, while the boronic ester substituted core (**5**) served as the other coupling partner. For these compounds, the reactions were carried out sequentially before purification of the crude products by flash chromatography. All reactions were run in the microwave at 120 °C for 30 min, which greatly reduced the reaction time.



Scheme 4.3: Synthesis of elaborated compounds **OSA_1054 – 1061** (Round 2) and **OSA_1062 – 1070** (Round 3). Reagents and conditions: (iv) boronic acid or boronic ester, PdCl₂(dppf)·CH₂Cl₂, K₂CO₃, 3:1 dioxane:water, 100 °C, overnight; (v) aryl bromide, PdCl₂(dppf)·CH₂Cl₂, K₂CO₃, 3:1 dioxane:water, 120 °C, 30 min, microwave.

4.4 X-RAY CRYSTALLOGRAPHY OF **OSA_1054 – 1061**

Analysis of the crystallographic data was carried out by our collaborator at the University of Warwick, Dr. Laura Diaz Saez. Structures of MurD crystals soaked with **OSA_1054**, **1055** and **1058** were obtained with a resolution ranging from 2.1 to 3.9 Å. Unfortunately, the compounds could not be identified bound to the target.

Structures of MurE crystals soaked with **OSA_1054 – 1061** were obtained with a resolution ranging from 1.8 to 3.6 Å. As for MurD, no compounds could be identified bound to the target for MurE either. However, several of the MurE crystal structures were found to have a more closed conformation in the presence of the compounds compared to the open conformation of the target's apo structure. This could imply that the compounds have an influence on conformational changes. It should be noted that a similar phenomenon was observed for the dual inhibitor compounds.

5 DISCUSSION

The design of all elaborated compounds from Elaboration Round 2 and 3 will be extensively discussed in this chapter, while their synthesis is described in the Results chapter.

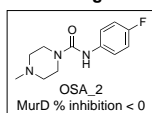
5.1 ELABORATION ROUND 1

5.1.1 SAR analysis

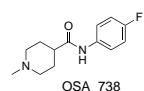
For the first Elaboration Round of the 'FBDD hit-to-lead' approach, Dr. Klug and Dr. Idiris synthesised analogues based on the four structurally different original fragment hits that were found to bind a potential allosteric pocket (Figure 1.6). These analogues contain several functional groups that can potentially engage in additional interactions with the target; the synthesis was made simpler by the commercial availability of suitable coupling partners. Following synthesis, the compounds were biochemically tested by PhD candidate Rebecca Steventon for their activity against MurD to provide data for SAR-analysis and subsequent semi-rational Elaboration Rounds. The compounds with the best inhibitory activity were also assessed against MurE, resulting in the identification of six compounds with dual inhibitory activity against both MurD and MurE (Figure 1.8). As four out of the six dual inhibitors contained a *1-methylpiperidine-4-(N-phenyl)carboxamide core*, it was decided that the subsequent SAR studies would be conducted on new analogues containing the same core.

As Figure 5.1 shows, there were 28 compounds with a *1-methylpiperidine-4-(N-phenyl)carboxamide core* which were designed as analogues of original fragment hit **OSA_2**. After a thorough analysis of the structures in relation to their MurD % inhibition data (Figure 1.7), an SAR diagram (Figure 5.2A) was created to summarise the positions of the molecule that could be modified to improve activity. For the R₁ substituent (ortho substituent), it was observed that aromatic rings (**OSA_753** and **754**) increased the inhibition activity compared to original fragment hit **OSA_2**, while introduction of a bromine atom (**OSA_750**) resulted in inactivity. For the R₂ substituent (meta substituent), the opposite was true. Aromatic and non-aromatic rings resulted in the loss of activity (**OSA_756**, **761**, **764**), while a bromine atom (**OSA_751**) increased the activity. Much like the R₁ substituent, the R₃ (para substituent) position showed a similar pattern of increased activity with specific aromatic rings (**OSA_757** and **759**) and a decreased activity with non-aromatic rings (**OSA_762**, **763**, and **766**) and halogen substitutions (**OSA_741**, **OSA_752**). Since all the compounds have a low molecular weight, small changes can induce major effects. This is perfectly illustrated by changing the R₃ methyl (**OSA_742**) into a methoxy group (**OSA_747**) or the 4-pyridinyl (**OSA_759**) into a 3-pyridinyl group (**OSA_760**), causing a highly active compound to become inactive, possibly due to altered polarity or dimensions.

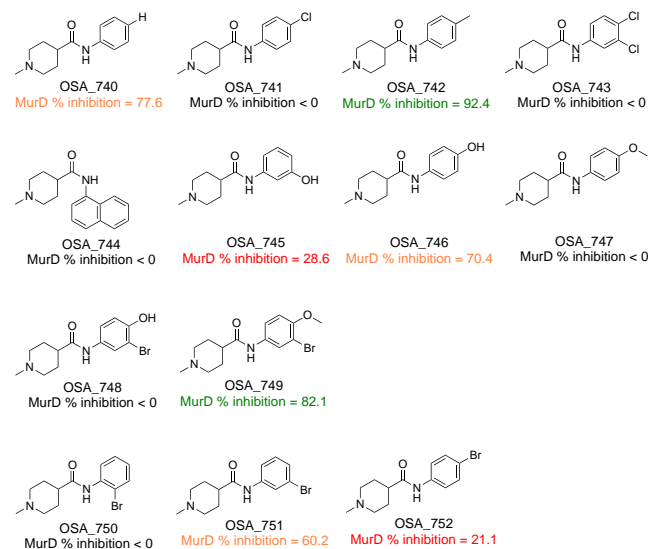
Parent fragment: Original Fragment Hit



Piperazine modification



Aryl modification



Extended analogues

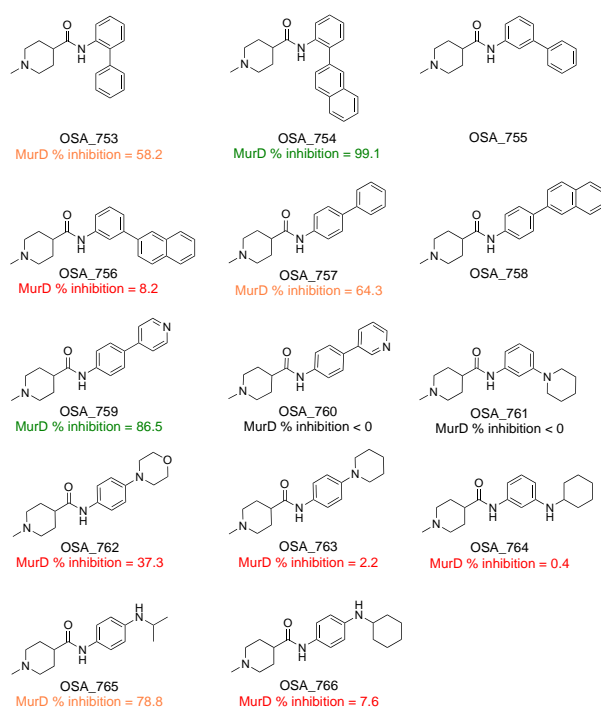


Figure 5.1: Elaboration Round 1 piperazine and aryl modifications, and extended analogues of original fragment hit **OSA_2** (parent fragment) with their corresponding MurD % inhibition. Compounds without MurD % inhibition either precipitated when used in the assay or interfered with the assay system. (Figure adapted from <https://github.com/opensourceantibiotics/murligase/wiki/MurD-Round-1>.⁽³¹⁾)

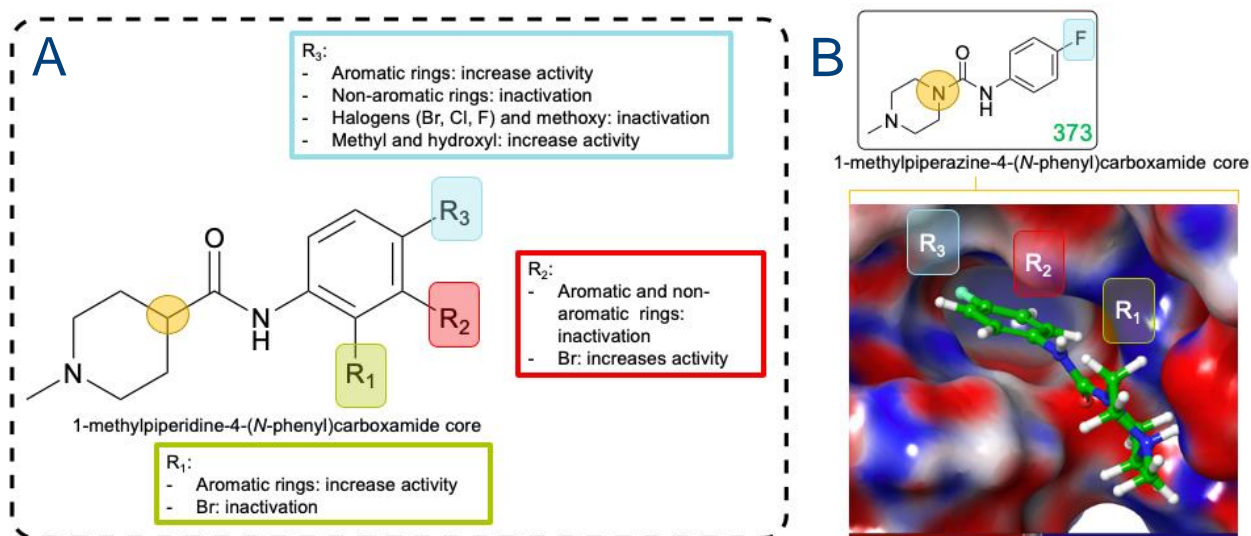


Figure 5.2: A) SAR diagram based on analogues of original fragment hit **OSA_2** with a 1-methylpiperidine-4-(N-phenyl)carboxamide core. B) Electrostatic potential map of original fragment hit **OSA_2** inside the allosteric pocket of MurD, generated with Maestro, Schrödinger, Version 12.9.137.

The electrostatic potential map of original fragment hit **OSA_2** in complex with the binding pocket (Figure 5.2B) shows that the R₁ and R₃ substituents both point towards negatively charged polar regions (red). While the R₂ substituent points to a slightly positively charged polar region (blue), which is also more spacious.

5.1.2 Analysis of the binding pocket

Figures 5.1 and 5.2 also show that the original fragment hit **OSA_2** or ‘parent fragment’ has a piperazine and not a piperidine core like its analogues. The rationale behind the substitution of the piperazine by a piperidine was that the piperidine core was easier to synthesise, and that the piperidine nitrogen would be more basic and thus more protonated. The more the *N*-methyl of the piperazine or piperidine is protonated, the greater the affinity of the compounds to the protein target, as this protonated nitrogen atom can engage in a strong interaction with the binding pocket.

More specifically, as shown in the 2D ligand interaction diagram in Figure 5.3, the protonated piperazine nitrogen of **OSA_2** interacts with Glu-132 by forming a salt bridge (2.51 Å) and a hydrogen bond (1.60 Å). Moreover, most of the piperazine ring is significantly solvent exposed. The urea carbonyl forms a hydrogen bond with the backbone NH of Lys-311 (1.79 Å), while the urea NH is making a hydrogen bond with a water molecule (2.14 Å). Lastly, the phenyl ring is involved in an edge-to-face π – π stacking interaction with His-312 (5.2 Å). Thus, the aim of the first Elaboration Round was to preserve these interactions while extending them to other residues in the binding pocket. Unfortunately, to this date it has not been possible to obtain crystallographic data for the elaborated compounds to confirm whether this is the case.

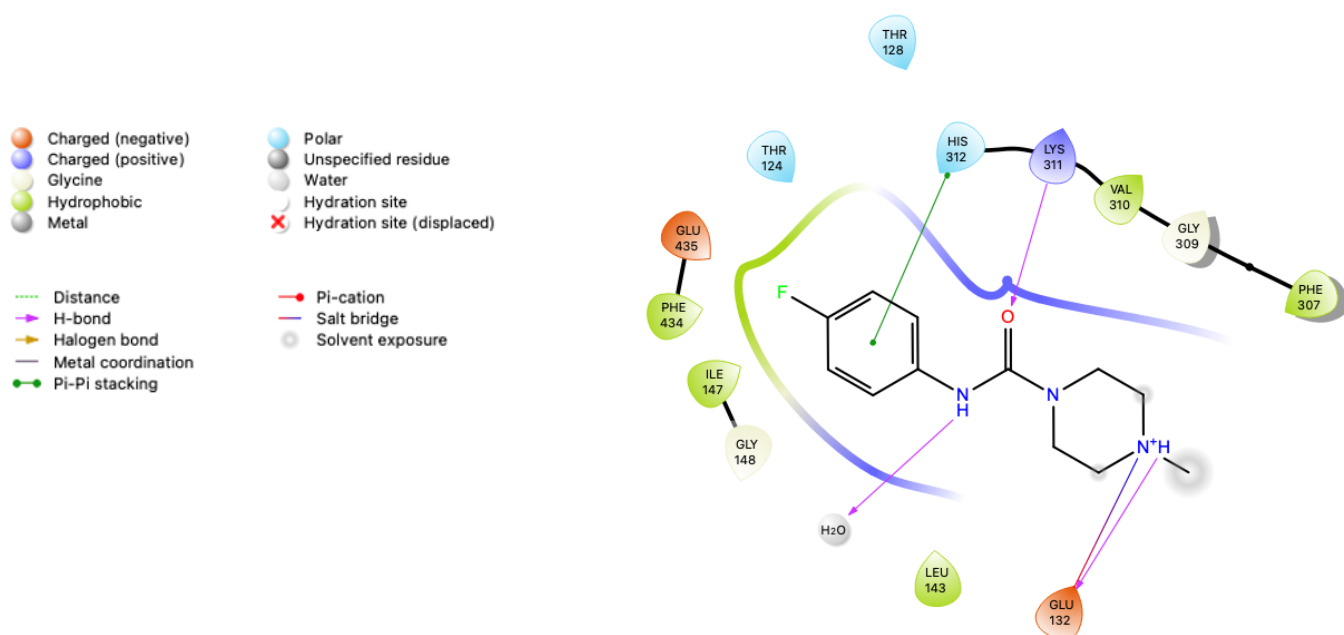


Figure 5.3: Ligand interaction diagram of original fragment hit **OSA_2** with residues from the allosteric pocket of MurD ligase generated with Maestro, Schrödinger, Version 12.9.137.

Since no crystallographic data was able to be obtained for the elaborated compounds, which proved to be a drawback, conclusions about the size, shape, and residues that might be important for interactions were drawn from the original fragment hit **OSA_2** in complex with the binding pocket of the protein target instead (Figure 5.4). In general, the size and shape of the pocket did not seem to provide enough room for fragment growing. When voluminous substituents were introduced at the R₂ or R₃ position of the phenyl ring, they were assumed to push the core out of the pocket, potentially resulting in the loss of interaction between the protonated piperazine or piperidine nitrogen and Glu-132. This assumption is supported by molecular docking of similar compounds.

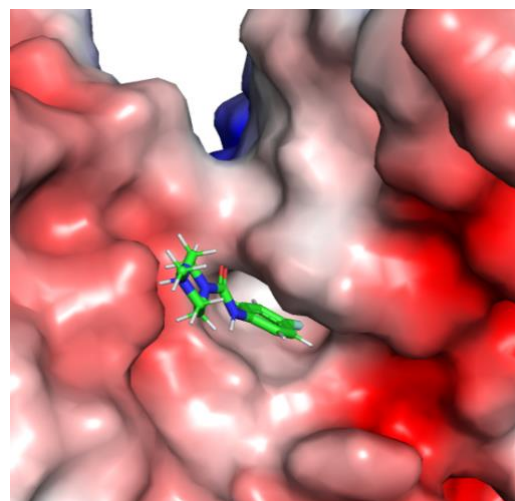


Figure 5.4: Electrostatic potential map of original fragment hit **OSA_2** in complex with MurD, showing the allosteric binding pocket. Generated with PyMOL, Schrödinger, Version 4.2.4.

Nevertheless, caution is required when interpreting docking results as the fragments show only weak interactions so that small changes can have a large impact on the binding pose.

On the other hand, two of the dual inhibitors contain an *N*-phenylisobutyramide core (Figure 5.5). This core lacks a protonated nitrogen and therefore also the associated salt bridge and hydrogen bond. This suggests that these interactions are not the main factor responsible for obtaining active compounds against both MurD and MurE, which validates the choice of bulky substituents in Elaboration Round 2 and 3.

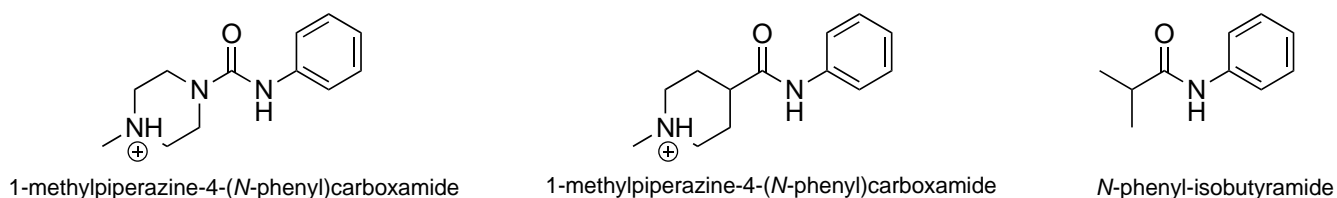


Figure 5.5: Protonated 1-methylpiperazine-4-(*N*-phenyl)carboxamide core of original fragment hit **OSA_2**. Protonated 1-methylpiperidine-4-(*N*-phenyl)carboxamide core of analogues from Elaboration Round 1, which includes four of the dual inhibitors, derived from original fragment hit **OSA_2**. *N*-phenylisobutyramide core of the two remaining dual inhibitors without protonated *N*-methyl.

5.2 ELABORATION ROUND 2

For further exploration of the allosteric pocket a second Elaboration Round was started that consisted of two parts. Firstly, a fragment growing approach could be applied to the solvent exposed piperidine side of the compounds which provides the possibility of growing the compound towards the substrate binding site. This part of the project was assigned to Dr. Klug. Secondly, more compounds with the same 1-methylpiperidine-4-(*N*-phenyl)carboxamide core, but with different phenyl substituents, can be designed and synthesised in a semi-rational way taking into account the SAR data together with the size, shape, and residues of the MurD allosteric pocket.

Table 5.1: Threshold values for important physicochemical properties - molecular weight (MW), lipophilicity (CLogP), hydrogen bond donors and acceptors - and typical values for the negative logarithm of half-maximal inhibitory concentration (pIC₅₀) according to the Rule of Three for fragments and Rule of Five for drugs. (Figure adapted from Schultes S⁽³⁷⁾).

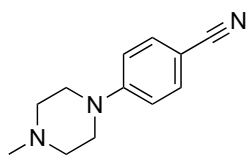
Type of compound	Fragment-like	Drug-like
Rule	Rule-of-Three	Rule-of-Five
Thresholds:		
MW	<300	≤500
CLogP	≤3	≤5
H-bond donors	≤3	≤5
H-bond acceptors	≤3	≤10
Typical Values:		
pIC ₅₀	4.4	8

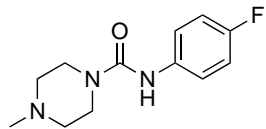
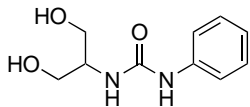
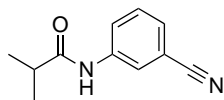
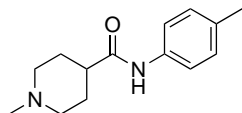
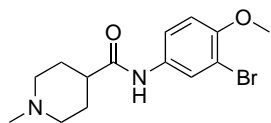
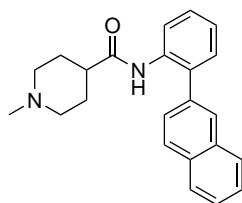
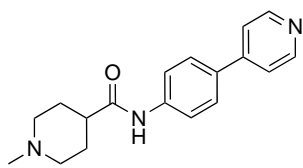
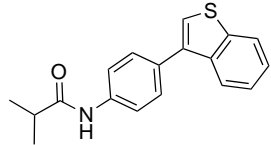
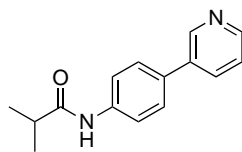
A core concept in FBDD is the Rule of Three (Ro3), which is considered as the fragment equivalent of Lipinski's Rule of Five (Ro5). Drug candidates complying with the Ro5 are expected to have good oral bioavailability and thus a higher chance of entering later stages of drug development. The Ro3 itself serves as a tool to evaluate fragments for their potential to be optimised into drug candidates that comply with the Ro5.⁽²⁵⁾ According to a study by Astex Pharmaceuticals, there is an increased chance of finding fragment hits when the Ro3 is applied.⁽³⁸⁾ Table 5.1 shows for both rules the thresholds and typical values for fragments (Ro3) and drugs (Ro5).

When evaluating the four original fragment hits derived from the commercially available fragment library using the Ro3, it can be observed that their MW (<300) and CLogP (≤3) are below the threshold values and therefore comply (Table 5.2). However, two fragments exceed the limit of hydrogen bond acceptors, while one fragment has an excess of hydrogen bond donors. Even though these fragments fail the Ro3 criteria, it has been stated that the Ro3 and Ro5 are only to be used as rough guidelines in drug design and that the emphasis is mainly on the MW and CLogP as the most important physicochemical properties to be fulfilled.⁽²⁵⁾ Hence, it is reasonable that the commercially available library was not originally designed to be fully compliant with the Ro3.⁽²⁸⁾ Doing so would impose enormous restrictions and significantly reduce the number of potential starting points for drug discovery campaigns.

In a similar way, it can be assessed whether the dual inhibitors (Table 5.2), which are elaborations of the original fragment hits, meet the requirements of the rule. It is clear that **OSA_749**, **OSA_754** and **OSA_788** are no longer classified as fragments since their MW or CLogP considerably exceeds the limits of the Ro3. This is, of course, the intention of fragment elaboration and growing. It can also be noted that all compounds have one hydrogen bond donor.

Table 5.2: Original fragment hits **OSA_1 – 4** and dual inhibitors (**OSA_742, 749, 754, 759, 788, 789**) with corresponding structures, molecular weight (MW), lipophilicity (CLogP, calculated using ChemDraw), and number of hydrogen bond donors and acceptors.

Fragment number	Compound Structure	MW	CLogP	H-bond donors	H-bond acceptors
OSA_1		201.3	1.6	0	3

OSA_2		237.3	1.5	1	4
OSA_3		224.3	0.7	4	5
OSA_4		188.2	1.4	1	3
OSA_742		232.3	1.7	1	3
OSA_749		327.2	1.6	1	4
OSA_754		344.5	3.3	1	3
OSA_759		295.4	1.9	1	4
OSA_788		295.4	4.9	1	2
OSA_789		240.3	2.4	1	3

In addition to the physicochemical properties, the affinity of the fragments for the target protein plays an important role in the selection and optimisation of the hit. The purpose of fragment elaboration is to grow the fragment hits into drug-sized inhibitors. Therefore, each compound of Elaboration Round 2 was designed to be at least three heavy atoms heavier than the original fragment hit, while keeping the CLogP consistently below 3, as this aids with solubility at high concentrations. In order to increase the affinity of the fragments for the binding pocket, substituents with more hydrogen bond acceptors and donors were introduced. Based on visual analysis of the pocket, they were presumed to engage in new interactions with the surrounding residues. The rationale behind this was the presence of Glu-435 and Asn-439, which bear hydrogen bond acceptor atoms in their side chains, and Lys-330 and Arg-313, which bear hydrogen donor atoms in their side chains, in close proximity of the binding site (Figure 5.6). These amino acid residues could possibly form additional hydrogen bonds with the compounds, in addition to the already existing hydrogen bonds with Glu-132 and Lys-31, thus increasing the affinity.

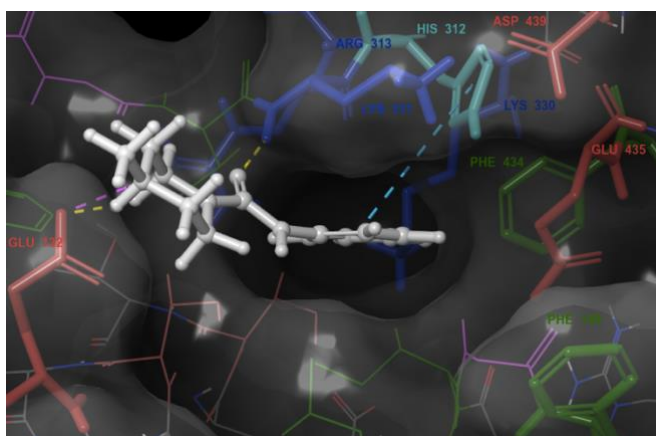


Figure 5.6: Visualisation of amino acid residues present in the allosteric binding pocket which is bound by original fragment hit **OSA_2** (white). Glu-435 and Asp-439 (red), Lys-330 and Arg-313 (blue), and Phe-434 and Phe-149 (green). Generated with Maestro, Schrödinger, Version 12.9.137.

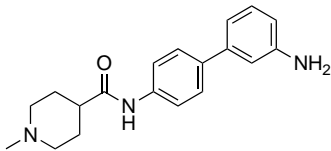
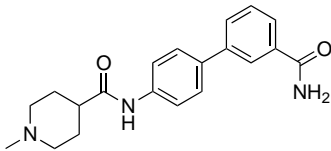
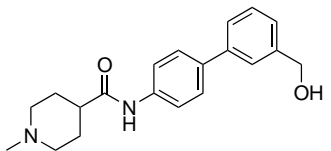
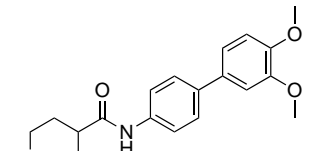
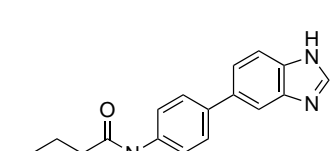
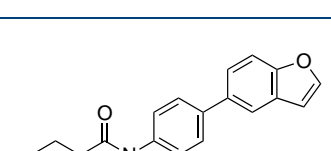
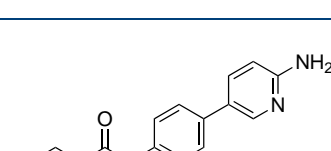
Moreover, half of the compounds with dual inhibitor activity contained aromatic substituents in the para position of the phenyl ring (**OSA_754** with 4-pyridinyl, **OSA_788** with benzothiophen-3-yl and **OSA_789** with 3-pyridinyl) (Table 5.2). Therefore, each compound of Elaboration Round 2 was designed with an additional phenyl group in the para position of the 1-methylpiperidine-4-(N-phenyl)carboxamide core. Based on visual analysis, the supplementary phenyl group may participate in π - π stacking with the aromatic rings of Phe-434 and Phe-149 present in the binding pocket, in addition to His-312 (Figure 5.6).

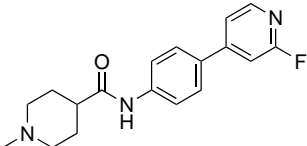
It is essential to be aware that this assessment assumes that the compounds of Elaboration Round 1 all bind in the same allosteric pocket as the original fragment hits. However, since no structural information is available from these compounds in complex with the protein target, this cannot be confirmed.

With this extensive analysis – and caveat - in mind, eight compounds (Table 5.3) were designed and synthesised for Elaboration Round 2, albeit limited to the chemicals that were available in the laboratory at the time. Compounds **OSA_1054**, **1055**, and **1056** all have at least one additional hydrogen bond donor or acceptor in the R₂ position. Compounds **OSA_1057**, **1058** and **1059** can be considered to have both R₂ and R₃ substituents, which are assumed to perfectly align in the cavity due to their geometry.

Lastly, compounds **OSA_1060** and **OSA_1061** are alterations on pyridine compounds from Elaboration Round 1. Table 5.3 shows that the eight compounds have a MW of more than 300 Da, but their CLogP remains consistently ≤ 3 , with compound **OSA_1059** as an outlier. It can also be concluded that these compounds comply with Lipinski's Ro5.

Table 5.3: Compounds **OSA_1054 – 1061** of Elaboration Round 2 with corresponding structures, molecular weight (MW), lipophilicity (CLogP, calculated using ChemDraw), and number of hydrogen bond donors and acceptors.

Compound number	Compound Structure	MW	CLogP	H-bond donors	H-bond acceptors
OSA_1054		309.4	1.9	2	4
OSA_1055		337.4	1.6	2	5
OSA_1056		324.4	2.1	2	4
OSA_1057		354.4	2.4	1	5
OSA_1058		334.4	1.8	2	5
OSA_1059		334.4	3.7	1	4
OSA_1060		310.4	0.4	2	5

OSA_1061		313.4	1.8	1	4
-----------------	---	-------	-----	---	---

5.3 ELABORATION ROUND 3

Although the SAR analysis provided a good starting point for Elaboration Round 2, the biochemical data on MurD % inhibition had to be interpreted with caution. In fact, this measurement was performed at a concentration of 1 mM, which is 25 times greater than the average IC₅₀ value for fragments and 2000 times greater than that for drugs (Table 5.1).⁽³⁷⁾ As this could have led to biased results, a dose-response curve was generated for the dual inhibitors (Figure 1.8 and Table 5.2) allowing for the actual IC₅₀ values to be derived. This experiment was carried out by our collaborator at the University of Warwick, PhD candidate Rebecca Steventon, after Elaboration Round 2 was already completed. Unfortunately, no data could be collected on dual inhibitor compound **OSA_788**, as it began to precipitate each time it was used in an assay.

As shown in Figure 5.7, for dual inhibitor compound **OSA_759**, a promising dose-response curve was obtained with an IC₅₀ value of 21.6 μM. According to a study by Schultes S. *et al.*, a typical pIC₅₀ value for favourable fragments fluctuates around 4.4, corresponding to an IC₅₀ value of 40 μM.⁽³⁷⁾ Thus, fragment **OSA_759** is the only of the identified dual inhibitors with an IC₅₀ value lower than the typical value found in the literature, providing a new starting point for designing compounds.

Additional assays were performed to investigate the mode of inhibition, and these showed that compound **OSA_759** inhibits the Mur ligases in a non-competitive manner to ATP. However, to get a clearer picture of whether it still binds to the potential allosteric pocket adjacent to the ATP binding site, crystallographic structure elucidation is necessary.

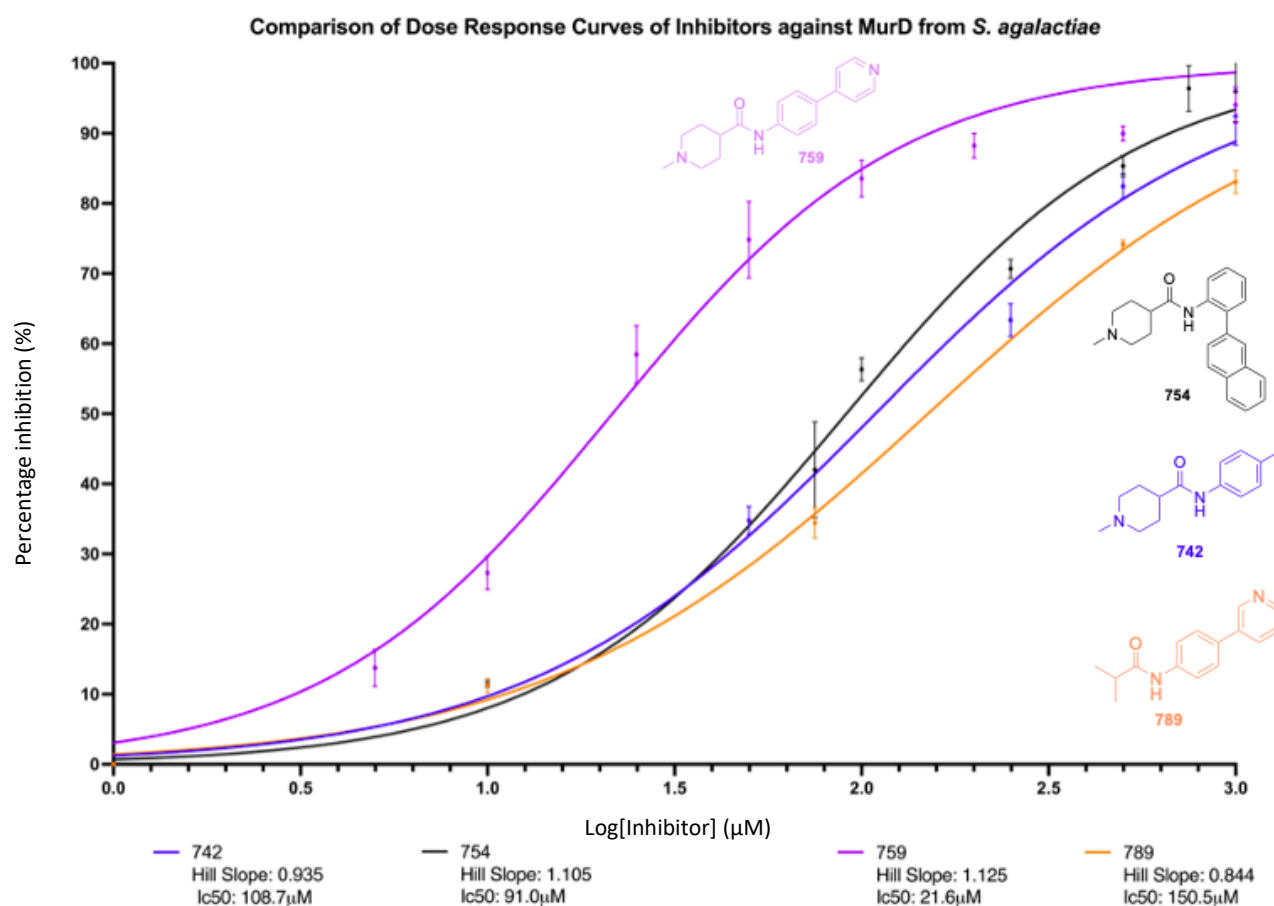


Figure 5.7: Dose-response curves with corresponding IC₅₀ values for dual inhibitor compounds **OSA_742**, **754**, **759**, and **789** from Elaboration Round 1. (Figure adapted from <https://github.com/opensourceantibiotics/murliqase/wiki/Dual-Inhibitors>.⁽³²⁾)

After analysing the chemical space of dual inhibitor compound **OSA_759** from Elaboration Round 1, 15 analogues were designed and synthesised with substituents in the meta- or para-positions of the *1-methylpiperidine-4-(N-phenyl)carboxamide* core (Table 5.3). Four of the para-analogues (**OSA_1062**, **1067**, **1068**, and **1069**) contain a fluoro or trifluoromethyl group, which are considered important functional groups in medicinal chemistry. When fluorine is incorporated into small-molecule drug candidates, significant changes in their physicochemical and pharmacokinetic behaviour are induced, such as improved membrane penetration and more stabilised drug metabolism. Moreover, fluorine-containing functional groups can positively influence the binding affinity of the compound for the target protein.⁽³⁹⁾

Furthermore, several positional isomers were synthesised throughout Round 1, 2, and 3 which were constructed as pairs, i.e., dual inhibitor Compound **OSA_759** (Round 1) and compound **OSA_1062**, compound **OSA_1061** and **1066**, compound **OSA_1063** and **1064**, and compound **OSA_1067** and **1068**. For the remaining para- and meta-analogues, the focus was on including unique and diverse substituents.

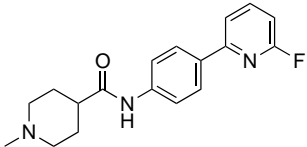
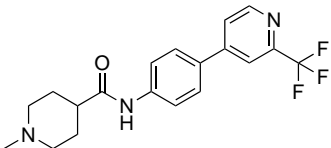
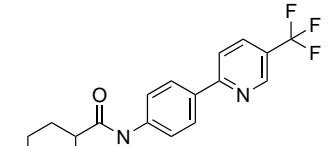
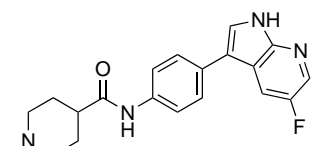
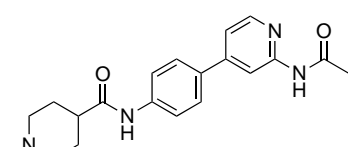
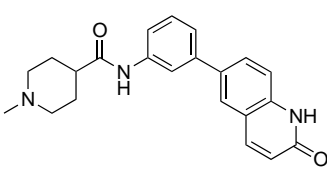
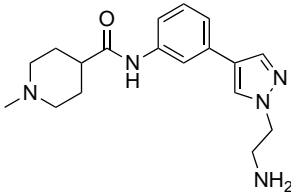
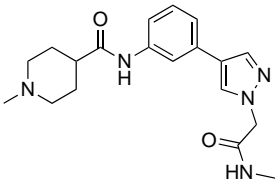
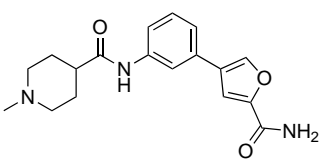
For this third Round too, shown in Table 5.4, all compounds have a MW of more than 300 Da (except for compound **OSA_1062**), and their CLogP remains consistently ≤ 3 . Also, it can be concluded that these compounds comply with Lipinski's Ro5.

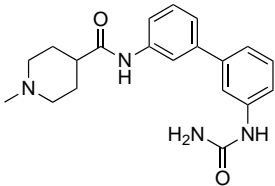
Since the substituents needed for the synthesis of compounds **OSA_1066 – 1075** were too costly as boronic acids or boronic esters, it was decided to purchase them as bromine analogues which function as the organohalide coupling partner in the Suzuki-Miyaura reaction. Consequently, it was necessary to convert the *1-methylpiperidine-4-(N-phenyl)carboxamide* core to a boronic ester *via* a Miyaura borylation to generate the other coupling partner. In the subsequent Suzuki reaction, the function of the coupling partners was essentially reversed compared to the synthesis of the other compounds. This approach was immensely timesaving in contrast to converting each bromine substituent into the corresponding boronic ester so that the coupling partners would remain constant.

Important to note is that all final products designed and synthesised for Round 2 and Round 3 of the 'FBDD Hit-to-Lead' approach were found to be novel compounds, according to a structure search using SciFinder. The novelty of the compounds emphasises the need for full characterisation, which includes m.p. determination, LRMS, HRMS, ¹H NMR, ¹³C NMR and infrared spectroscopy.

*Table 5.4: Compounds **OSA_1062 – 1070** and **OSA_1088 – 1092** from Elaboration Round 3 with corresponding structures, molecular weight (MW), lipophilicity (CLogP, calculated using ChemDraw), and number of hydrogen bond donors and acceptors.*

Compound number	Compound Structure	MW	CLogP	H-bond donors	H-bond acceptors
OSA_1062		295.4	1.6	1	4
OSA_1063		319.4	2.5	1	4
OSA_1064		319.4	2.5	1	4
OSA_1065		373.5	1.3	2	6

OSA_1066		313.4	2.0	1	4
OSA_1067		363.4	2.5	1	4
OSA_1068		363.4	2.7	1	4
OSA_1069		352.4	1.7	2	5
OSA_1070		352.4	0.6	2	6
OSA_1088		361.4	1.8	2	5
OSA_1089		327.4	0.6	2	6
OSA_1090		355.4	0.16	2	7
OSA_1091		327.4	0.8	2	6

OSA_1092		352.4	1.8	3	6
-----------------	---	-------	-----	---	---

5.4 FUTURE PERSPECTIVES

As discussed in the most recent monthly meeting, compounds from Elaboration Round 2 and 3 are expected to be evaluated using three different assays that complement each other.⁽⁴⁰⁾ First, the enzymic assay will be carried out where the compounds target % inhibition can be determined. A stopped Pi release assay can be used to assess the residual activity of the Mur ligases in the presence of the compounds. Ultimately, dose-response curves can be constructed from which the IC₅₀ can be derived.⁽³¹⁾ Since this assay requires the compounds to be pure, purification of **OSA_1056** and **1062**, and **OSA_1066 – 1070** will be completed by Dr. Tse. Secondly, surface plasmon resonance (SPR) analysis, which is an optical technique used for the detection of molecular interactions between the compounds and the Mur ligases will be performed. Here, dose-response curves of the dissociation rate constant (K_d), which is a measure of binding affinity, can be generated.⁽³⁴⁾ Finally, new crystal soaking experiments will be done to structurally confirm the binding site of the compounds by X-ray crystallography. All these experiments will be carried out by our collaborators at the University of Warwick and the University of Oxford.

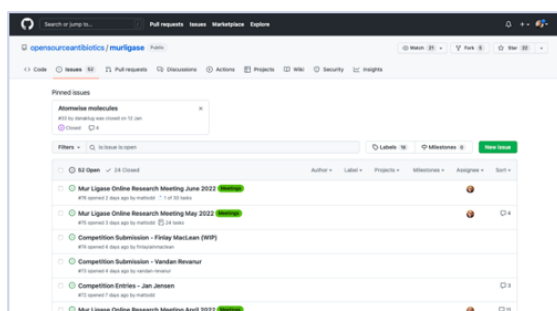
Based on the data that will be obtained for compounds **OSA_1054 – 1070**, further fragment elaboration will be initiated to ultimately achieve an inhibitor with good affinity and potency for at least two of the Mur ligases. Ideally, the drug candidate that emerges from the Elaboration Rounds should comply to Lipinski's Ro5, which is a predictor for good oral absorption, and should be able to efficiently penetrate the bacterial cell.

5.5 RETROSPECTION ON OPEN SCIENCE

As extensively discussed in the Introduction, this project took place in an Open Source context. In essence, three platforms were used to make all the premises of Open Source research possible (Figure 5.8). Twitter, or other social media, was used to involve a wider audience with the project (A). GitHub is a platform, originally created for software development, where collaborators started discussions and asked questions related to the key advances of the project, from chemistry to biology (B). A personalised electronic laboratory notebook was used to record all experimental details and results, which are publicly available and were viewable in real-time (C).



A



B



C

Figure 5.8: Three key platforms for the OSA Mur ligase project. (A) OSA Twitter where things can be shared with collaborators around the world;⁽⁴¹⁾ (B) OSA GitHub where all aspects of the project are discussed;⁽⁴²⁾ (C) Electronic Laboratory Notebook where all experimental information is recorded.⁽⁴³⁾

In addition, monthly meetings were organised where the overall strategy and recent results were discussed. These are also public and were always uploaded to YouTube and linked in GitHub afterwards. All content that originates from GitHub is licensed as CC-BY-4.0.⁽¹²⁾

It can be concluded that the openness of the project contributed greatly to various aspects of this research project. First, information about the different parts of the Mur ligase project could be readily retrieved by using the wiki page on GitHub.⁽²⁶⁾ The fact that all information is gathered in one place that can be accessed at any time has greatly facilitated the writing of this thesis. The issue tool on GitHub was used for sharing ideas and asking questions about the project.⁽⁴²⁾ The ability to speak with qualified experts involved in the project efficiently resolved any problems that arose. The advantage of doing this openly rather than privately is that people can elaborate on it rather than having to ask the same question repeatedly. Finally, it was remarkable how often scientists with no previous connection to the project participated in discussions. This emphasises one of the key elements of Open Source research, namely that a wider audience can be involved, from every background and level, all over the world.⁽¹¹⁾

6 REFERENCES

1. Ten threats to global health in 2019 [Internet]. [cited 2021 Dec 4]. Available from: <https://www.who.int/news-room/spotlight/ten-threats-to-global-health-in-2019>
2. 10 global health issues to track in 2021 [Internet]. [cited 2021 Dec 4]. Available from: <https://www.who.int/news-room/spotlight/10-global-health-issues-to-track-in-2021>
3. Khardori N, Stevaux C, Ripley K. Antibiotics: From the Beginning to the Future: Part 2. *Indian J Pediatr*. 2020 Jan 5;87(1):43–7. Available from: <http://www.archivepp.com/text.asp?2016/7/3/110/186181>
4. Morel CM, Lindahl O, Harbarth S, de Kraker MEA, Edwards S, Hollis A. Industry incentives and antibiotic resistance: an introduction to the antibiotic susceptibility bonus. *J Antibiot (Tokyo)*. 2020;73(7):421–8. Available from: <http://dx.doi.org/10.1038/s41429-020-0300-y>
5. Renwick MJ, Brogan DM, Mossialos E. A systematic review and critical assessment of incentive strategies for discovery and development of novel antibiotics. *J Antibiot (Tokyo)*. 2016 Feb 14;69(2):73–88. Available from: <http://www.nature.com/articles/ja201598>
6. Laxminarayan R, Matsoso P, Pant S, Brower C, Røttingen JA, Klugman K, et al. Access to effective antimicrobials: A worldwide challenge. *Lancet*. 2016;387(10014):168–75. Available from: <https://linkinghub.elsevier.com/retrieve/pii/S0140673615004742>
7. McKenna M. The antibiotic paradox: why companies can't afford to create life-saving drugs. *Nature*. 2020 Aug 20;584(7821):338–41. Available from: <https://www.nature.com/articles/d41586-020-02418-x>
8. Hutchings M, Truman A, Wilkinson B. Antibiotics: past, present and future. *Curr Opin Microbiol* [Internet]. 2019;51(Figure 1):72–80. Available from: <https://doi.org/10.1016/j.mib.2019.10.008>
9. Årdal C, Balasegaram M, Laxminarayan R, McAdams D, Outterson K, Rex JH, et al. Antibiotic development — economic, regulatory and societal challenges. *Nat Rev Microbiol*. 2020;18(5):267–74. Available from: <http://dx.doi.org/10.1038/s41579-019-0293-3>
10. Plackett B. Why big pharma has abandoned antibiotics. *Nature*. 2020 Oct 22;586(7830):S50–2. Available from: <https://www.nature.com/articles/d41586-020-02884-3>
11. Klug DM, Idris FIM, Blaskovich MAT, von Delft F, Dowson CG, Kirchhelle C, et al. There is no market for new antibiotics: this allows an open approach to research and development. *Wellcome Open Res*. 2021 Jun 11;6:146. Available from: <https://wellcomeopenresearch.org/articles/6-146/v1>
12. Balasegaram M, Kolb P, McKew J, Menon J, Oliaro P, Sablinski T, et al. An open source pharma roadmap. *PLOS Med*. 2017 Apr 18;14(4):e1002276. Available from: <https://dx.plos.org/10.1371/journal.pmed.1002276>
13. Home · opensourceantibiotics/GeneralTopics Wiki · GitHub [Internet]. [cited 2021 Aug 13]. Available from: <https://github.com/opensourceantibiotics/GeneralTopics/wiki>
14. Kouidmi I, Levesque RC, Paradis-Bleau C. The biology of Mur ligases as an antibacterial target. *Mol Microbiol*. 2014 Oct;94(2):242–53. Available from: <https://onlinelibrary.wiley.com/doi/10.1111/mmi.12758>
15. York A, Lloyd AJ, del Genio CI, Shearer J, Hinxman KJ, Fritz K, et al. Structure-based modeling and dynamics of MurM, a *Streptococcus pneumoniae* penicillin resistance determinant present at the

cytoplasmic membrane. *Structure*. 2021 Jul;29(7):731-742.e6. Available from: <https://linkinghub.elsevier.com/retrieve/pii/S0969212621000745>

16. Tomašić T, Zidar N, Kovač A, Turk S, Simčič M, Blanot D, et al. 5-Benzylidenethiazolidin-4-ones as Multitarget Inhibitors of Bacterial Mur Ligases. *ChemMedChem*. 2010 Feb 1;5(2):286–95. Available from: <https://onlinelibrary.wiley.com/doi/10.1002/cmdc.200900449>
17. Aminov RI. A Brief History of the Antibiotic Era: Lessons Learned and Challenges for the Future. *Front Microbiol*. 2010;1(DEC):1–7. Available from: <http://journal.frontiersin.org/article/10.3389/fmicb.2010.00134/abstract>
18. Tommasi R, Brown DG, Walkup GK, Manchester JI, Miller AA. ESKAPEing the labyrinth of antibacterial discovery. *Nat Rev Drug Discov*. 2015;14(8):529–42. Available from: <https://doi.org/10.1038/nrd4572>
19. Hameed P S, Manjrekar P, Chinnapattu M, Humnabadkar V, Shanbhag G, Kedari C, et al. Pyrazolopyrimidines Establish MurC as a Vulnerable Target in *Pseudomonas aeruginosa* and *Escherichia coli*. *ACS Chem Biol*. 2014 Oct 17;9(10):2274–82. Available from: <https://pubs.acs.org/doi/10.1021/cb500360c>
20. Humnabadkar V, Prabhakar KR, Narayan A, Sharma S, Guptha S, Manjrekar P, et al. UDP- N - Acetylmuramic Acid I -Alanine Ligase (MurC) Inhibition in a tolC Mutant *Escherichia coli* Strain Leads to Cell Death. *Antimicrob Agents Chemother*. 2014 Oct;58(10):6165–71. Available from: <https://journals.asm.org/doi/10.1128/AAC.02890-14>
21. Perdih A, Kovač A, Wolber G, Blanot D, Gobec S, Solmajer T. Discovery of novel benzene 1,3-dicarboxylic acid inhibitors of bacterial MurD and MurE ligases by structure-based virtual screening approach. *Bioorg Med Chem Lett*. 2009 May;19(10):2668–73. Available from: <https://linkinghub.elsevier.com/retrieve/pii/S0960894X09004636>
22. Perdih A, Hrast M, Barreateau H, Gobec S, Wolber G, Solmajer T. Benzene-1,3-dicarboxylic acid 2,5-dimethylpyrrole derivatives as multiple inhibitors of bacterial Mur ligases (MurC–MurF). *Bioorganic Med Chem*. 2014;22(15):4124–34. Available from: <http://dx.doi.org/10.1016/j.bmc.2014.05.058>
23. Perdih A, Hrast M, Pureber K, Barreateau H, Grdadolnik SG, Kocjan D, et al. Furan-based benzene mono- and dicarboxylic acid derivatives as multiple inhibitors of the bacterial Mur ligases (MurC–MurF): experimental and computational characterization. *J Comput Aided Mol Des*. 2015 Jun 8;29(6):541–60. Available from: <http://link.springer.com/10.1007/s10822-015-9843-6>
24. Barreateau H, Sosič I, Turk S, Humljan J, Tomašić T, Zidar N, et al. MurD enzymes from different bacteria: Evaluation of inhibitors. *Biochem Pharmacol*. 2012 Sep;84(5):625–32. Available from: <https://linkinghub.elsevier.com/retrieve/pii/S0006295212004042>
25. Kirsch P, Hartman AM, Hirsch AKH, Empting M. Concepts and Core Principles of Fragment-Based Drug Design. Merz KM, Ringe D, Reynolds CH, editors. *Molecules*. 2019 Nov 26;24(23):4309. Available from: <https://www.mdpi.com/1420-3049/24/23/4309>
26. Overview · opensourceantibiotics/murligase Wiki · GitHub [Internet]. [cited 2022 Jan 5]. Available from: <https://github.com/opensourceantibiotics/murligase/wiki/Overview>
27. Jahnke W, Erlanson DA, de Esch IJP, Johnson CN, Mortenson PN, Ochi Y, et al. Fragment-to-Lead Medicinal Chemistry Publications in 2019. *J Med Chem*. 2020 Dec 24;63(24):15494–507. Available from: <https://pubs.acs.org/doi/10.1021/acs.jmedchem.0c01608>
28. DSI-poised Library - Enamine [Internet]. [cited 2022 Jan 4]. Available from: <https://enamine.net/compound-libraries/fragment-libraries/dsi-poised-library>

29. DSI-Poised Library - - Diamond Light Source [Internet]. [cited 2022 Jan 4]. Available from: <https://www.diamond.ac.uk/Instruments/Mx/Fragment-Screening/Fragment-Libraries0/DSI-Poised-Library.html>
30. Initial MurD Hits · opensourceantibiotics/murligase Wiki · GitHub [Internet]. [cited 2022 Jan 5]. Available from: <https://github.com/opensourceantibiotics/murligase/wiki/Initial-MurD-Hits>
31. MurD Round 1 · opensourceantibiotics/murligase Wiki · GitHub [Internet]. [cited 2022 Jan 5]. Available from: <https://github.com/opensourceantibiotics/murligase/wiki/MurD-Round-1>
32. Dual Inhibitors · opensourceantibiotics/murligase Wiki · GitHub [Internet]. [cited 2022 May 4]. Available from: <https://github.com/opensourceantibiotics/murligase/wiki/Dual-Inhibitors>
33. Roberts JD, Weigert FJ. Carbon-13 nuclear magnetic resonance spectroscopy. Determination of carbon-fluorine couplings. *J Am Chem Soc.* 1971 May 1;93(10):2361–9. Available from: <http://xlink.rsc.org/?DOI=ar9221900030>
34. SPR with the Atomwise library · opensourceantibiotics/murligase Wiki · GitHub [Internet]. [cited 2022 May 13]. Available from: <https://github.com/opensourceantibiotics/murligase/wiki/SPR-with-the-Atomwise-library>
35. Klug DM, Tschiegg L, Diaz R, Rojas-Barros D, Perez-Moreno G, Ceballos G, et al. Hit-to-Lead Optimization of Benzoxazepinoindazoles As Human African Trypanosomiasis Therapeutics. *J Med Chem.* 2020 Mar 12;63(5):2527–46. Available from: <https://pubs.acs.org/doi/10.1021/acs.jmedchem.9b01506>
36. Neeve EC, Geier SJ, Mkhali IAI, Westcott SA, Marder TB. Diboron(4) Compounds: From Structural Curiosity to Synthetic Workhorse. *Chem Rev.* 2016 Aug 24;116(16):9091–161. Available from: <https://pubs.acs.org/doi/10.1021/acs.chemrev.6b00193>
37. Schultes S, de Graaf C, Haaksma EEJ, de Esch IJP, Leurs R, Krämer O. Ligand efficiency as a guide in fragment hit selection and optimization. *Drug Discov Today Technol.* 2010;7(3):e157–62. Available from: <https://linkinghub.elsevier.com/retrieve/pii/S1740674910000363>
38. Congreve M, Carr R, Murray C, Jhoti H. A ‘Rule of Three’ for fragment-based lead discovery? *Drug Discov Today.* 2003 Oct;8(19):876–7. Available from: <https://linkinghub.elsevier.com/retrieve/pii/S135964460302765X>
39. Shah P, Westwell AD. The role of fluorine in medicinal chemistry. *J Enzyme Inhib Med Chem.* 2007 Jan 4;22(5):527–40. Available from: <http://www.tandfonline.com/doi/full/10.1080/14756360701425014>
40. Mur Ligase Online Research Meeting May 2022 · Issue #75 · opensourceantibiotics/murligase · GitHub [Internet]. [cited 2022 May 17]. Available from: <https://github.com/opensourceantibiotics/murligase/issues/75>
41. OSantibiotics (@OSantibiotics) / Twitter [Internet]. [cited 2022 May 13]. Available from: <https://twitter.com/osantibiotics>
42. Issues · opensourceantibiotics/murligase · GitHub [Internet]. [cited 2022 May 13]. Available from: <https://github.com/opensourceantibiotics/murligase/issues>
43. Kato Leonard - LabArchives, Your Electronic Lab Notebook [Internet]. [cited 2022 May 17]. Available from: <https://tinyurl.com/OSA-KatoLeonard>

ADDENDA

The addenda include the NMR spectra of all synthesised compounds and the mass spectra (high resolution) of the final **OSA** compounds from Elaboration Round 2 and 3.

ADDENDUM 1 - NMR: SYNTHESIS OF BROMO SUBSTITUTED CORE (compound **3a and **3b**)**

1. *N*-(4-Bromophenyl)-1-methylpiperidine-4-carboxamide (**3a**)

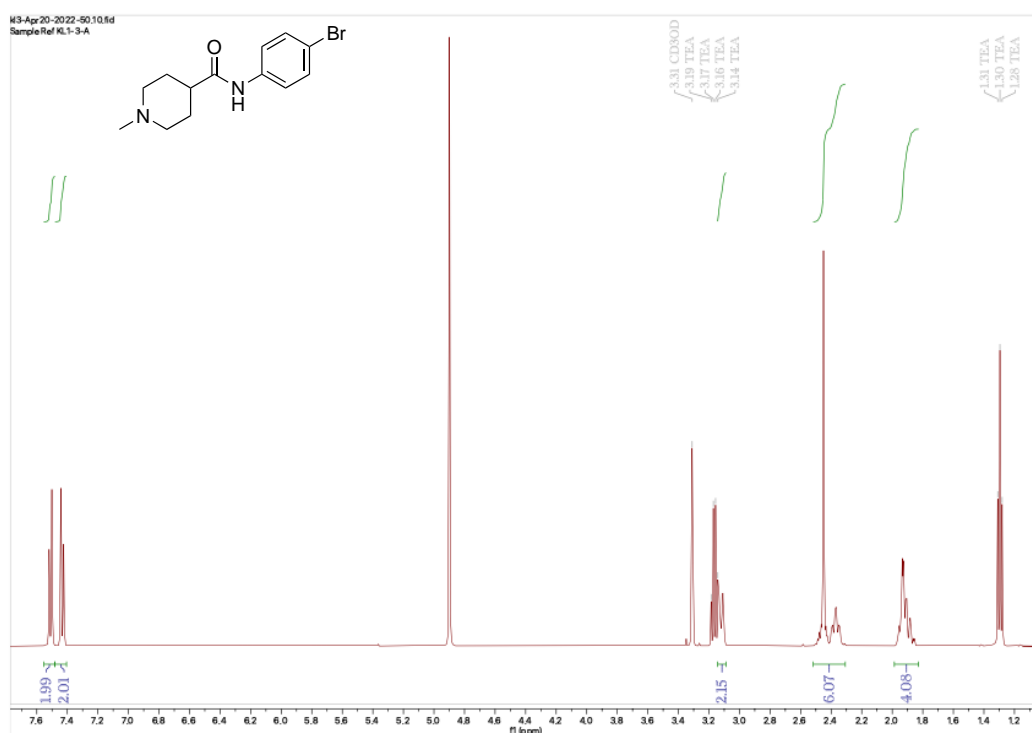


Figure 1: ¹H NMR compound **3a**

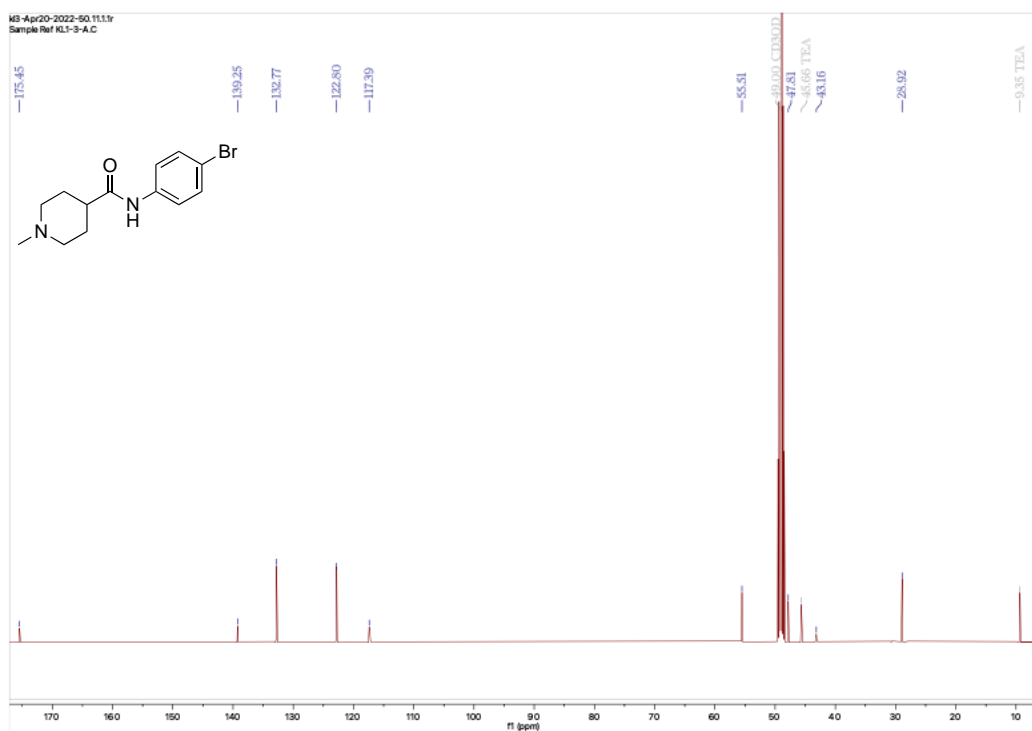


Figure 2: ¹³C NMR compound **3a**

2. *N*-(3-Bromophenyl)-1-methylpiperidine-4-carboxamide (**3b**)

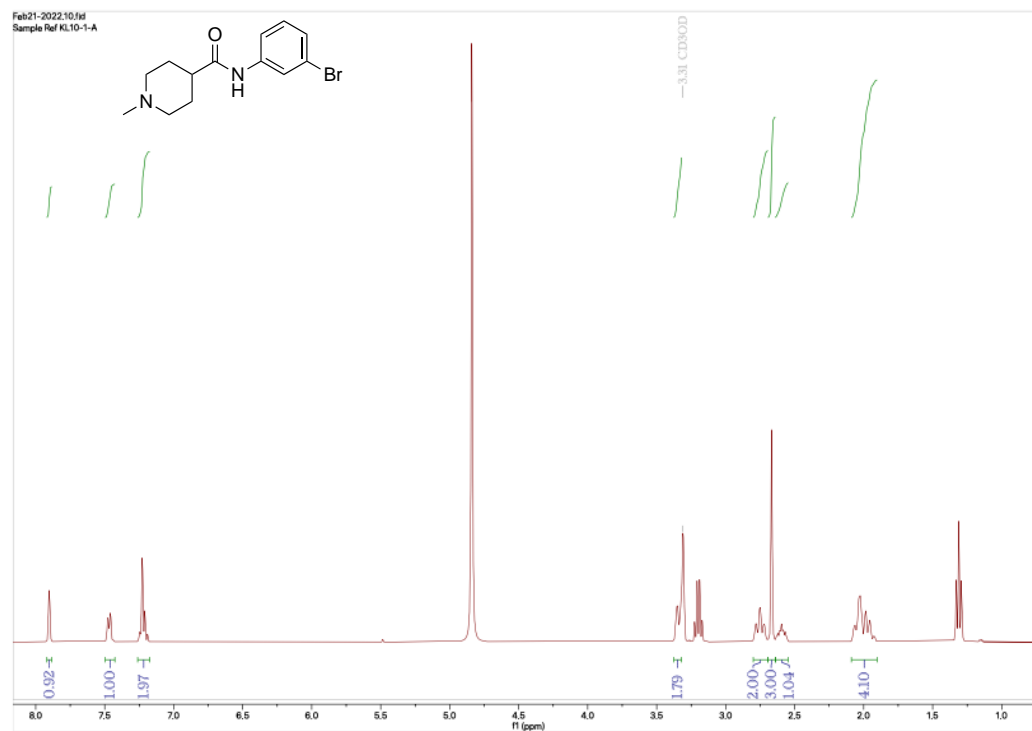


Figure 3: ¹H NMR compound **3b**

ADDENDUM 2 - NMR: SYNTHESIS OF THE BORONIC ESTER SUBSTITUTED CORE (compound 5)

1. *N*-(4-(4,4,5,5-Tetramethyl-1,3,2-dioxaborolan-2-yl)phenyl)-1-methylpiperidine-4-carboxamide (**5**)

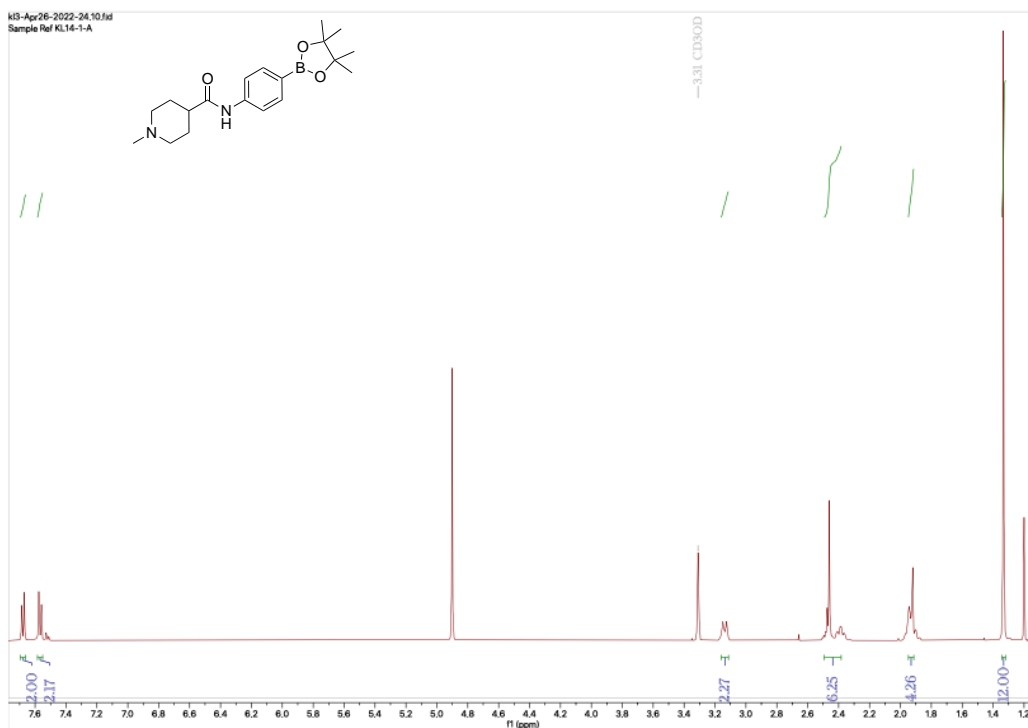


Figure 4: ¹H NMR compound 5

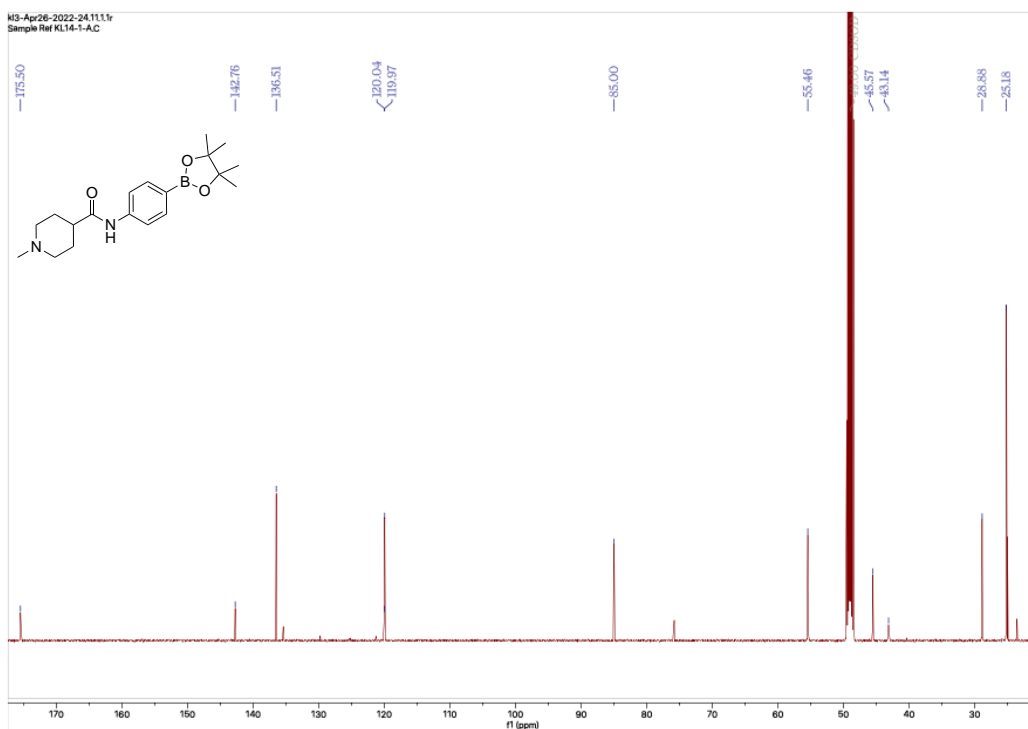


Figure 5: ¹³C NMR compound 5

ADDENDUM 3 - NMR: SYNTHESIS OF OSA_1054 – 1068

1. N-(3'-Amino-[1,1'-biphenyl]-4-yl)-1-methylpiperidine-4-carboxamide (OSA_1054)

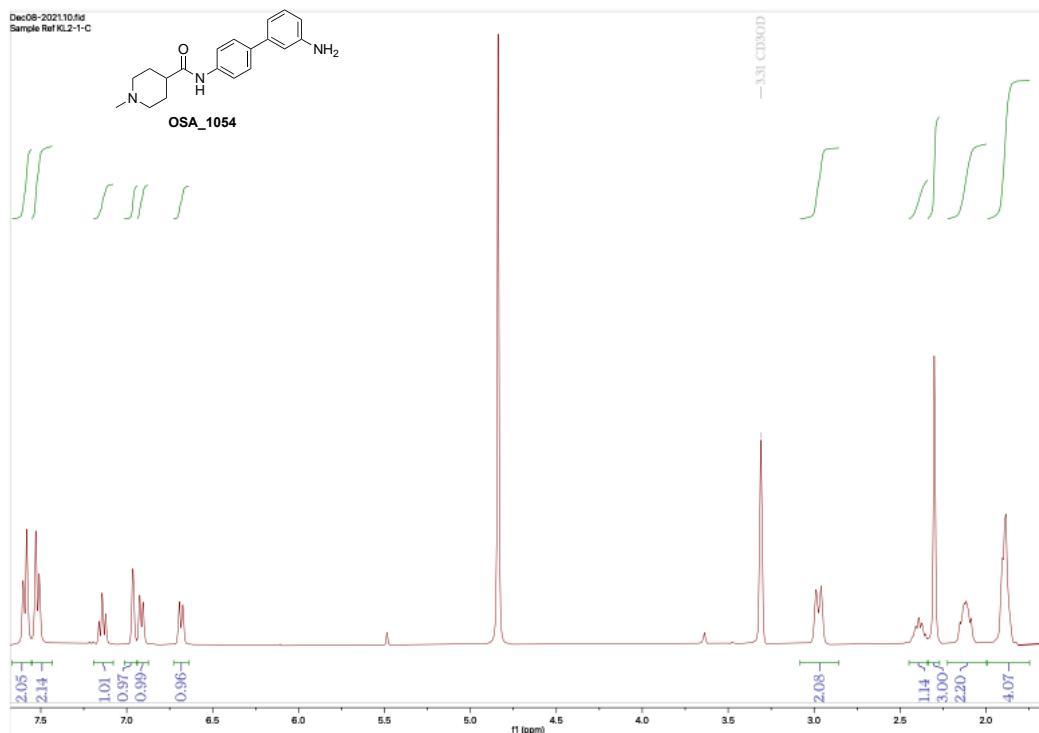


Figure 6: ¹H NMR compound OSA_1054

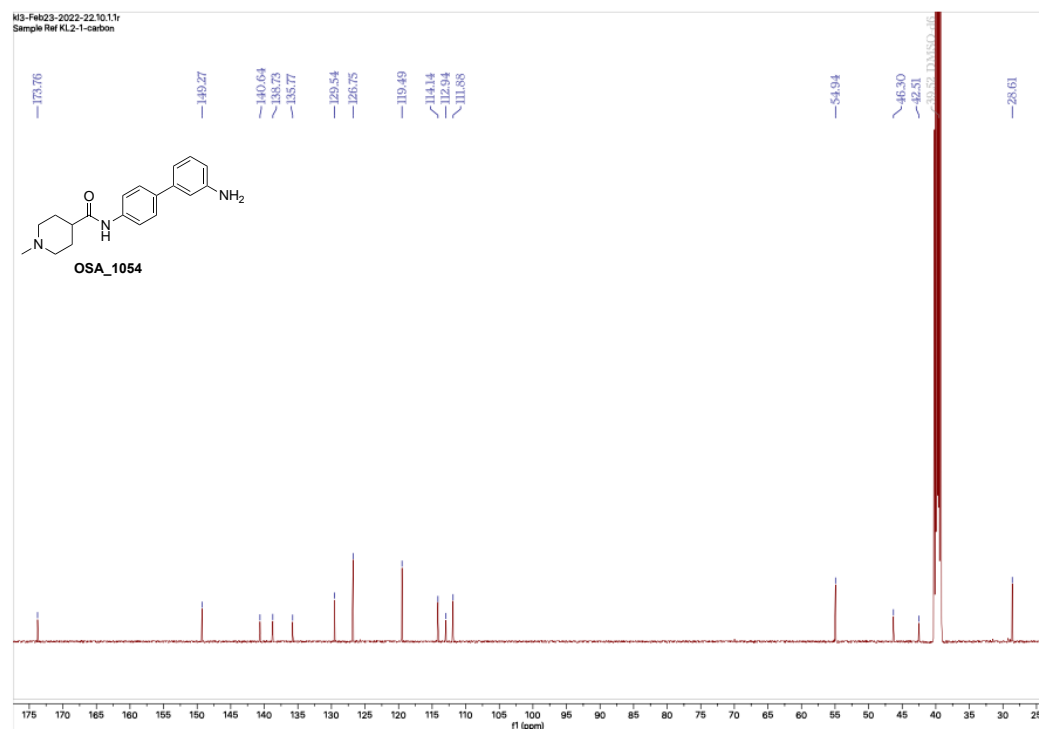


Figure 7: ¹³C NMR compound OSA_1054

2. *N*-(3'-Carbamoyl-[1,1'-biphenyl]-4-yl)-1-methylpiperidine-4-carboxamide (OSA 1055)

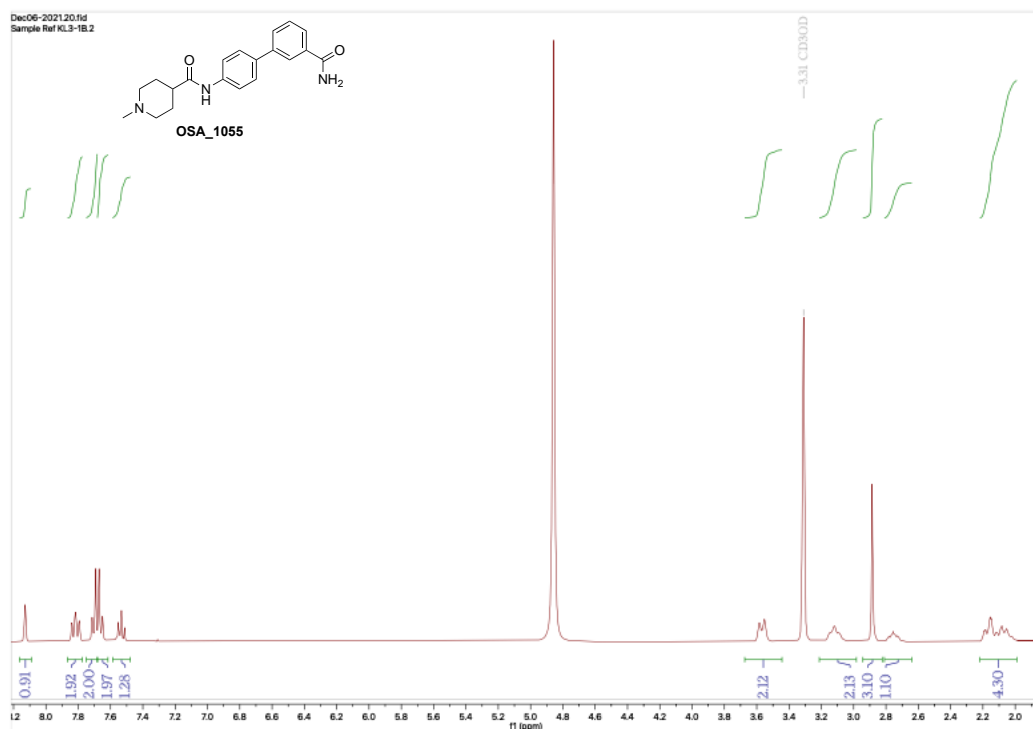


Figure 8: ^1H NMR compound **OSA_1055**

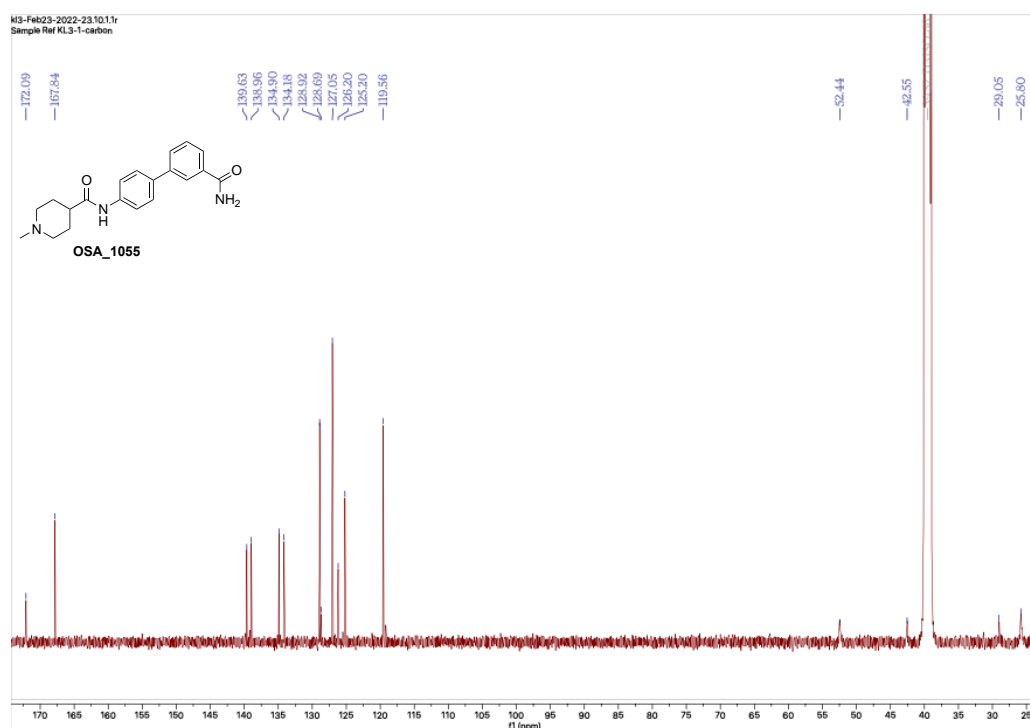


Figure 9: ^{13}C NMR compound OSA_1055

3. *N*-(3'-(Hydroxymethyl)-[1,1'-biphenyl]-4-yl)-1-methylpiperidine-4-carboxamide (OSA_1056)

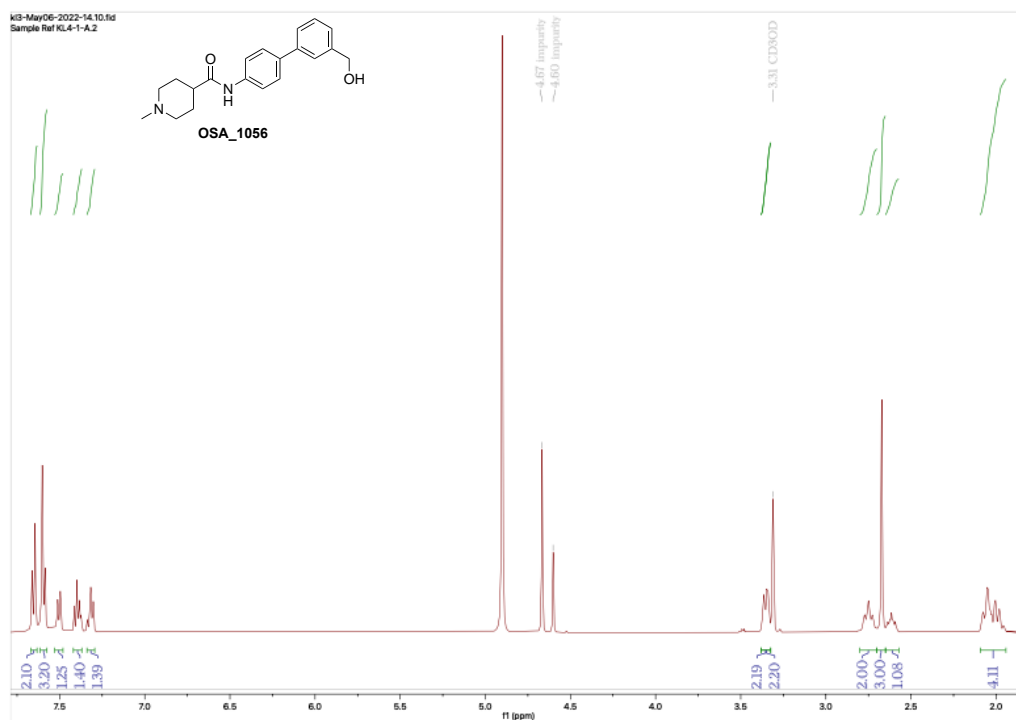


Figure 10: ^1H NMR compound OSA_1056

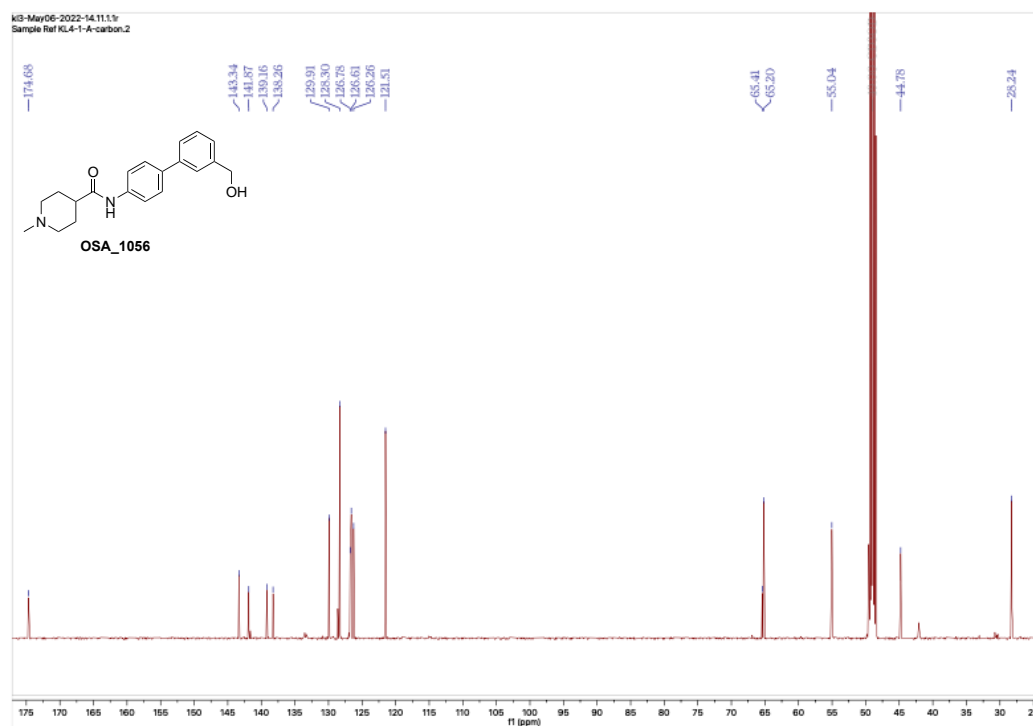


Figure 11: ^{13}C NMR compound OSA_1056

4. *N*-(3',4'-Dimethoxy-[1,1'-biphenyl]-4-yl)-1-methylpiperidine-4-carboxamide (OSA_1057)

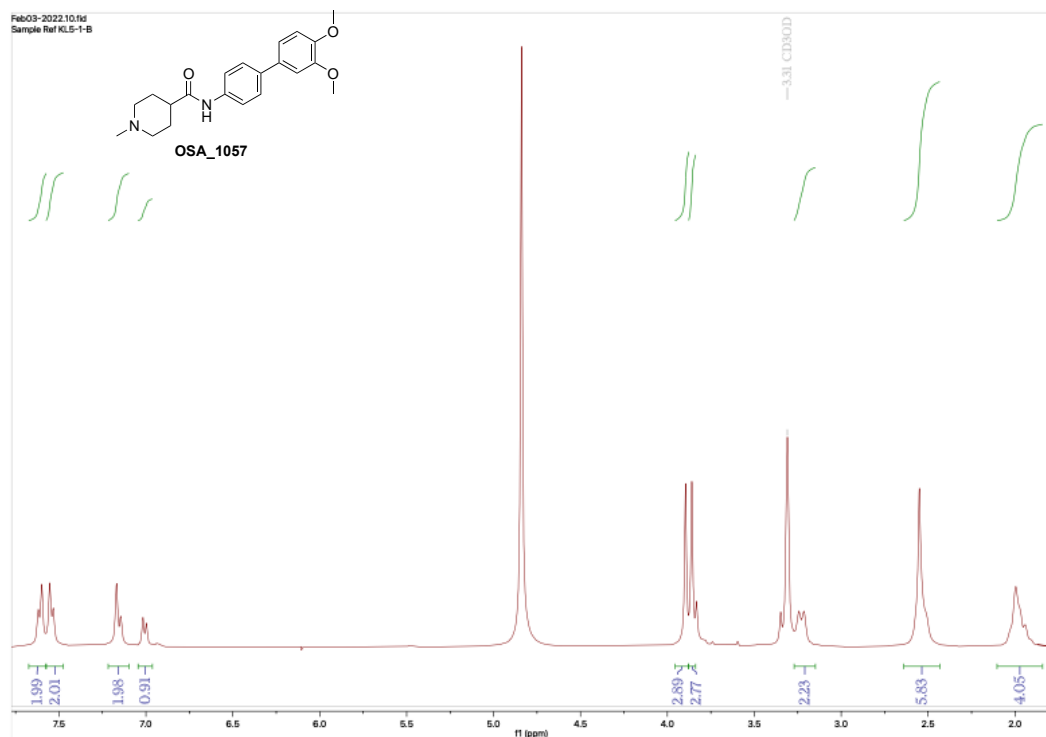


Figure 12: ¹H NMR compound OSA_1057

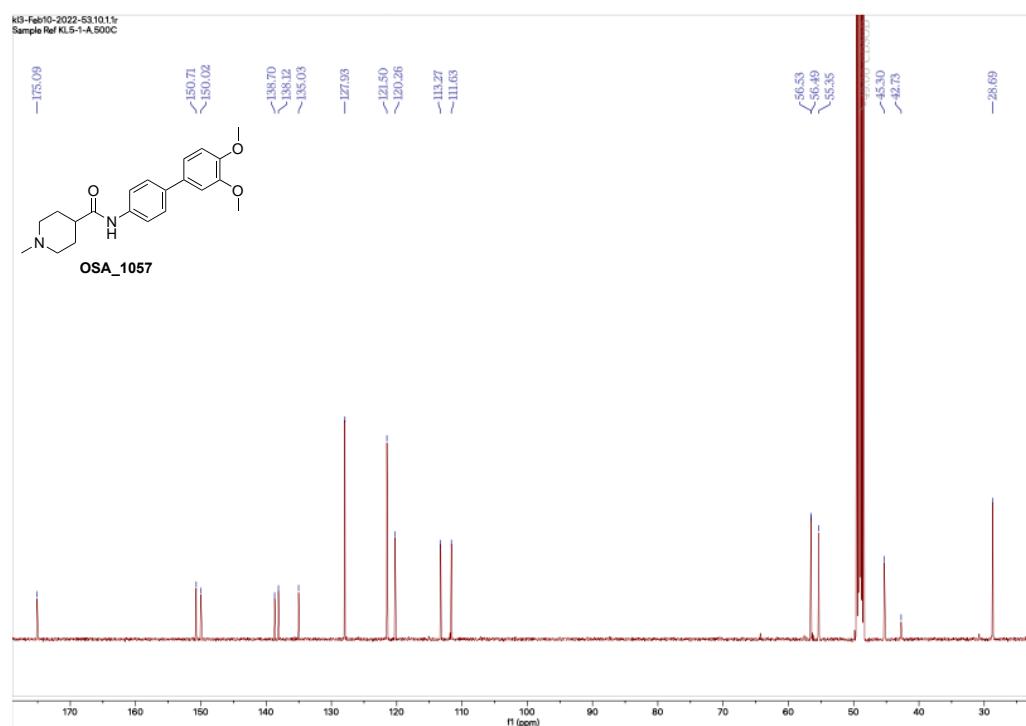


Figure 13: ¹³C NMR compound OSA_1057

5. *N*-(4-(1*H*-Benzo[d]imidazol-5-yl)phenyl)-1-methylpiperidine-4-carboxamide (**OSA_1058**)

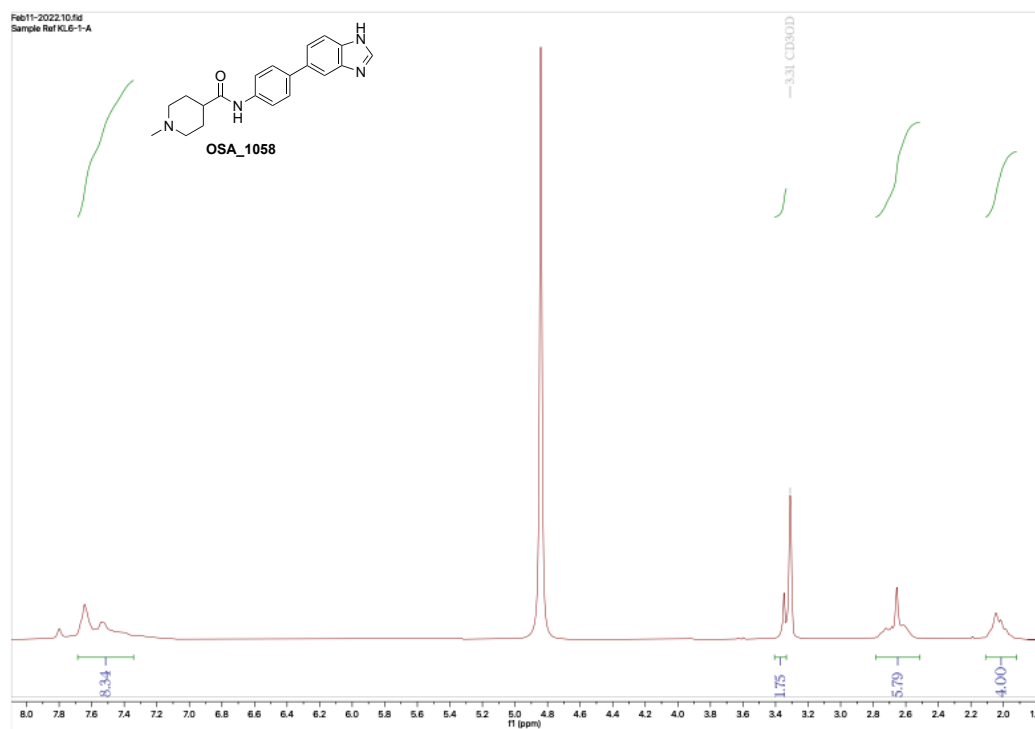


Figure 14: ¹H NMR compound **OSA_1058**

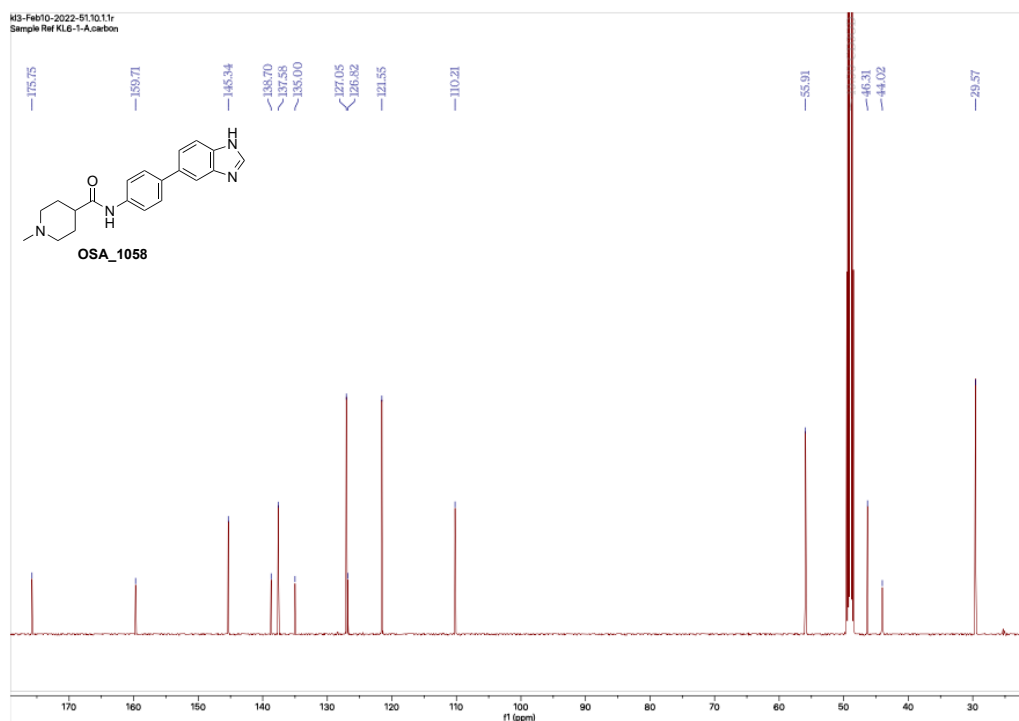


Figure 15: ¹³C NMR compound **OSA_1058**

6. *N*-(4-(Benzofuran-5-yl)phenyl)-1-methylpiperidine-4-carboxamide (OSA 1059)

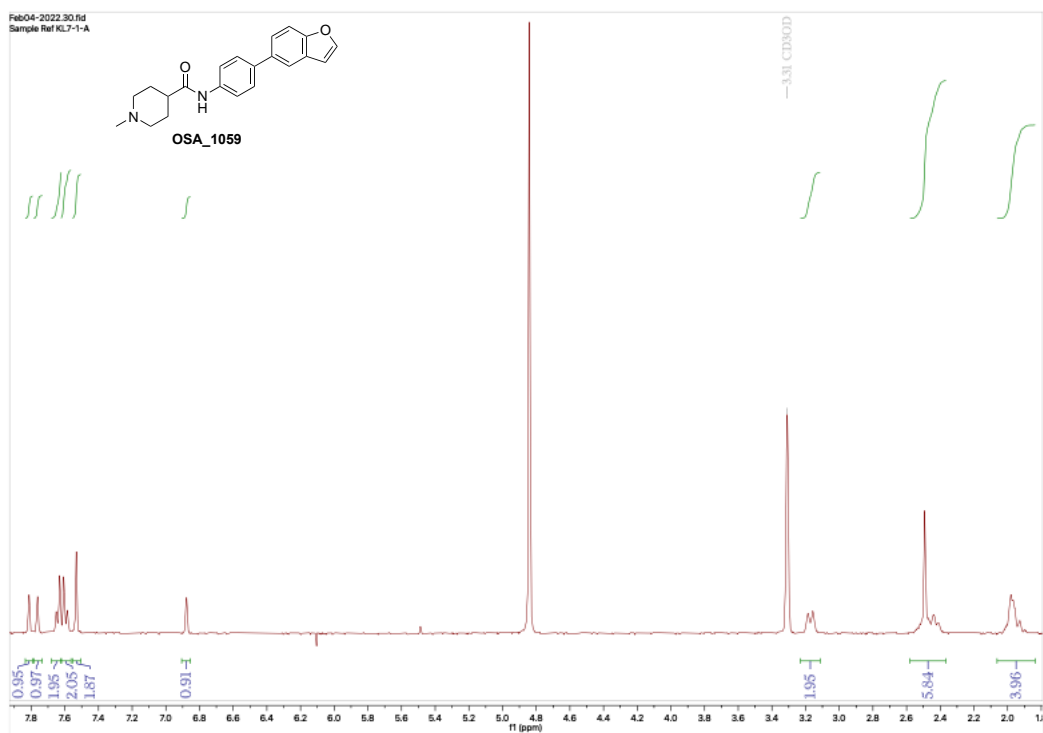


Figure 16: ¹H NMR compound **OSA_1059**

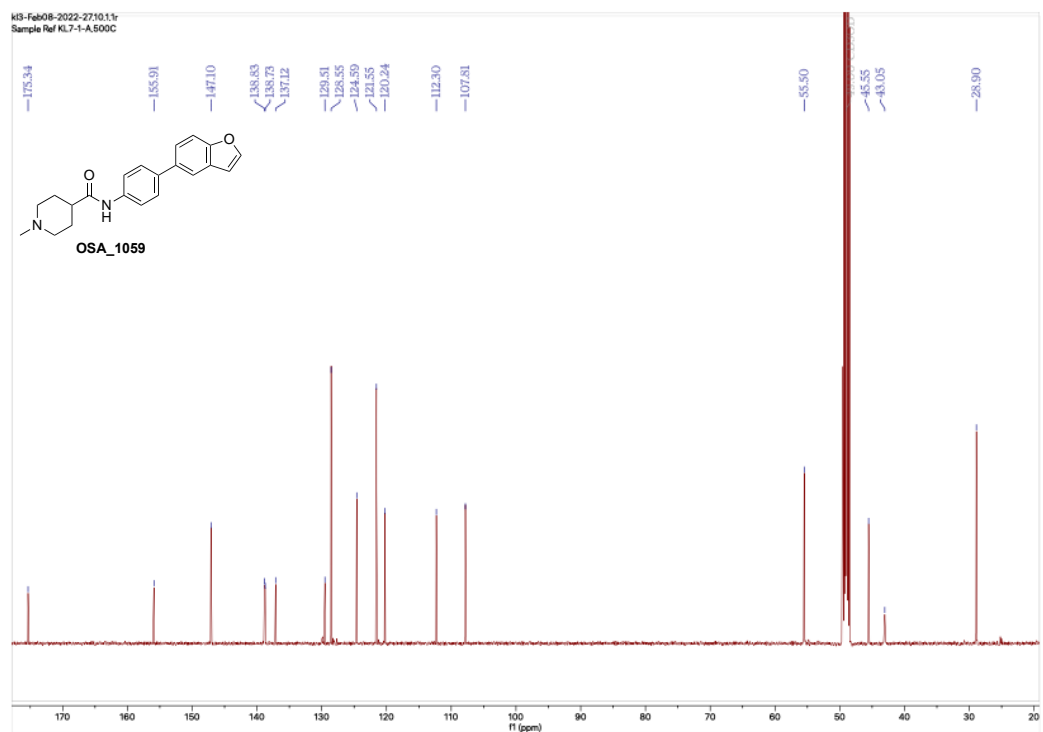


Figure 17: ¹³C NMR compound **OSA_1059**

7. *N*-(4-(6-Aminopyridin-3-yl)phenyl)-1-methylpiperidine-4-carboxamide (OSA 1060)

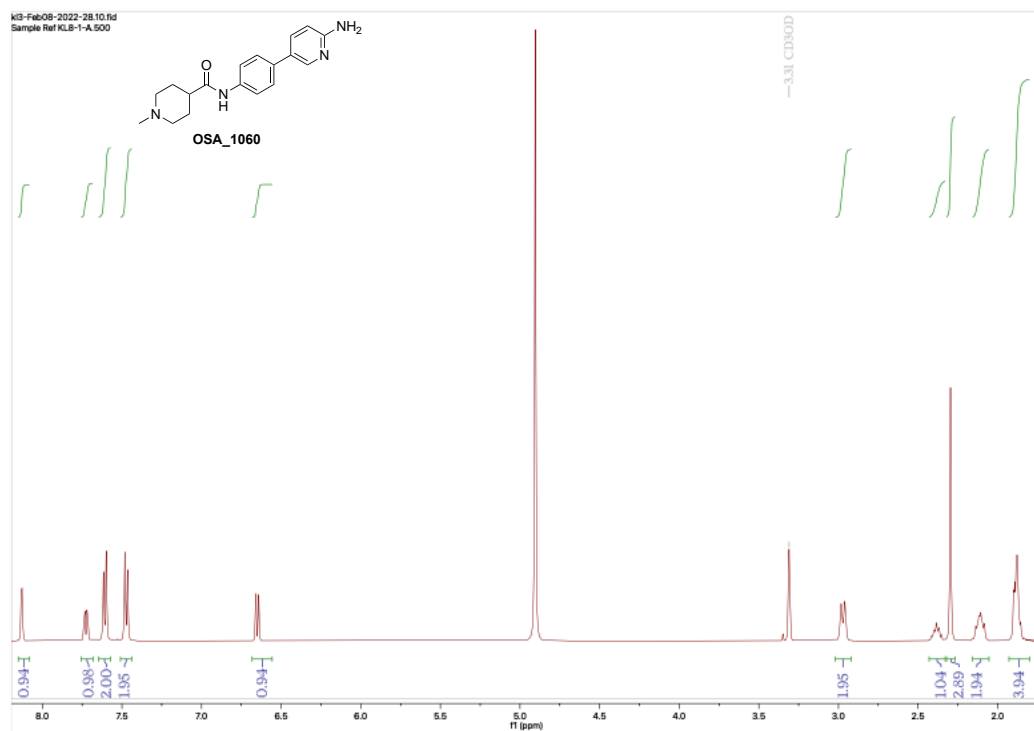


Figure 18: ¹H NMR compound **OSA_1060**

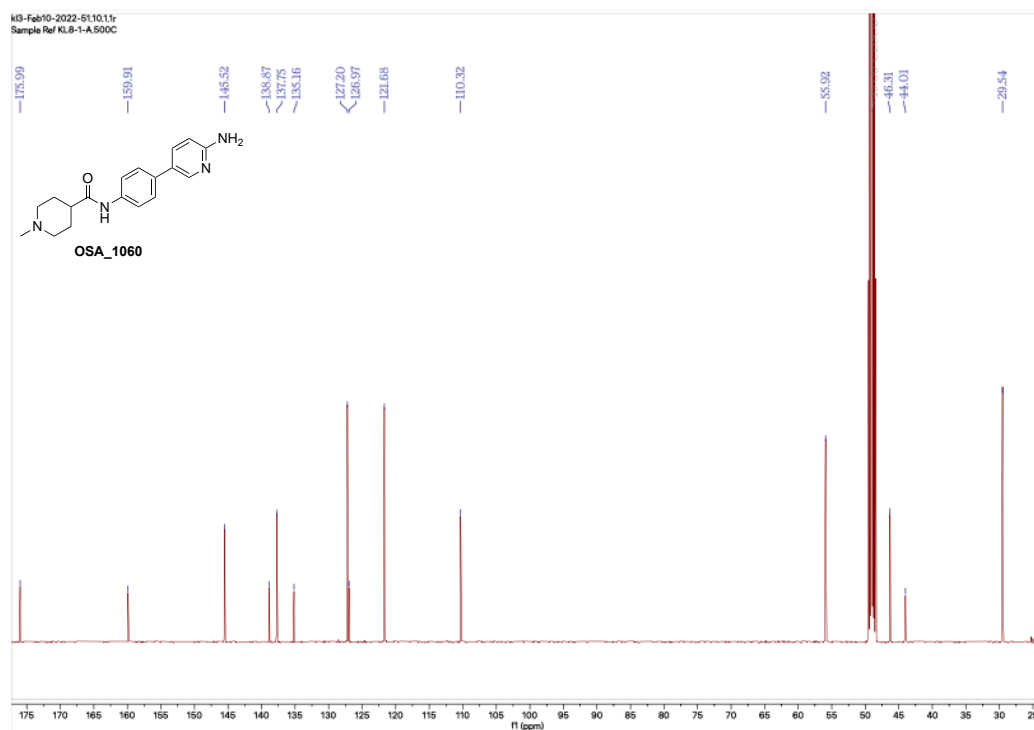


Figure 19: ¹³C NMR compound **OSA_1060**

8. *N*-(4-(2-Fluoropyridin-4-yl)phenyl)-1-methylpiperidine-4-carboxamide (OSA 1061)

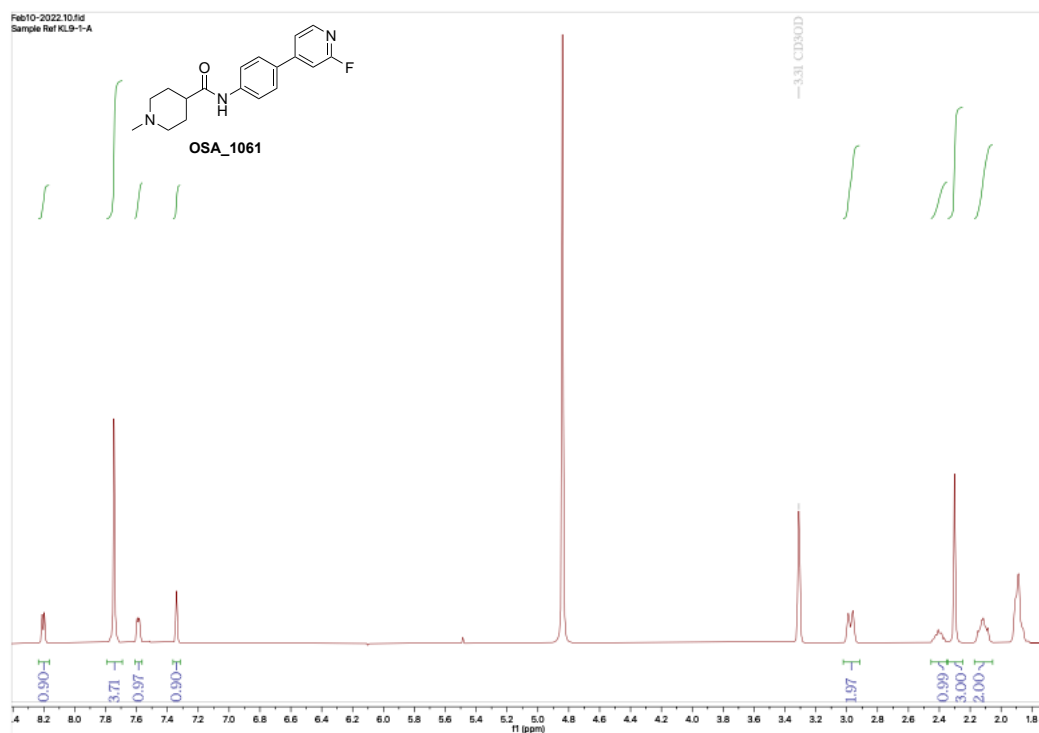


Figure 20: ¹H NMR compound **OSA_1061**

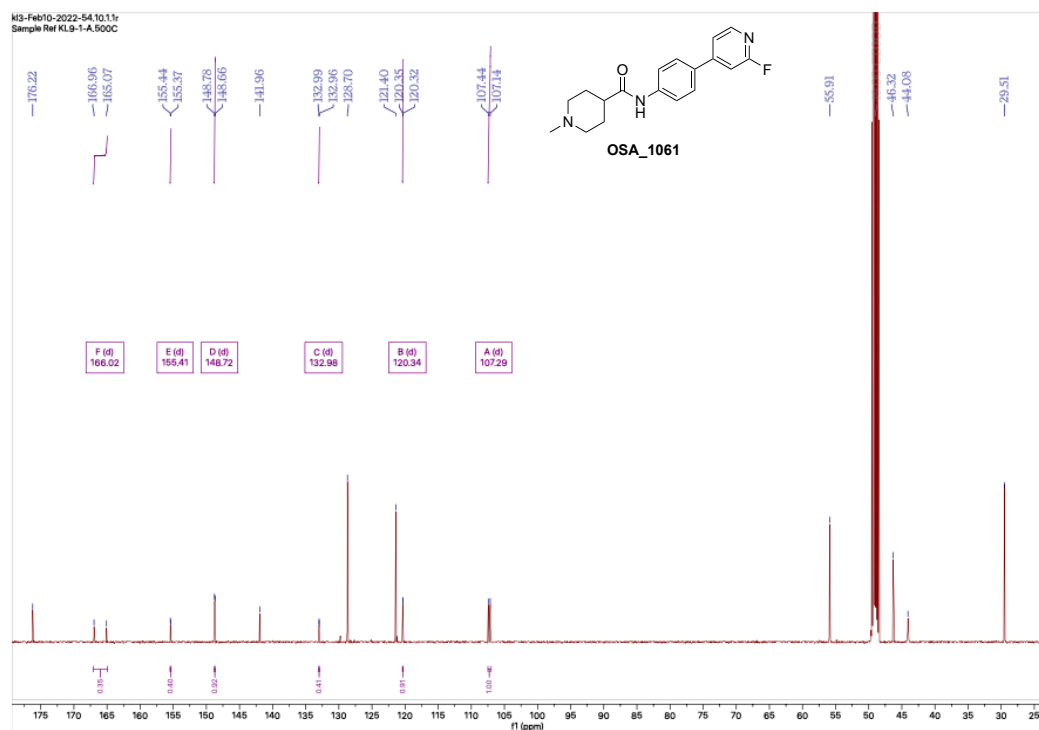


Figure 21: ¹³C NMR compound **OSA_1061**

9. *N*-(3-(Pyridin-4-yl)phenyl)-1-methylpiperidine-4-carboxamide (OSA_1062)

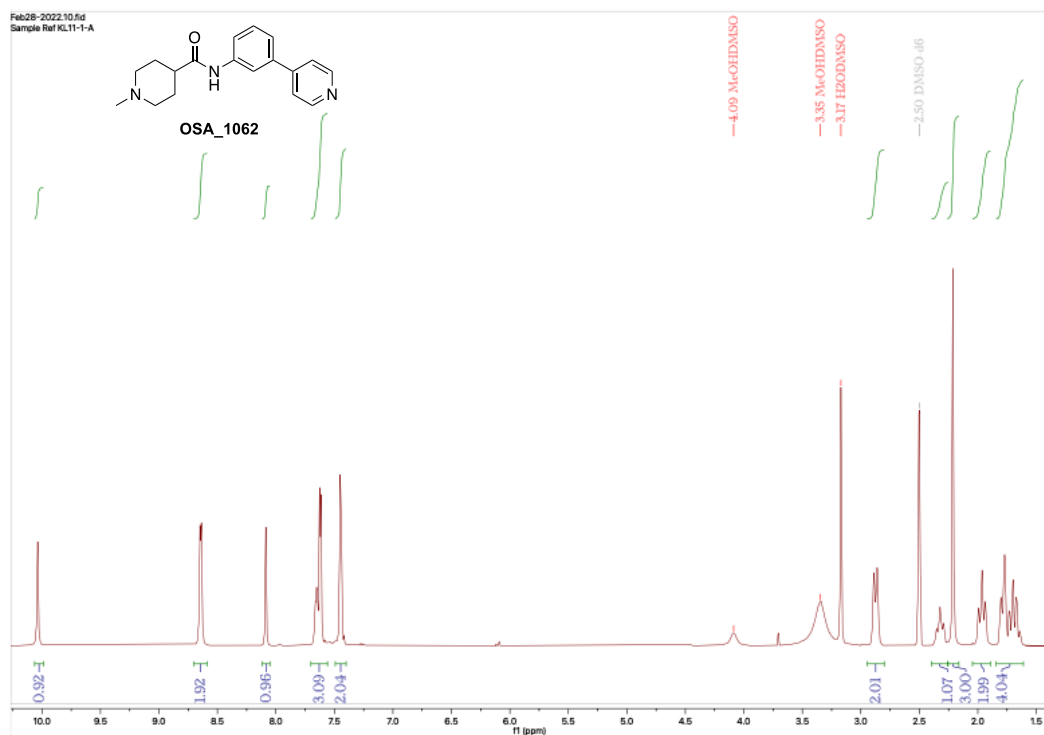


Figure 22: ^1H NMR compound **OSA_1062**

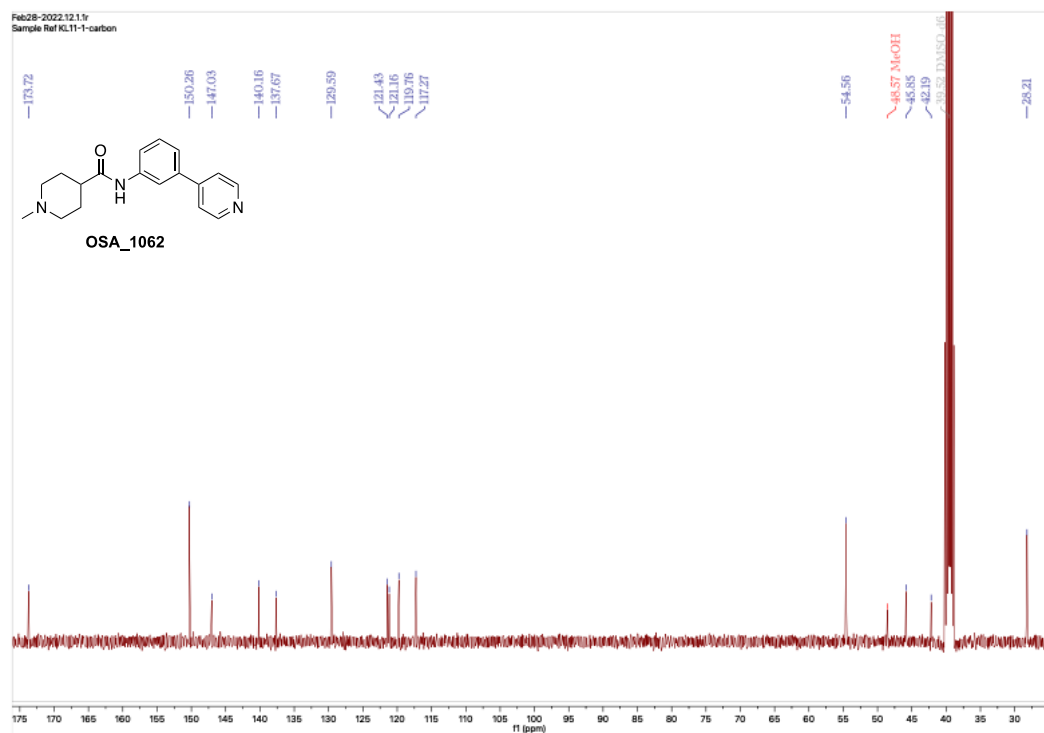


Figure 23: ^{13}C NMR compound **OSA_1062**

10. *N*-(4'-Cyano-[1,1'-biphenyl]-3-yl)-1-methylpiperidine-4-carboxamide (OSA 1063)

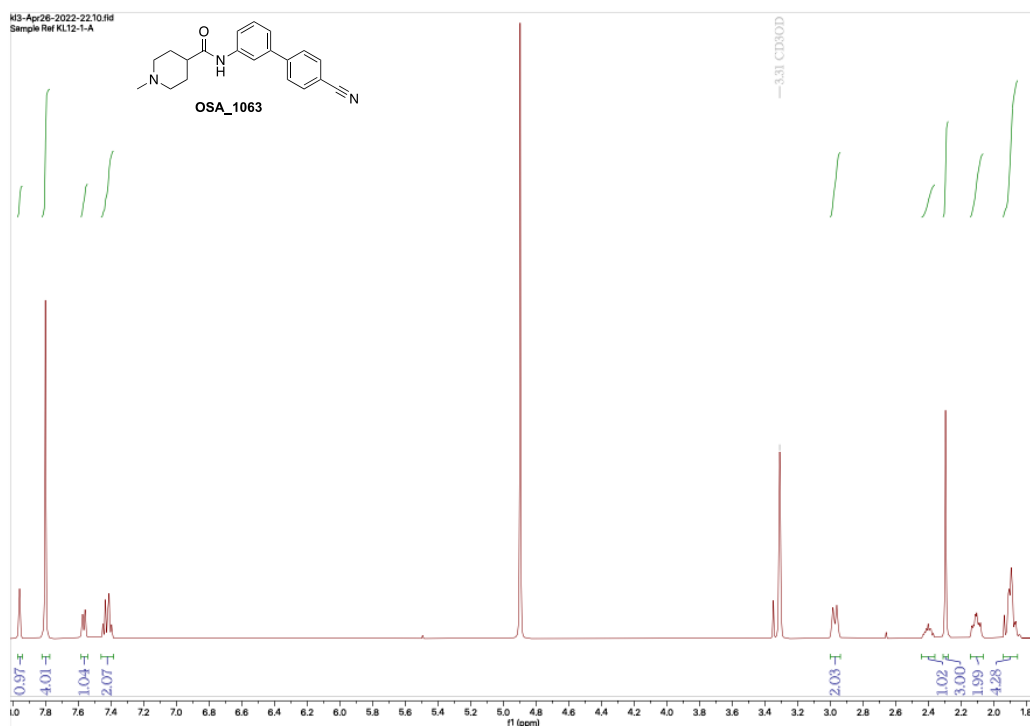


Figure 24: ¹H NMR compound **OSA_1063**

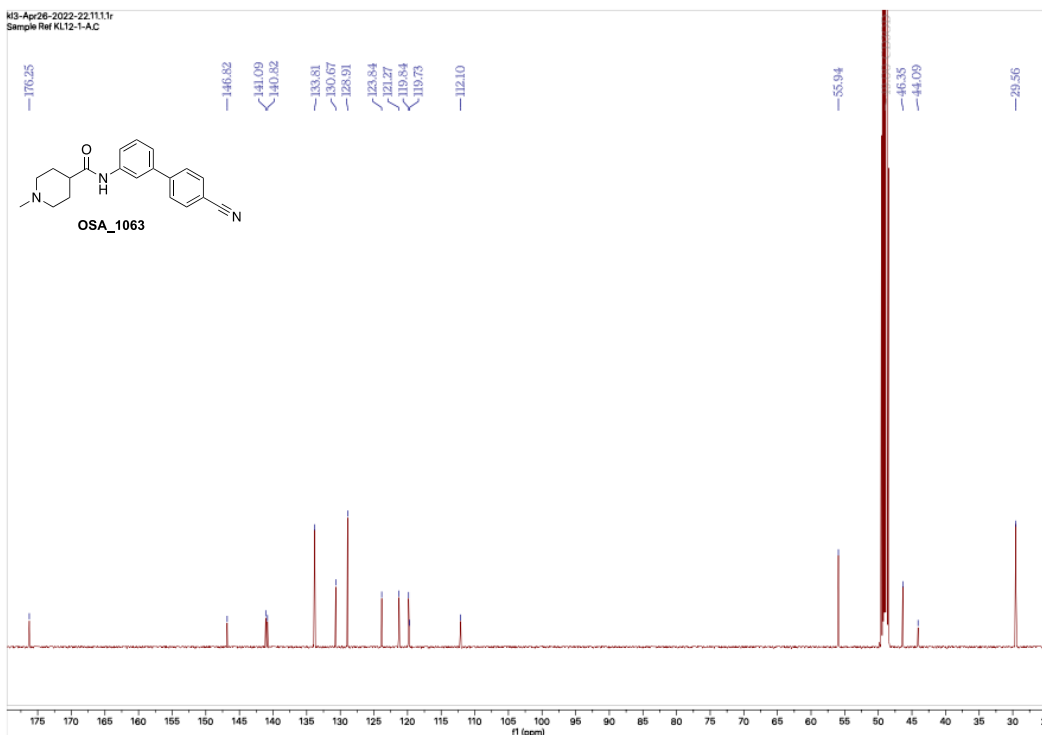


Figure 25: ¹³C NMR compound **OSA_1063**

11. *N*-(4'-Cyano-[1,1'-biphenyl]-4-yl)-1-methylpiperidine-4-carboxamide (OSA_1064)

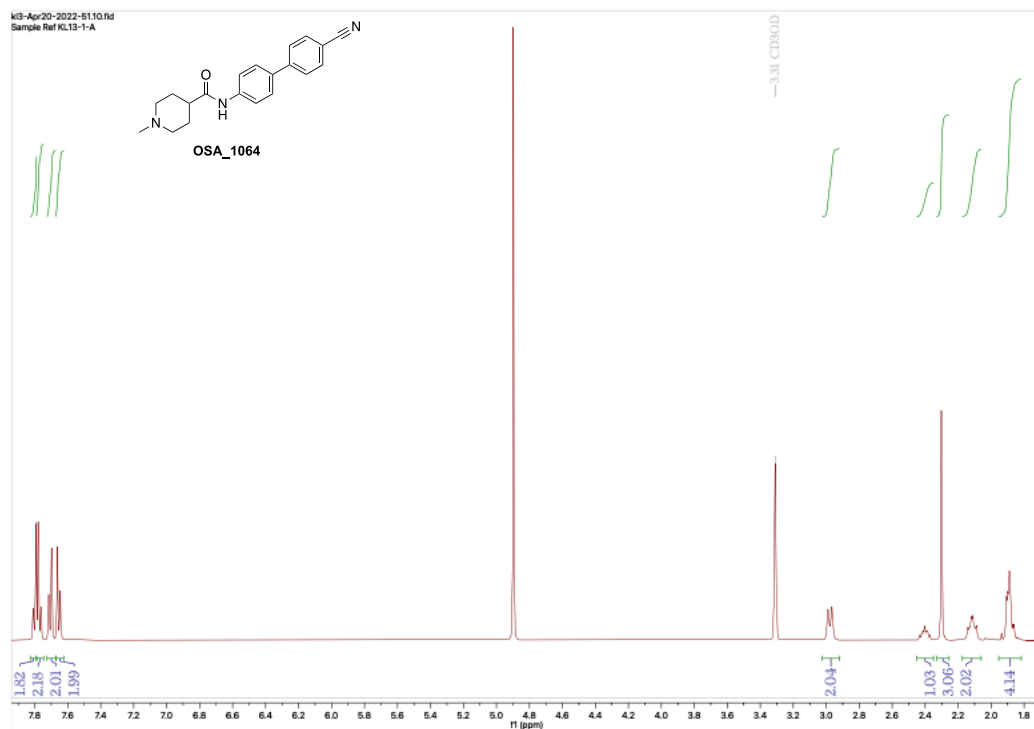


Figure 26: ^1H NMR compound **OSA_1064**

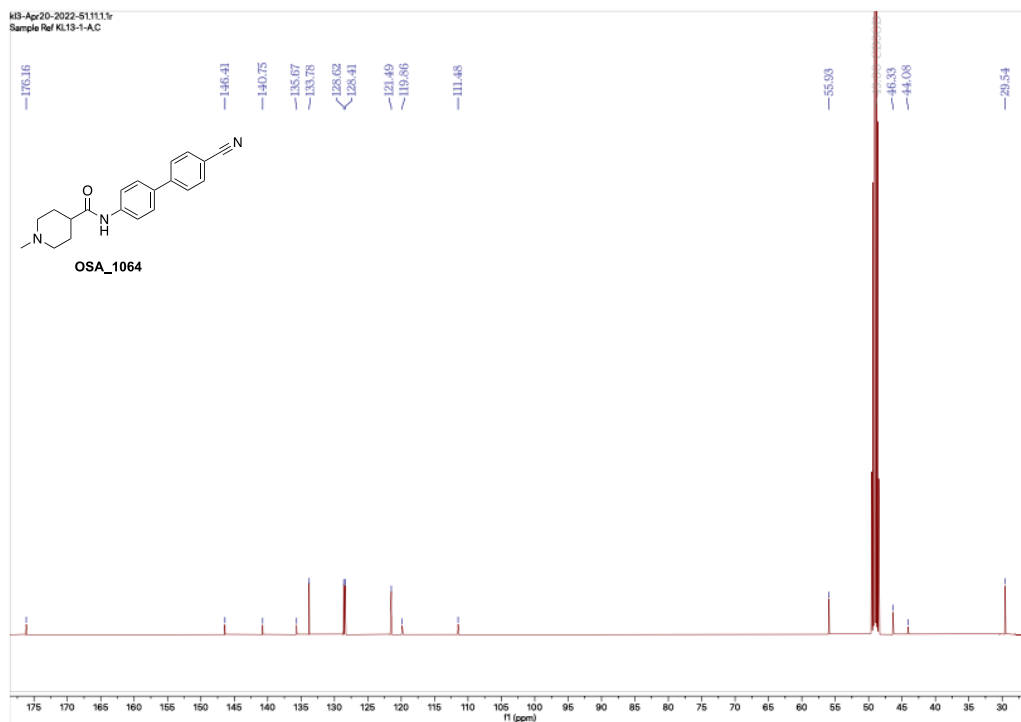


Figure 27: ^{13}C NMR compound **OSA_1064**

12. *N*-(4'-Sulfamoyl-[1,1'-biphenyl]-4-yl)-1-methylpiperidine-4-carboxamide (OSA 1065)

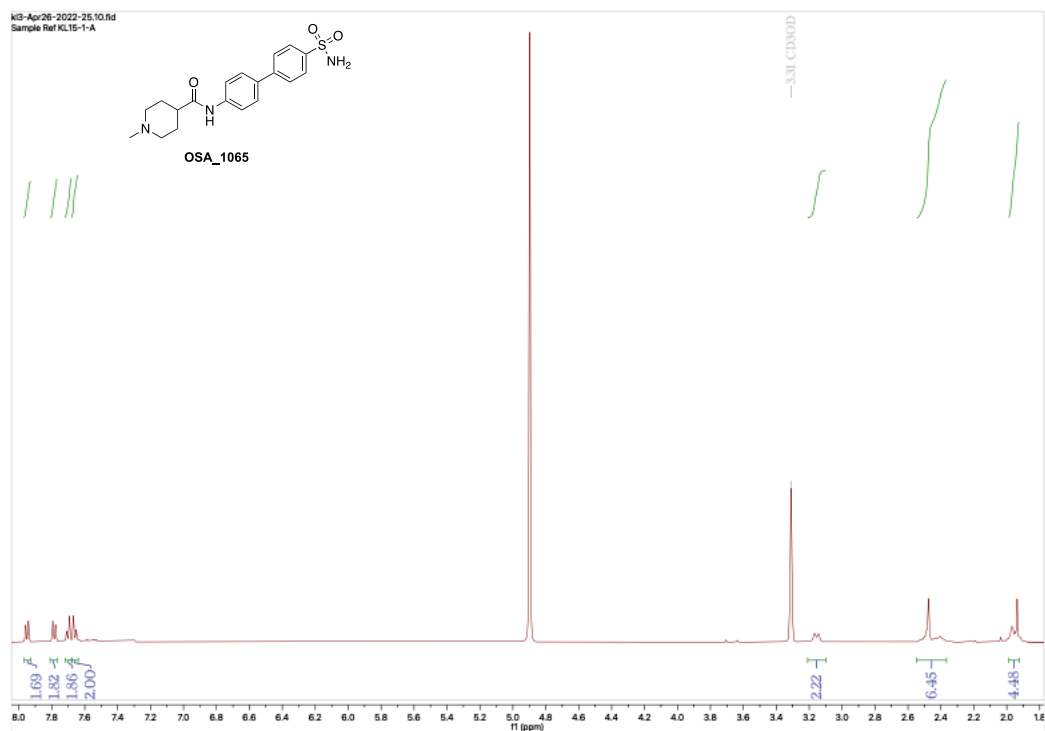


Figure 28: ¹H NMR compound OSA_1065

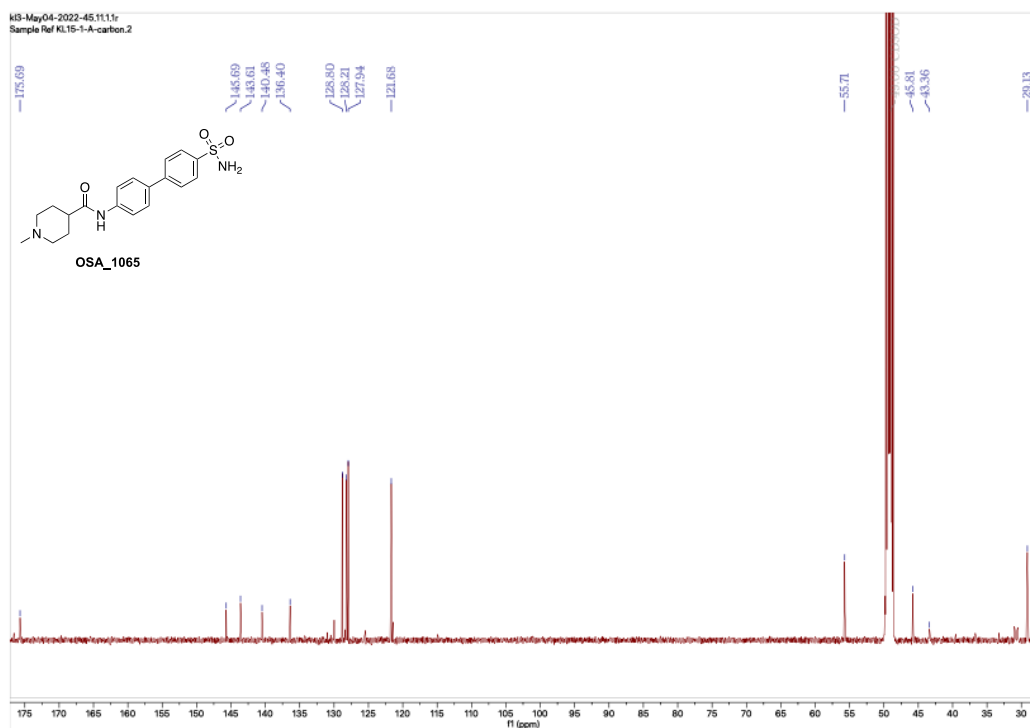


Figure 29: ¹³C NMR compound OSA_1065

13. *N*-(4-(6-Fluoropyridin-2-yl)phenyl)-1-methylpiperidine-4-carboxamide (OSA 1066)

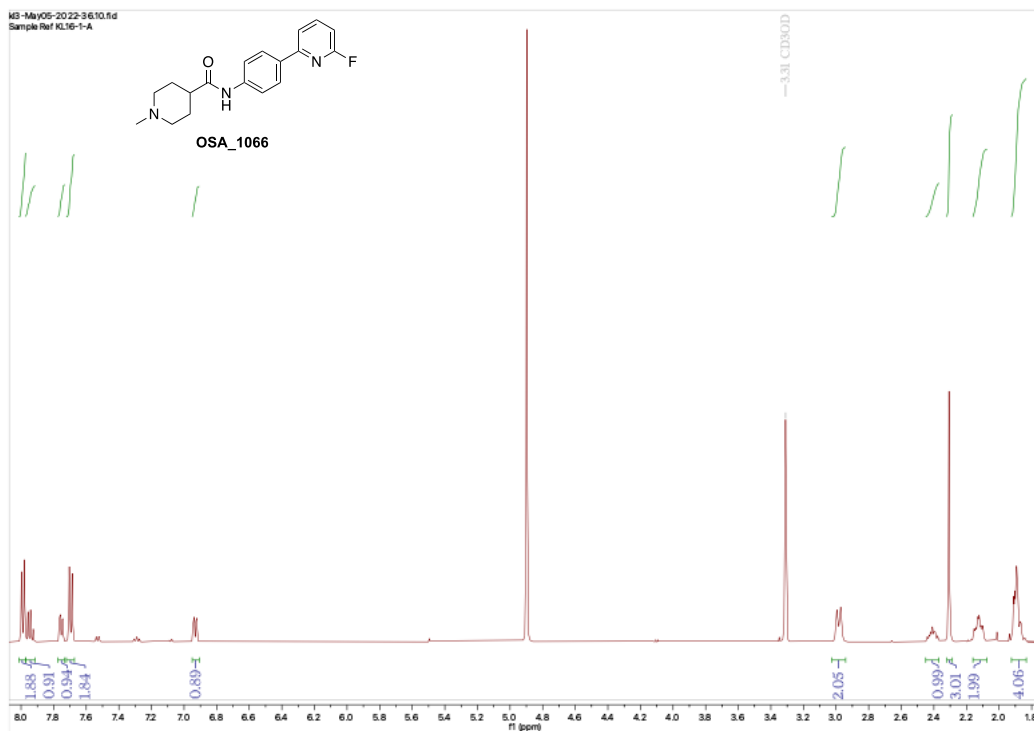


Figure 30: ¹H NMR compound **OSA_1066**

14. *N*-(4-(2-(Trifluoromethyl)pyridin-4-yl)phenyl)-1-methylpiperidine-4-carboxamide (OSA 1067)

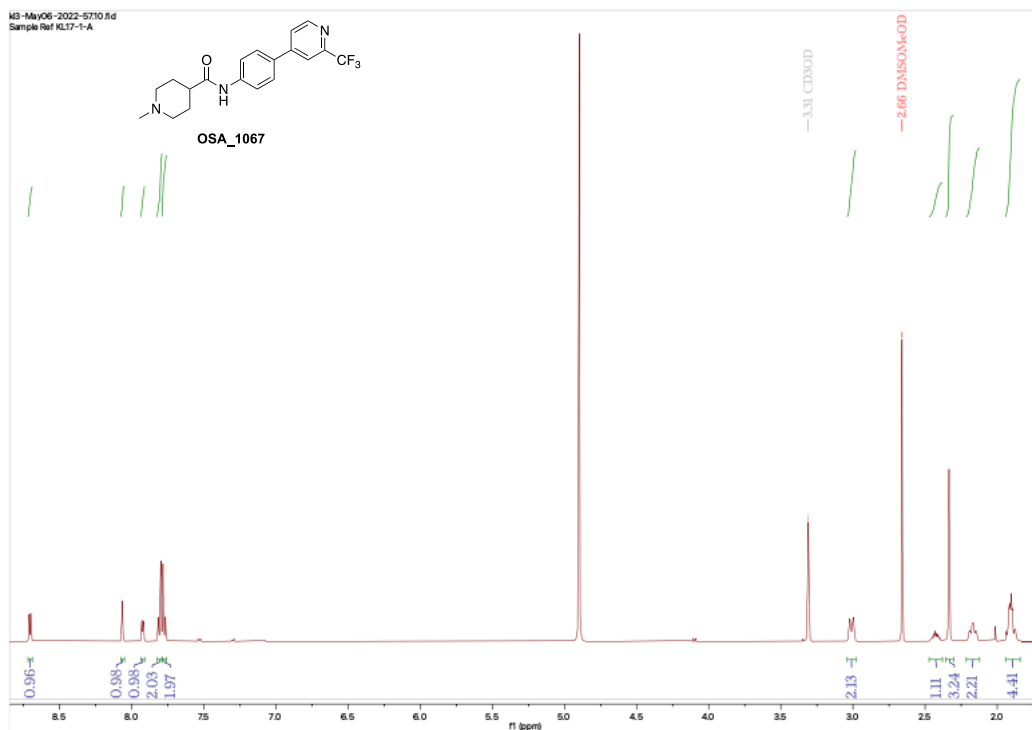


Figure 31: ¹H NMR compound **OSA_1067**

15. *N*-(4-(5-(Trifluoromethyl)pyridin-2-yl)phenyl)-1-methylpiperidine-4-carboxamide (OSA_1068)

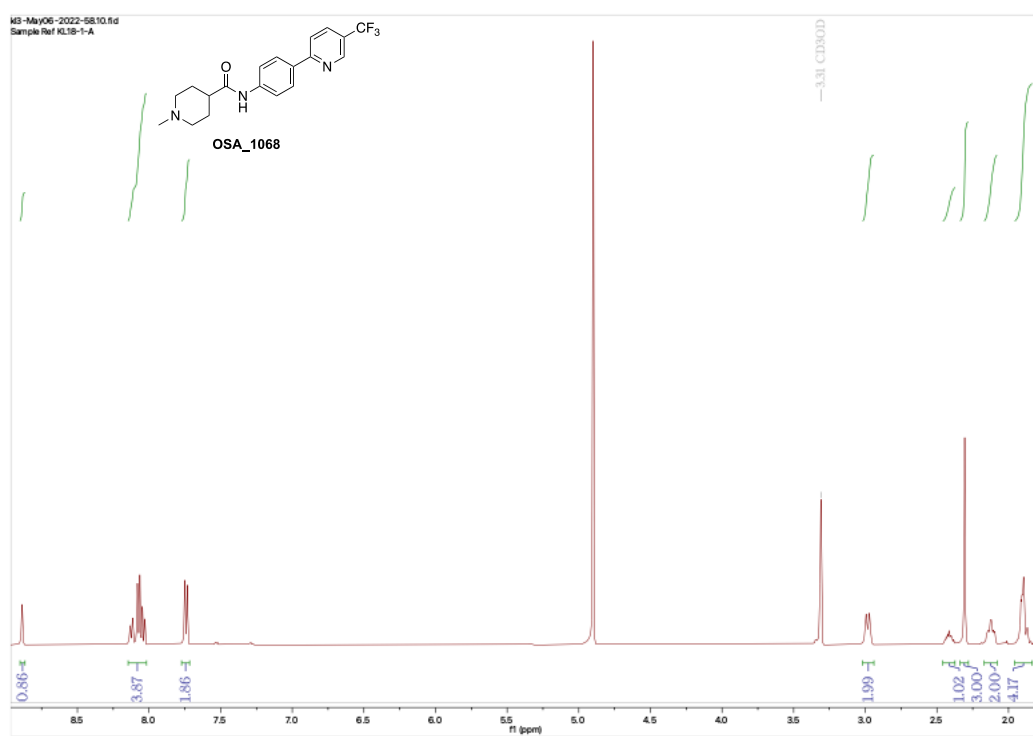


Figure 32: ^{13}C NMR compound **OSA_1068**

ADDENDUM 4 - HRMS: SYNTHESIS OF OSA_1054 – 1065

1. *N*-(3'-Amino-[1,1'-biphenyl]-4-yl)-1-methylpiperidine-4-carboxamide (OSA 1054)

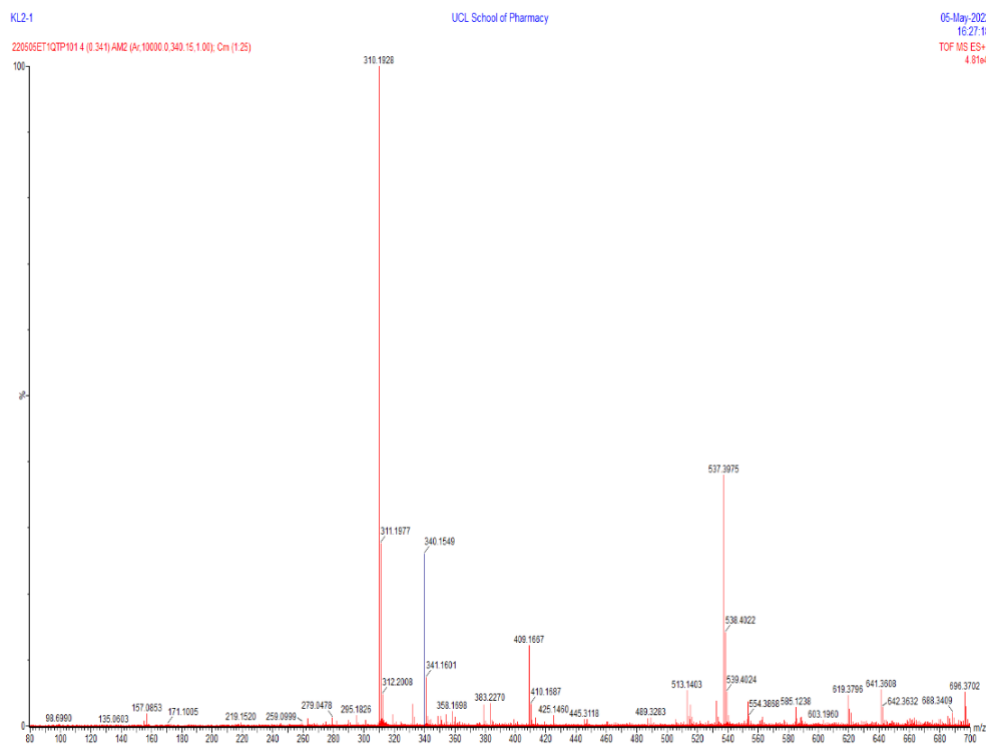


Figure 33: HRMS compound **OSA_1054**

2. *N*-(3'-Carbamoyl-[1,1'-biphenyl]-4-yl)-1-methylpiperidine-4-carboxamide (OSA 1055)

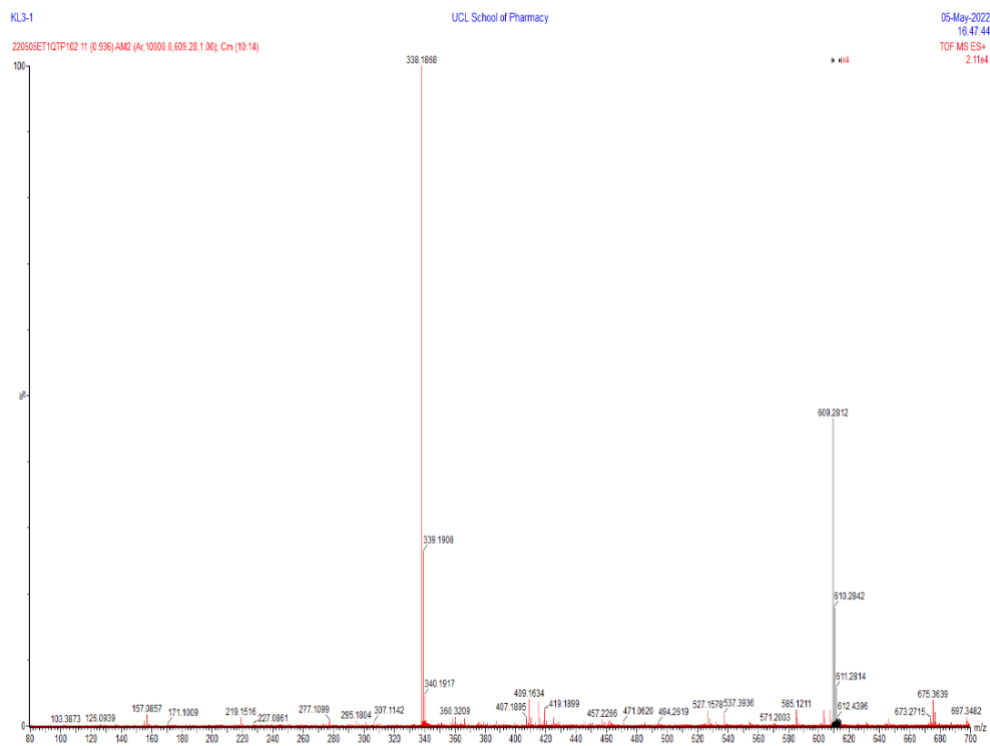


Figure 34: HRMS compound **OSA_1055**

3. *N*-(3'-(Hydroxymethyl)-[1,1'-biphenyl]-4-yl)-1-methylpiperidine-4-carboxamide (OSA 1056)

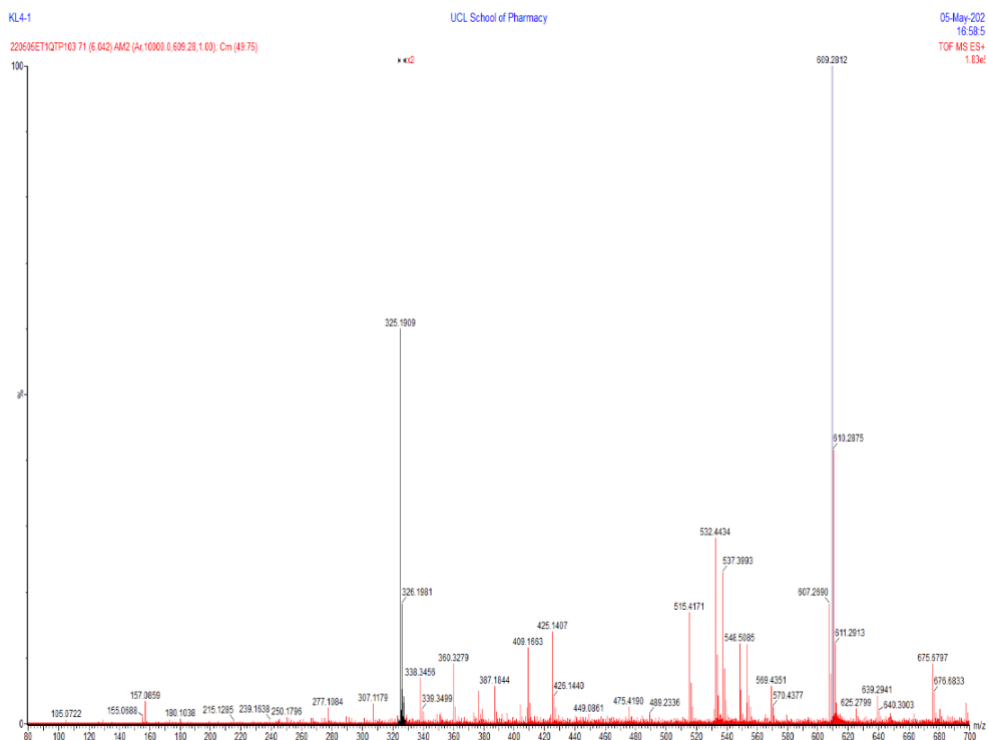


Figure 35: HRMS compound **OSA_1056**

4. *N*-(3',4'-Dimethoxy-[1,1'-biphenyl]-4-yl)-1-methylpiperidine-4-carboxamide (OSA 1057)

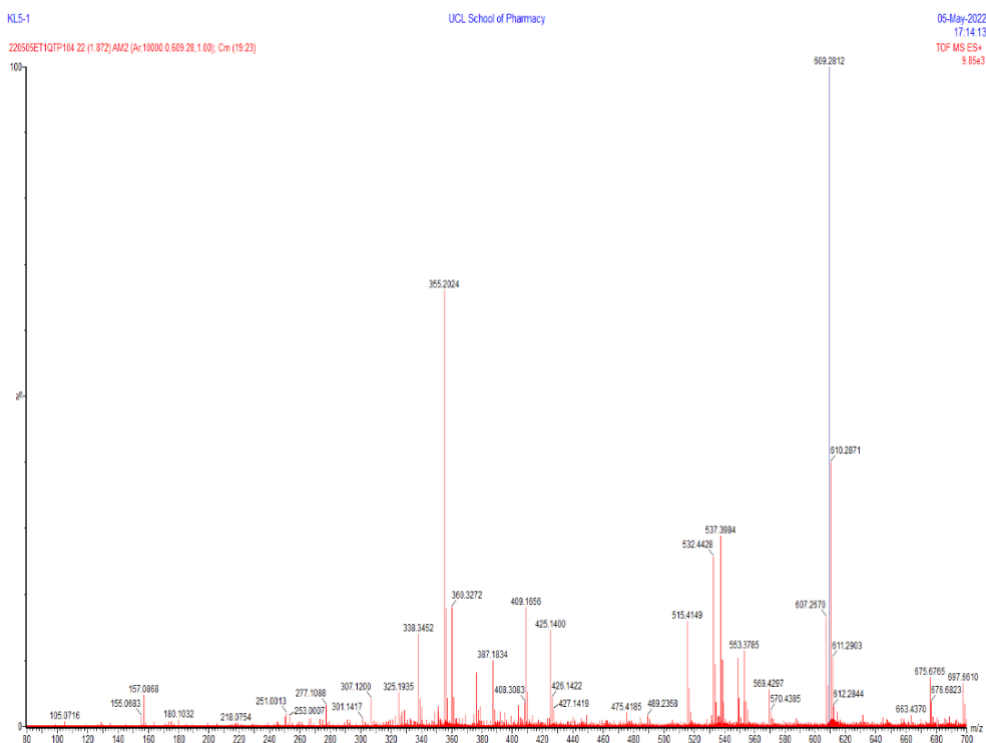


Figure 36: HRMS compound **OSA_1057**

5. *N*-(4-(1*H*-Benzo[d]imidazol-5-yl)phenyl)-1-methylpiperidine-4-carboxamide (OSA 1058)

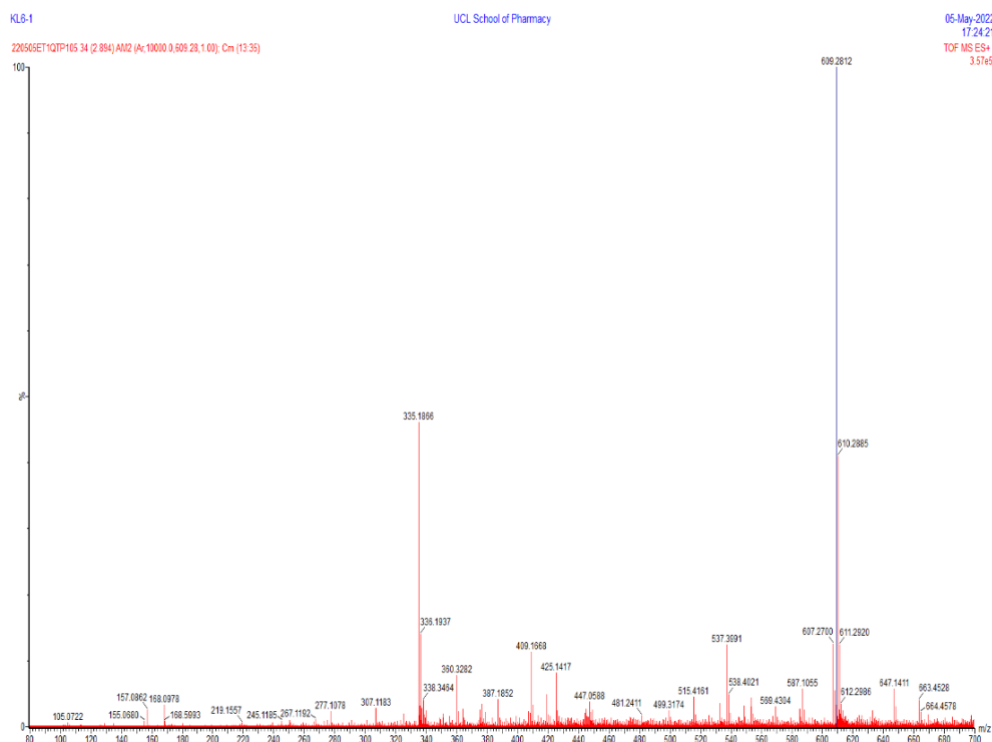


Figure 37: HRMS compound OSA_1058

6. *N*-(4-(Benzofuran-5-yl)phenyl)-1-methylpiperidine-4-carboxamide (OSA 1059)



Figure 38: HRMS compound OSA_1059

7. *N*-(4-(6-Aminopyridin-3-yl)phenyl)-1-methylpiperidine-4-carboxamide (OSA 1060)

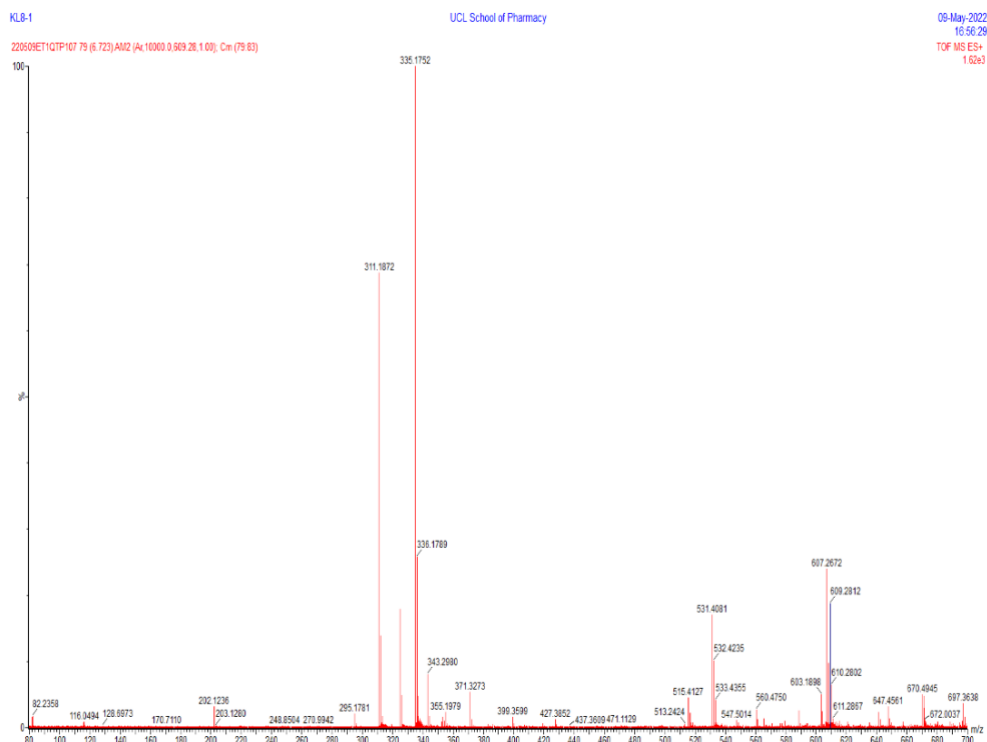


Figure 39: HRMS compound **OSA_1060**

8. *N*-(4-(2-Fluoropyridin-4-yl)phenyl)-1-methylpiperidine-4-carboxamide (OSA 1061)

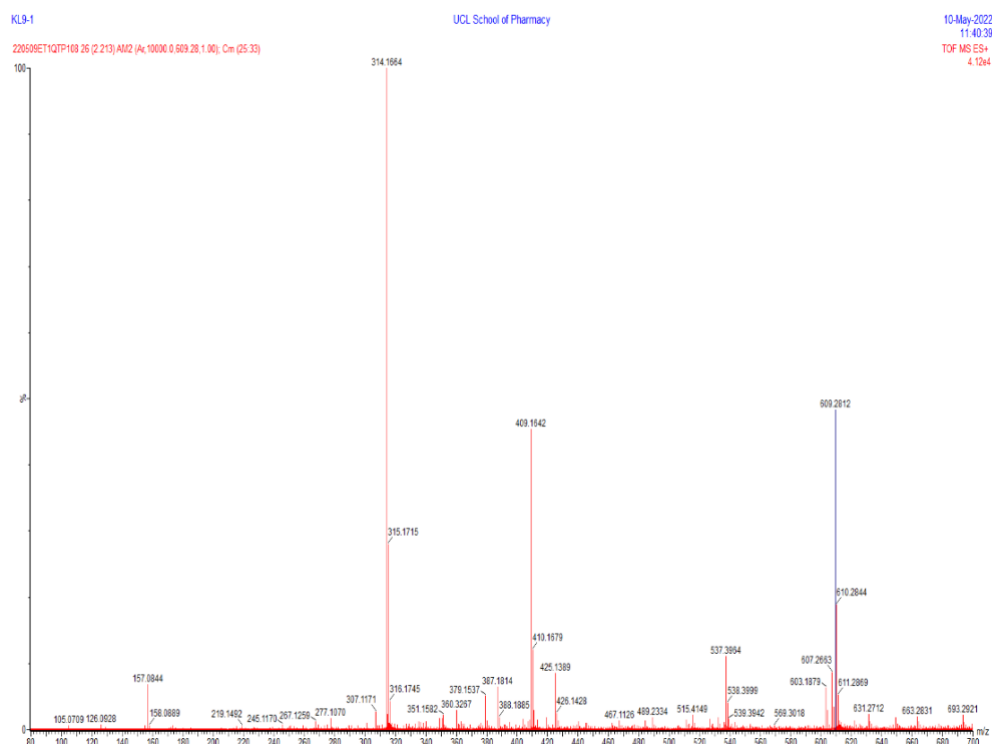


Figure 40: HRMS compound **OSA_1061**

9. *N*-(3-(Pyridin-4-yl)phenyl)-1-methylpiperidine-4-carboxamide (OSA 1062)

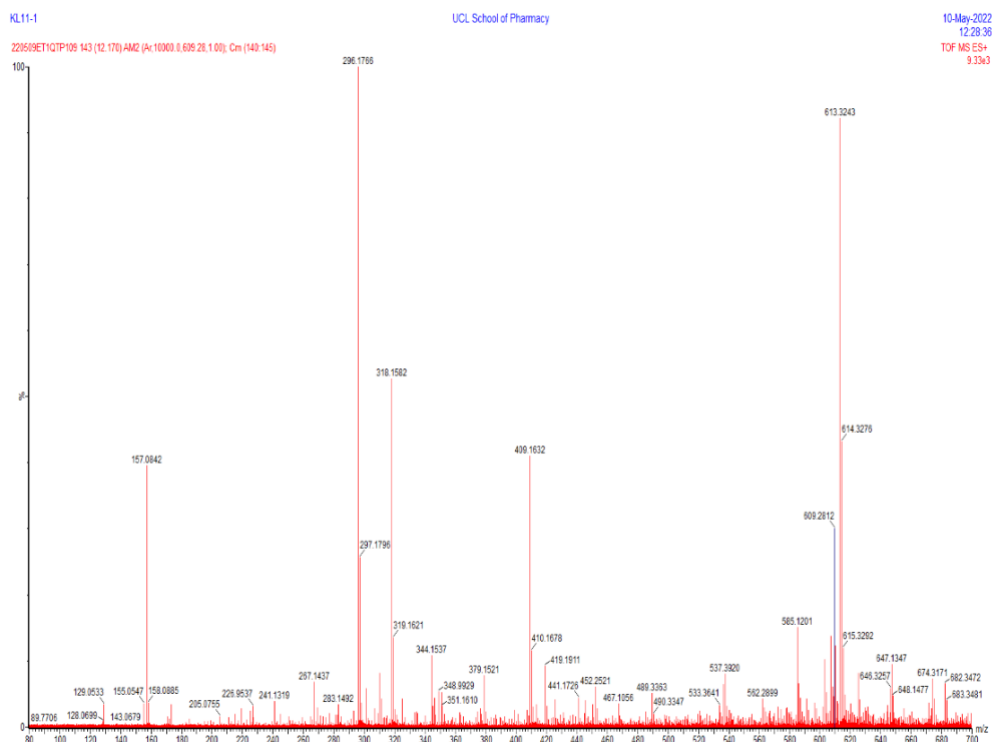


Figure 41: HRMS compound **OSA_1062**

10. *N*-(4'-Cyano-[1,1'-biphenyl]-3-yl)-1-methylpiperidine-4-carboxamide (OSA 1063)

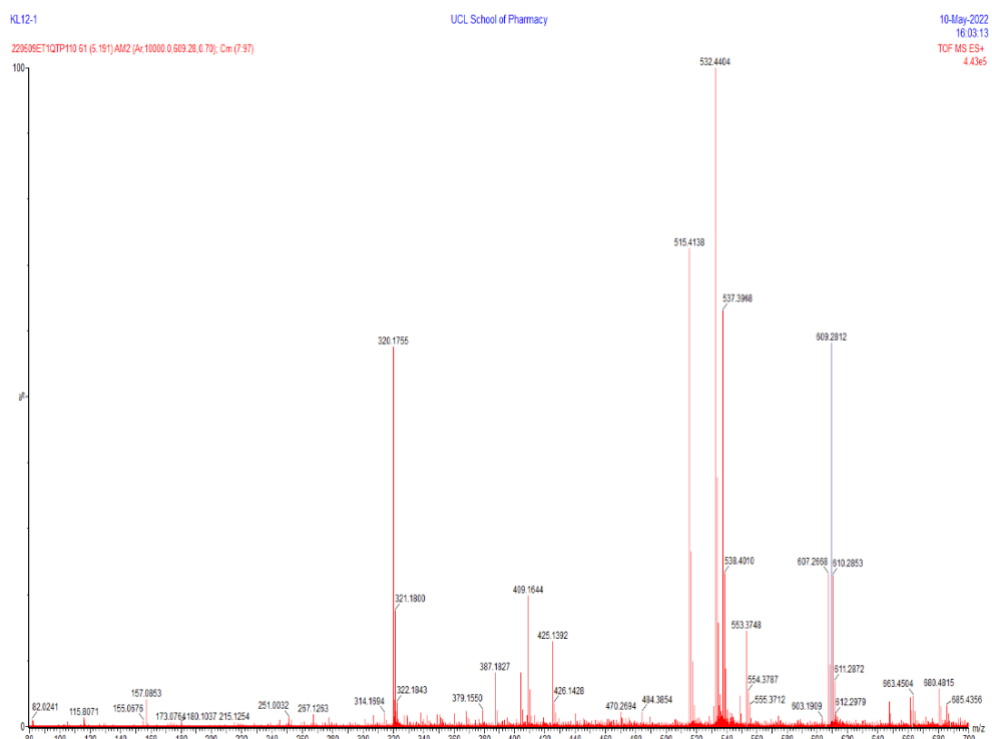


Figure 42: HRMS compound **OSA_1063**

11. *N*-(4'-Cyano-[1,1'-biphenyl]-4-yl)-1-methylpiperidine-4-carboxamide (OSA 1064)

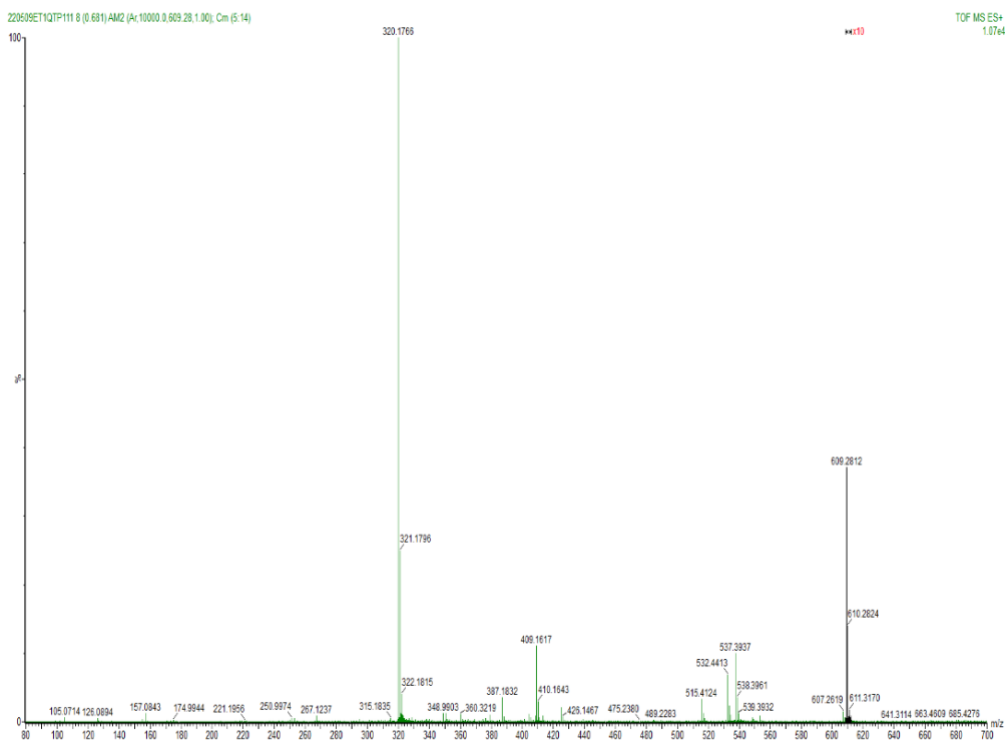


Figure 43: HRMS compound **OSA_1064**

12. *N*-(4'-Sulfamoyl-[1,1'-biphenyl]-4-yl)-1-methylpiperidine-4-carboxamide (OSA 1065)

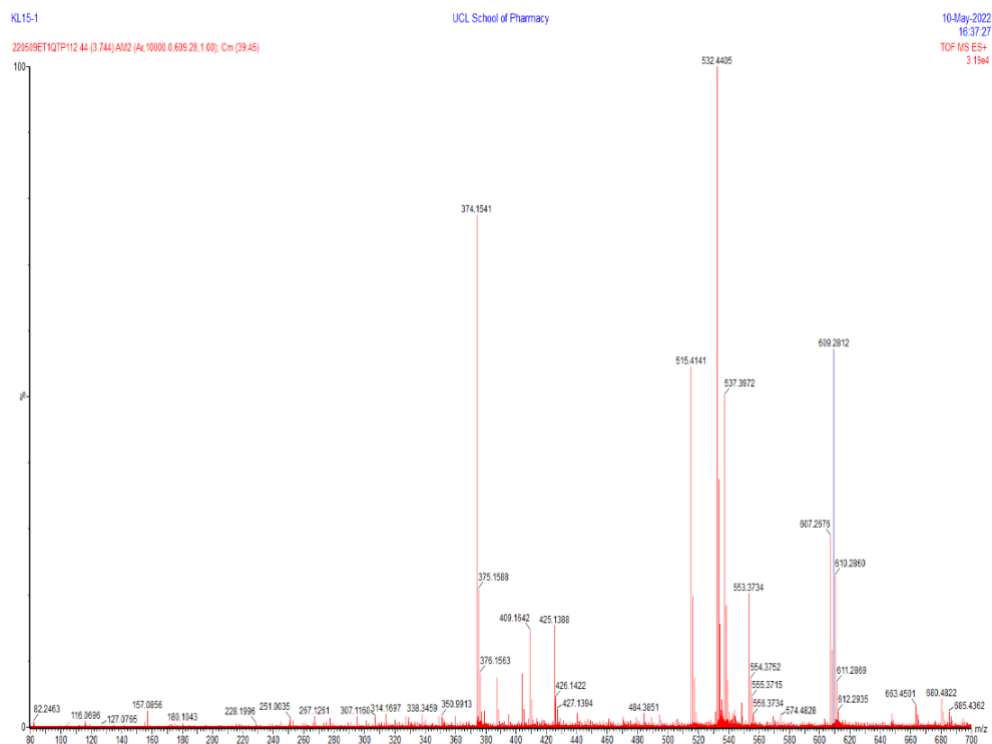


Figure 44: HRMS compound **OSA_1065**

